# DESIGN AND IMPLEMENTATION OF A DECENTRALIZED CONTROLLER FOR FLOTATION PROCESS

**by**

**MOEGAMAT TASHREEQ SAMODIEN**

**Thesis submitted in fulfilment of the requirements for the degree**

**Master of Engineering Degree**
**Electrical Engineering**

**Faculty of Engineering and Built Environment**

**at the Cape Peninsula University of Technology**

**Supervisor:** DR Nomzamo Tshemese-Mvandaba
**Co-Supervisor:** DR Mkhululi Elvis Siyanda Mnguni

**Bellville Campus**
**26 July 2024**

## DECLARATION

I, Moegamat Tashreeq Samodien, hereby declare that the information contained in this thesis is entirely original to me and that it has never been turned in for credit toward a degree. Moreover, it expresses my personal viewpoints rather than those of the Cape Peninsula University of Technology.

| | |
|---|---|
| | 12 December 2024 |
| Signed | Date |

# ACKNOWLEDGMENT

For this section, I would like to voice my appreciation to everyone who has been a part of the development of this research work that I have conducted.

I would like to thank:

- My parents and family, for their continuous believe and support in me.
- Dr. Tshemese-Mvandaba, for directing me and all her assist and guidance during the writing of my thesis and the motivation provided and support throughout the course of this study.
- Dr. Mnguni, for consenting to co-supervise this study and advising me throughout this research.
- Acknowledgements and appreciations to those whom I have unknowingly left out but provided support and were beneficial towards me and my studies.

# ABSTRACT

This research aims to design and implement a decentralized flotation process in real-time hardware in the loop scheme. The research objective is to supply sufficient literature on the flotation process and control development methods. To develop an open-loop and design controllers for the closed-loop model of the flotation process. The behaviour of the closed-loop system is investigated using the MATLAB/Simulink software environment. The investigation is based on the set point-tracking and disturbance suppression of the closed-loop system designed.

The research is expected to identify the best performance between the decentralized and decoupling control methodology. The controllers are designed individually based on the developed transfer function of the flotation process. The first controller is a decentralized and decoupled PI controller. The second controller is a decentralized and decoupled Advanced controller. The advanced controller consists of a Model Reference Adaptive controller using the Massachusetts Institute of Technology (MIT) rule. The results of the relevant controllers are compared against each other by adjusting the manipulated variables, (air flow rate and wash water) and monitoring the Froth layer height and Gas holdup in the collection zone. These controllers are also subjected to disturbances that may occur in practice.

The advanced controller modelled in the MATLAB/Simulink environment is translated to the Beckhoff Automation TwinCAT 3.1 environment for implementation on a Beckhoff PLC. The TwinCAT development environment is used for real-time simulation and analysis. The closed-loop hardware system behaviour is investigated under various process and disturbance conditions. The system simulation and hardware implementation results are to be compared. The PLC is then used for hardware in-loop implementation of the closed-loop system of the flotation process. The outcomes of the thesis are applicable to a flotation process implementing the proposed designed control strategy.

## Key words:

*Froth flotation; Decentralised control; Multiple Input Multiple Output; Model Reference Adaptive control; Relative Gain Array; Hardware-in-the-Loop.*

# LIST OF ABBREVIATIONS

| | |
|---|---|
| AC: | Adaptive Control |
| Eg: | Gas Holdup in the collection zone |
| FL: | Fuzzy Logic |
| Hf: | Froth Layer Height |
| DCS: | Distributed Control Systems |
| DNA: | Direct Nyquist Array |
| MPC: | Model Predictive Control |
| MIMO: | Multiple Input Multiple Output |
| MRAC: | Model Reference Adaptive Control |
| MIT: | Massachusetts Institute of Technology |
| PCB: | Printed Circuit Board |
| PI: | Proportional + Integral |
| PID: | Proportional + Integral+ Derivative |
| PLC: | Programmable Logic Control |
| RGA: | Relative Gain Array |
| RNGA: | Relative Normalised Gain Array |
| SISO: | Single Input Single Output |

## TABLE OF CONTENTS

## TABLE OF FIGURES:

## LIST OF TABLES:

# CHAPTER 1 : INTRODUCTION

## 1.1 Introduction

Froth flotation simply known as flotation is a physical and chemical separation technique used to separate valuable minerals from ore. This technique was originally developed for the mining industry and dates to the early 20th century, (Maurice, et al., 2007). Today this robust technique is used in other industries such as wastewater management and recycling. Modern day flotation circuits require process control, along with various control strategies for each plant. The objectives of these controllers are to achieve regulatory control (flow rate, froth density and froth depth) and maintain a productive operation.

This thesis focuses on the design of a decentralized advance control scheme for the froth flotation process. This control scheme will allow for adequate regulatory control of wash water flow rate and airflow rate. The process performance is based on the froth depth and the air holdup in the collection zone. The literature involves various advance control schemes that are used for industrial applications. The remaining literature contains the factors and challenges that may affect the controllability of the flotation process.

The purpose of this chapter is to provide a general background on flotation control in the industry. The problem awareness is discussed, and the problem statement is mentioned with regards to the flotation process industrial implementation challenges. The aim and objectives of this research are stated, along with the delimitation and motivation of the research mentioned in the thesis.

## 1.2 Background

In the last two decades, optimizing modern industrial controllers has become a popular study area. The use of advanced mathematical techniques to analyse and build modern control systems piqued the interest of researchers (Grimble, 2019). The growing popularity of sophisticated industrial control innovation, according to author Grimble (2019), stems from the evolving challenges of control implementation. The tuning approach of advance controllers to optimize performance criteria in a specific time frame is one of the focus areas for improvement.

Modern industrial control often involves of a multivariable process which in general, consist of numerous instrumentation and measurements, (Garrido et al., 2012; Salgado & Conley, 2004). This occasionally leads to complications with these control signals. Multivariable processes proved challenging to control due to variable interactions. As a solution, controller developers propose a matrix control architecture. These controller architectures are either centralized or decentralized, (Salgado & Conley, 2004).

For multivariable processes with strong variable interactions between them, a centralized approach is preferred, (Garrido et al., 2012). However, the centralized control architecture often renders traditional PID tuning methods inapplicable due to its full matrix structure. According to Garrido et al., (2012) controller manufacturers often consider depraved decoupling of the multiple variables to be the result of poor controller performance in practice. Engineers often use the approach of a decoupled network with a decentralized controller to solve this issue, (Garrido et al., 2012).

## 1.3 Problem awareness

Controllability and optimisation of a flotation process is considered challenging achievement due to its non-linear characteristics. The flotation process control consists of numerous variables and incalculable disturbances contributing to its performance, (Quintanilla, et al., 2021). A multivariable process such as column flotation consists of many interconnecting variables rendering the input-output pairings quite challenging. Selecting the incorrect input-output pairing or incorrect control structure could impose limitations on the controller performance. Advance controller designs might not be able to overcome these limitations, (Schmidt, 2002).

Model predictive control (MPC) strategy has been the proposed solution to dealing with the non-linear control of the system, (le Roux & Craig, 2019). Authors le Roux and Craig conducted research into MPC based on variables that are available for manipulation to the primary control plant and evaluate the controllability of the target variables. However, their approach does not consider the disturbances and only considers three variables.

## 1.4 Problem statement

Automated froth flotation control applications are considered scarce in the industry due to improper control tuning and poor control strategies. As a result, the preferred method of control is manual as opposed to automatic.

### 1.3.1 Sub problem 1 based on design

The frequent and spontaneous disturbances within a flotation cell, together with the high volume of variables required to achieve optimal performance will make it challenging to model. However, there are studies conducted into modelling a flotation column, but less literature on the development of a closed loop model with disturbance rejection.

### 1.3.2 Sub problem 2 based on implementation

Controllers are often poorly implemented or tuned; this raises concern for automated controllers used in practice. These controllers are not performing to their desired design objectives.

## 1.5 Aim and objectives

### 1.5.1 Aim

The aim of this research is to design and implement a decentralised flotation process in a real-time hardware in the loop scheme.

### 1.5.2 Objectives

- Literature review based on the flotation process and the methods for control design.
- To develop an open loop model based on the flotation process and simulate it using MATLAB/Simulink software environment.
- To design controllers for the closed loop model of the flotation process.
- To build the closed loop system in MATLAB/Simulink environment and to investigate its behavior for set-point tracking control and disturbance rejection.
- To transform the designed controller from MATLAB/Simulink environment into a Beckhoff PLC via TwinCAT 3 simulation environment.
- To determine the inputs and outputs of the Beckhoff PLC and establish communication between a Beckhoff PLC, for hardware in-loop implementation of the closed loop system.
- To investigate the closed loop Hardware in the Loop system behaviour under various process and disturbance conditions. Comparison of the results obtained from MATLAB simulation and Hardware-in-the-Loop implementation.

## 1.6 Research question

This research addresses the following questions:

- What is the best approach to the designing and implementation of an advanced controller that allows for real-time set point-tracking and disturbance rejection of column flotation?
- How well does performance of the implemented controller measure up to its simulated design?

## 1.7 Delimitation of the research

The flotation process consists of a circuit of cells to refine the mineral ore to achieve maximum concentration grade. For this research, the focus is on the controllability of a singular flotation column cell.

This study focuses on manipulation of two fundamentally controlled variables such as wash water flow rate and air flow rate. Additional fundamental variables such as Pulp level, pH and reagent addition shall not be considered as controlled variables.

There is numerous control strategies implemented in a flotation process such as Distributed control systems (DCS), Programmable Logic controller (PLC), Model-Predictive Control methods (MPC), fuzzy logic (FL) and Proportional-integral-derivative (PID) control. For controller development the MPC control strategy is utilized for mathematical modelling of the variables. The implementation consists of a PLC controller with a PID strategy and a model reference advanced controller. This thesis will not make use of the details of the other control strategies as the research is focused on an advanced decentralized and decoupled controller design and implementation.

## 1.8 Motivation of the research

Froth flotation separation is a versatile mineral separation technique utilized in numerous industries. The common usage for froth flotation is in the mining industry, which contributes roughly around 200 billion Rand per annum to South Africa’s Gross Domestic Product (GDP), (Saifadin, 2020). However, the potential for the flotation process lies within the automated controllability. In most cases control has been rendered unsuccessful due to a lack of automated performance of the process itself. By developing an advanced controller that uses Real-Time optimization, the economic efficiency and process performance could increase.

## 1.9 Thesis outline

The title of this thesis is “Design and implementation of a decentralized controller for flotation process”. The focus of this thesis is to address the challenges of control implementation of a column flotation process. This section gives a brief overview of each chapter in this thesis:

Chapter 1: Announces the background to flotation, the research question, objectives and methodology used to accomplish these objectives. The motivation of research and the delimitation of the research is also mentioned in this chapter.

Chapter 2: An induction into the theory and practice of flotation as well as industrial control. This chapter also presents an insight into future developments and trends in research on flotation.

Chapter 3: A discussion on column flotation control and all its components. This chapter highlights the merits and challenges of modelling a flotation column and implementing a controller.

Chapter 4: The mathematical model of a flotation column is presented. The behaviour of the flotation column without any control action is simulated and discussed.

Chapter 5: Introduces a decentralized and decoupled PI controller for a column flotation process. The design and simulations of the controller is mentioned in this chapter along with its challenges and limitations.

Chapter 6: An advance controller is developed based on the limitations of the decentralized and decoupled PI controller. The performance of both the advanced controller and decentralized PI controller are analysed and discussed.

Chapter 7: This chapter presents an implementation of the advance controller developed in the previous chapter. Using real-time simulation and HIL testing the implemented controller’s performance is measured against the performance of the simulated advance controller.

Chapter 8: Provides a summary of the research conducted, including the results and conclusions drawn based on the findings of the research. The recommendations and future work are also mentioned in this chapter.

## 1.10 Conclusion

Multivariable systems control has become the focal point of control systems research in the past few years. This is due to the evolution of control system technology and the consistent growth of industrial processes. As industrial processes shifted towards MIMO systems structural complications began to immerge. Interconnecting relationships or interaction between variables proved difficult to control. These variables are often decoupled and then decentralized to improve controller performance.

The column flotation process often uses manual control at base levels due to poor controller performance. The process modelling is often complexed due to the interrelationships between variables and is highly sensitive to modelling errors. Existing controllers often fail due to irregularities within the feed, resulting in manual control being the popular opinion between plant managers and operators.

The outcome of this proposed research is the adaptation of a decentralized controller to a column flotation process. This research focuses on an advance control approach to manage the multivariable nature of the flotation process. The objective is to improve the process controllability by developing a reliable and robust controller for set point tracking and disturbance rejection. This study makes use of the existing data and experimental data from a column flotation cell as a foundation. To analyse and make comparison, the author gathers experimental data collected from the literature review. The author undertakes an experiment based on an actual flotation column utilizing available data to designing controllers that can stabilize the system and reject any disturbance.

# CHAPTER 2 : LITERATURE REVIEW

## 2.1 Introduction

The purpose of this chapter is to provide an understanding into what flotation is and to provide its industrial usage. Froth flotation is considered the most general method of separation in the mining industry. Although the process was only introduced in the late 19$^{th}$, and early 20$^{th}$ century the flotation process remains inefficient. Despite years of research and development, there are still economical gains to be made by optimising many of the present processes, (Shean & Cilliers, 2011). In this chapter, an investigation of the advantages and disadvantages associated with the utilization of flotation is presented. This chapter further investigates the factors that influence the controllability of the process when implemented in practical settings. Furthermore, the various important components integrated into the flotation process are detailed and discussed.

The second portion of this chapter introduces industrial control technology, and the strategies commonly used and seen in industrial applications. An analysis is done based on modern literature and similarities to this study as presented in the literature table.

## 2.2 Fundamentals of flotation

This section is intended to provide insight into flotation and how it is implemented in the modern era. To do this one needs to understand the fundamentals of the flotation process and why it is required. As high-grade ore became more scares in the late 19th century, mineral engineers turned their focus to a refinery process to treat lower-grade ore, (Bunyak, 2000). According to Bunyak, (2000), the first commercialized flotation mill was established in Broken Hill Australia in 1905. This was soon followed by experimental plants in other parts of the world. The successful development of the flotation process increased the productivity of metals and non-metals at a more cost-effective rate.

### 2.2.1 Description of the flotation process

Froth flotation is described as a separation process that uses differences in surface area properties of minerals. The mineral particles that repel water will attach themselves to the air bubble and float to the surface. The selection of particles is based on whether they are either hydrophobic or hydrophilic. Hydrophobic is referred to as the rejection of water whereas hydrophilic is referred to as the acceptance or absorption thereof. The hydrophobic particles are extracted from the cell when air is induced into the flotation pulp allowing particles to collide and attach themselves onto air bubbles to float to the surface of the water for extraction; this is known as the froth phase. The collision of bubble and solid particles requires what is known as an induction period. The induction period is the time taken for the solid particles to successfully attach to the air bubble, (Wills & Finch, 2016). A chemical compound, known as a flotation reagent, is used to prevent the air bubbles from bursting when it reaches the surface. The hydrophobic particles sink to the bottom of the system for extraction, known as the tailings.

True flotation is an interaction between liquid, solids, and gasses. Once these three phases interact, equilibrium is established among the surface tension of each phase (solid to gas, solid to liquid, and liquid to gas). These tensile forces develop an angle between the tangent and the point of contact of all three phases. The balance of these surface forces is represented using Young's equation.

$$\gamma_{SA} = \gamma_{LS} + \gamma_{LA} \cos\theta \qquad (2.1)$$

Where: $\gamma_{SA}$ is the tensile force between solid and air

$\gamma_{LS}$ is the tensile force between liquid and solid.

$\gamma_{LA}$ is the tensile force between liquid and air.

$\theta$ is the contact angle of the three phases.

The force or energy required to separate the solid particle to bubble interaction is known as the free energy change or work of adhesion ($\gamma_{WA}$).

$$\gamma_{WA} = \gamma_{LS} + \gamma_{LA} - \gamma_{SA} \qquad (2.2)$$

Substituting equation 2.1 into equation 2.2 resulting in the following equation:

$$\gamma_{WA} = \gamma_{L/A}(1 - \cos\theta) \quad (2.3)$$

To maximise the work of adhesion $\gamma_{WA}$ a greater contact angle $\theta$ is required, thus increasing the tensile forces that holds the solid particle to the bubble. The hydrophobic characteristics of minerals are measured by their contact angle. Minerals with a greater contact angle are said to be aerophilic, (Wills & Finch, 2016). A graphical representation of this three-phase relationship can be seen in Figure 2.1.

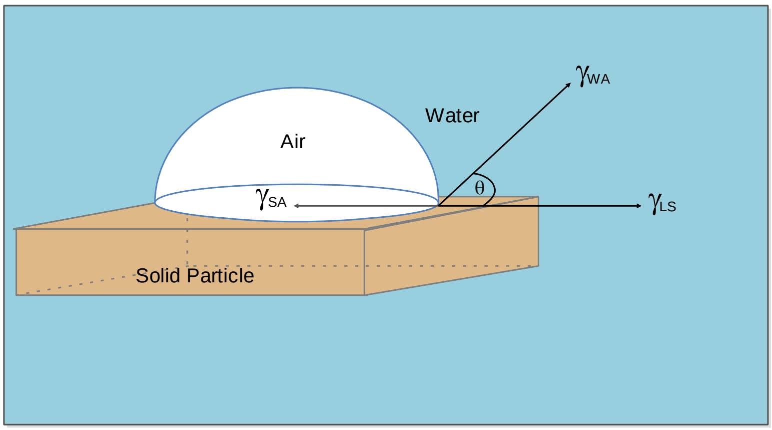


**Figure 2.1:** **A representation of forces and three-phase surface interaction during the flotation process. (Wills & Finch, 2016)**

Shean and Cilliers, (2011) describes the process control of froth flotation as a hierarchy of 4 interconnecting layers as presented in Figure 2.2. The lowest level is the instrumentation, which is an essential part of any control system. The base level flotation control uses traditional single input single output (SISO) to control primary variables such as pulp level, air flow rate, and reagent addition. The advanced flotation control consists of disturbance rejection from inconsistent feed grade and maintaining the system parameters such as concentration grade and recovery. The primary objective of optimising flotation control tier is to maximise the grade and recovery thus maximising the financial gains of the process.

The two higher tiers advanced flotation control and optimising flotation control attempt to achieve their objectives by manipulation of the base flotation level control. Thus, more complex methods of control to the traditional SISO PID control were required. The earliest attempt at grade and recovery control dates to the 1980's. After the 1980's adaptive control and neural networks have been effectively applied to the flotation systems to some degree, (Wills & Finch, 2016).

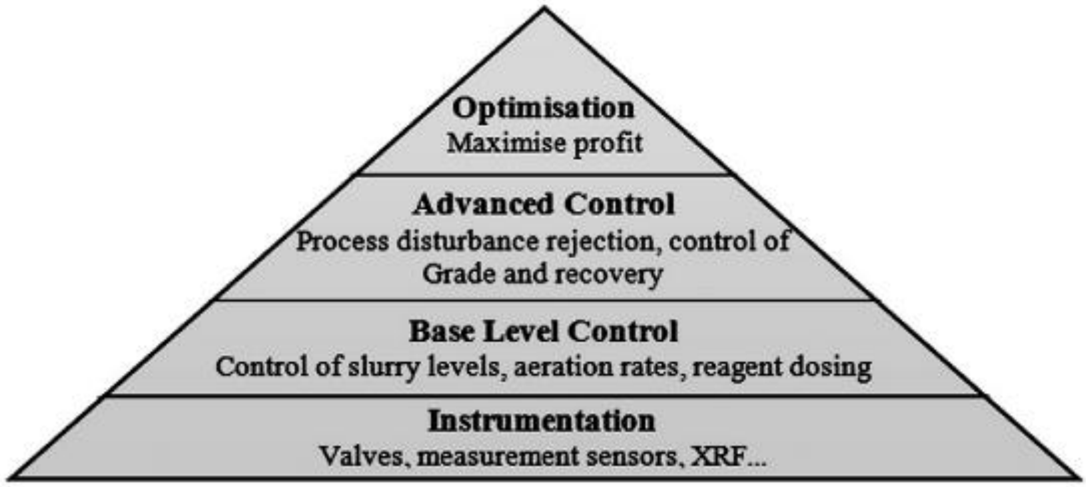


**Figure 2.2:** **Process control hierarchy of froth flotation, (Shean & Cilliers, 2011).**

### 2.2.2 Flotation circuits

In practice, a flotation circuit is regularly suggested over a single cell and bank operation. A flotation circuit or flowsheet consists of several flotation stages combined, with the tailing flowing back into the circuit, (Wills & Finch, 2016). These authors indicate that the circuit provides better separation as opposed to the single-cell operation. This is mainly due to the selectivity limit in the single cell. Figure 2.3 below represents a basic Rougher-Scavenger-Cleaner circuit configuration. The pulp is fed into the rougher cell for the initial stage of flotation. The concentrate of the rougher cell is then fed into the cleaner cell and the tailings are fed to the scavenger cell. The recovery of the scavenger cell and the tailings of the cleaner cell are recycled back into the rougher cell. The R-S-C configuration may use different types of flotation cells per stage. The rougher cell could consist of a column flotation, and the scavenger or cleaner could consist of mechanical flotation, (Wills & Finch, 2016).

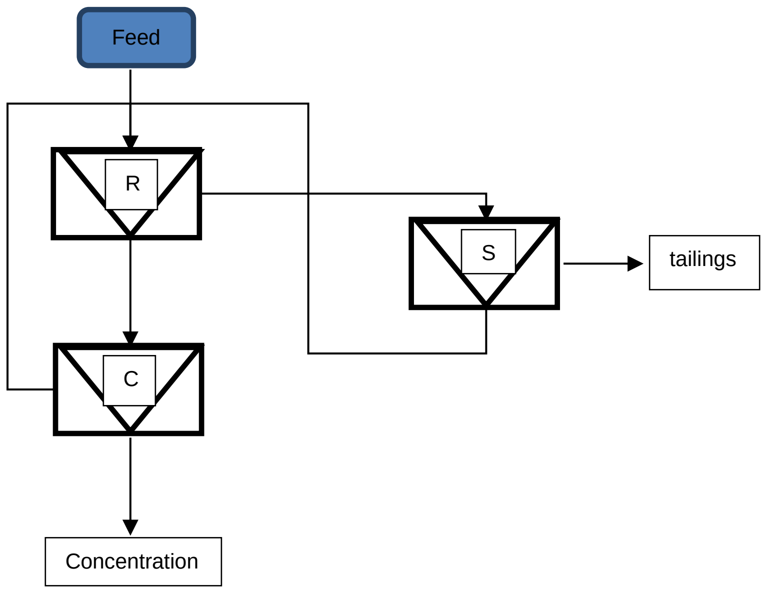


**Figure 2.3:** **R-S-C circuit configuration, (Wills & Finch, 2016)**

### 2.2.3 Types of flotation mechanisms

The type of flotation cell is a popular topic in modern literature for flotation circuit configuration. Modern flotation cells are often separated into three categories: mechanical, column, and pneumatic, (Wills & Finch, 2016). These categories are specified by the way entrainment is achieved.

#### 2.2.3.1 Mechanical mechanism:

These cells are aeriated by means of a mechanical impeller. A mechanical flotation impeller typically consists of a rotor and diffuser. However, the design of the cell and impeller varies based on the manufacturer. The air is either self-induced by the rotation of the impeller or induced through an external blower. During the rotation of the impeller, an air cavity is created behind the impeller blades. Air bubbles are then formed through shearing action. The impeller speed dictates the particle suspension and bubble dispersion throughout the cell, (Wills & Finch, 2016).

Mechanical flotation banks are either configured as cell-to-cell flow or as open flow. The cell-to-cell configuration uses adjustable weirs between each cell, (Fuerstenau & Somasundaran, 2003; Wills & Finch, 2016). Wills (2016), further states that the cell-to-cell configuration shows significant improvement in selectivity as opposed to open flow with regard to coal processing. Whereas open flow, also known as free flow configuration, allows for easier maintenance, and is suited for higher throughputs, (Fuerstenau & Somasundaran, 2003; Wills & Finch, 2016).

### 2.2.3.2 Column mechanism:

Column flotation gained its popularity in the coal mineral industry during the 1980's, (Wills & Finch, 2016). The column flotation cell, as seen in Figure 2.4, consists of a collection zone and a froth zone. The collection zone is known as the area in the column where the bubble particle collision occurs. Air is induced into the column through a sparger, generating air bubbles. The hydrophobic particles are transferred to the froth zone allocated above the feed. The wash water is used to prevent the contamination of feed and concentrate. Column flotation provided better fine particle separation efficiency and a cost-effective solution to automation than mechanical flotation. Column cells are often used as cleaner cells based on the fine particle performance, (Wills & Finch, 2016).

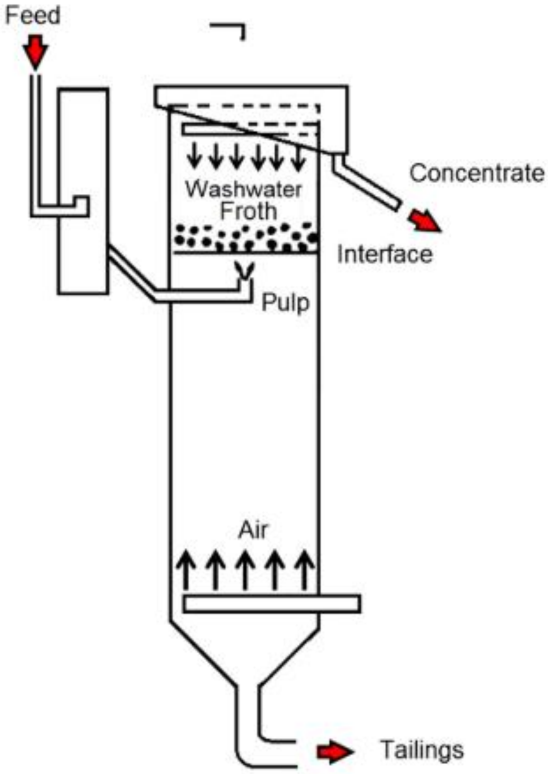


**Figure 2.4:** **Column flotation cell, (Wills & Finch, 2016)**

### 2.2.3.3 Pneumatic mechanism:

Pneumatic flotation cells consist of two separate vessels as opposed to mechanical and column flotation cells. Both mechanical and column flotation uses a single vessel for bubble-to-particle attachment and separation The first vessel is known as the reactor, this vessel is used to induce air for the bubble and particle collision and particle attachment. The second vessel known as a separator is used to gather the concentrate and tailings, (Imhof, 1988; Wills & Finch, 2016).

According to Wills & Finch (2016), the first commercialized pneumatic cell was introduced in the 1960's. The Devcra cell was considered as either a column or reactor/separator cell, however, the pulp and air come into contact and are then injected into the tank. The Devcra cells as seen in Figure 2.5, were installed as reported to reduce the cost of operations and floor plan area as well as improve metallurgic recovery as opposed to the mechanical cells that were replaced, (Wills & Finch, 2016).

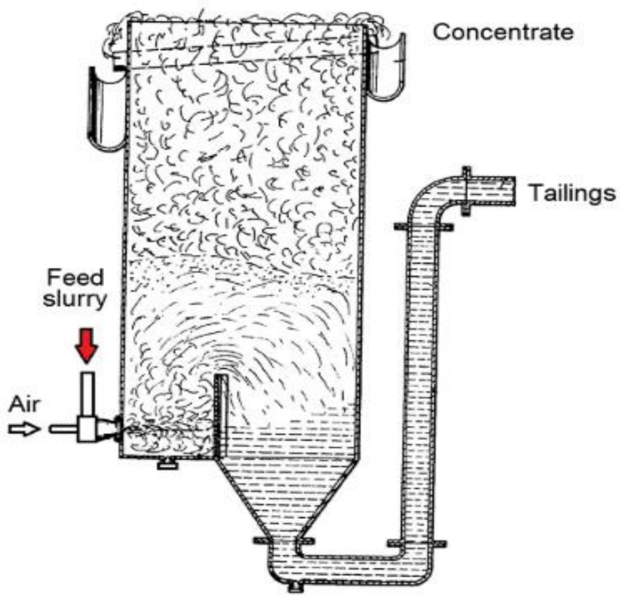


**Figure 2.5: Devcra flotation cell, (Wills & Finch, 2016)**

### 2.2.4 Flotation used in recycling

Flotation is generally an eco-friendly method used for the recycling process. The process utilises a flotation cell to separate the recyclable materials from waste materials. There are quite few literatures based on the flotation used for recycling plastic. A study based on the separation of polyvinyl chloride and polycarbonate from plastic waste by using froth flotation by authors Zhang et al., (2020). The study suggested a novel surface modification by treating these waste plastics with chlorine dioxide prior to the flotation process. Thus, aiding the separation of polyvinyl chloride and polycarbonate from the plastic, (Zhang et al., 2020). The results of the study showed an increase in concentration grade of 99% and recovery of 96% for polyvinyl chloride and polycarbonate respectively.

In a different study, the recycling of PCBs by means of reverse flotation was conducted by authors Yao et al., (2020). The reverse flotation process was used to extract metal particles from the waste PCBs. The metal particles subside and are extracted through the tailings of the flotation cell. The authors conducted an experiment to monitor the flotation performance under different temperatures and collector dosages. The collectors used in the experiment were diesel oil, composite collector, and laurylamine. The result of the experiment showed that diesel oil performed better for non-metal particles than the other collectors, demonstrating that reverse flotation is an efficient solution to the recycling of waste PCBs.

### 2.2.5 Flotation used in waste-water treatment

The most effective methods used for waste-water treatment consist of precipitation, flocculation, and flotation, (Halters et al., 2010). In waste-water treatment, the flotation process is used for the collection and separation of particles. The collection process occurs when particles in the water will have an equal negative surface charge at a pH value below the iso-electric-point. This creates an equilibrium of negative surface charge to the particles allowing them to repel each other and eventually reside. The separation process is used to extract the particles from the wastewater through dissolved-air flotation. The dissolved air is induced into the flotation cell allowing entrapment to occur between the air bubble and particle structure. The particle then floats to the froth layer, where it is extracted by a mechanical skimmer, (Halters et al., 2010).

Authors Halters et al., (2010) conducted a study to optimise waste-water treatment plants. Their method was to use precipitation, flocculation, and flotation as processes to remove aluminium from wastewater. An empirical model was developed based on an experiment that they conducted to maximise the amount of aluminium to be removed. The results of the study led to the amount of polyelectrolyte used in the flocculation process as a deciding factor.

### 2.2.6 Advantages and disadvantages of froth flotation

#### 2.2.6.1 Advantages:

- **Versatile:** Based on the variety of literature the froth flotation process has a vast number of applications in the mineral processing industry. The process has proven to be effective for metallic and non-metallic minerals, allowing the separation of most minerals.
- **Efficiency:** Based on true flotation, the fine sized mineral particles provide a good bubble to particle interaction. This results in greater mineral particle selection. The

efficiency of the process can be improved using a circuit configuration, (Wills & Finch, 2016).

#### 2.2.6.2 Disadvantages:

- **Pollution:** Flotation reagents used in the process consists of chemicals that are harmful to the environment. To reduce the amount of reagent used regular maintenance is conducted on these flotation machines.
- **Expensive:** Industrial flotation machines are considered as extremely complexed and expensive. The process is dependent on flotation reagents and could raise the operations cost based on the reagent dosage required, (Shean & Cilliers, 2011).

### 2.2.7 Factors affecting flotation control

There are some factors listed below to take into consideration for flotation control based on authors (Shean & Cilliers, 2011) and (Wills & Finch, 2016):

#### 2.2.7.1 Mineral composition:

The surface characteristics can be used to categorise minerals as either polar or non-polar. The minerals in the polar category are considered hydrophilic due to their effective reaction with water molecules. The polar category is further subcategorized into five groups but is beyond the scope of this research. Minerals in the non-polar category are considered as hydrophobic due to their weak reaction to water molecules. Although non-polar minerals hardly require any chemical reagents, oil is used to increase the hydrophobicity, (Wills & Finch, 2016).

#### 2.2.7.2 Particle size:

Based on true flotation, particle recovery is dependent on the size thereof. Finer particle sizes are often associated with low recovery due to bad collision efficiencies. Therefore, a decrease in particle sizes results in a decrease in flotation time. As particle size increases, so do the probability of bubble to particle detachment. Coarse particles also see low recovery rates due to detachment. Chemical reagents are used in practice to aid with detachment, (Wills & Finch, 2016).

#### 2.2.7.3 pH:

Flotation takes place on an alkaline medium to stabilize the collectors. The separation process relies on the equilibrium of reagent and pH concentration. The pH regulators such as Lime or Soda Ash are commonly used to regulate pulp alkalinity levels. In practice, these pH regulators are mixed with the slurry before flotation can occur. The alkali serves as a deactivator, precipitation occurs by removing heavy metal ions that can cause the prevention of flotation, (Afolabi et al., 2011).

#### 2.2.7.4 Chemical reagents:

- **Collectors**: Surfactants are used to alter the hydrophobicity characteristics through mineral surface absorption. These surfactants promote with the particle to bubble interaction, by destabilizing the solid-air-water interaction. In practice, collectors are used to reduce the time of inductance.
- **Frothers**: Surfactants used to interact with the air to water interface. In practice, frothers are used to maintain froth stability, to assist and preserve bubbles in the froth layer, and to reduce the velocity at which the bubbles rise.
- **Depressants**: A reagent used to prevent flotation of certain minerals by making them hydrophilic. In practice, they are used to make the flotation process more economical.
- **Activators**: A chemical surface modifier used to interact with the collector rendering it as hydrophobic.

- **Air flowrate:**
  In practice, air flowrate manipulation is used to regulate the entrainment recovery process. The entrainment recovery process is a mechanism used to recover fine particles through water transportation by air bubbles into the froth. A reduction in airflow rate results in a decrease in entrainment, (Wills & Finch, 2016).

- **Wash water flowrate:**
  Wash water is commonly used in column flotation to minimise entrainment and control the froth depth. This strategy is known to be a regular approach towards grade control and is considered as the main advantage of column flotation, (Wills & Finch, 2016).

## 2.3 Control systems in industrial processes

This section of the chapter is focused on the control system strategies available for industrial processes. The first and second parts of this section discuss the Centralized and Decentralized control processes respectively. The third portion of this section will discuss the numerous control system architectures available along with their merits and demerits.

### 2.3.1 Centralized and decentralized control

The modern control theory applied to large scaled systems such are considered as MIMO processes. These MIMO processes often consist of many interacting control loops causing difficulties and complexity to practically implement control of such systems. To address these concerns researchers and engineers proposed various design techniques based on centralized and decentralized control.

The centralized controller approach is considered as highly complexed as the controllers handle the same information as the MIMO process. In practice, these controllers are often challenging to tune and have poor control system integrity. As a result, the decentralized controller approach is usually an engineer's preferred choice. Decentralized controllers offer simple hardware and software realization, an easy-to-understand control structure with fewer controller tuning parameters and the loop failure tolerance can be determined in the design phase, (Xiong et al., 2006). Three different design strategies for decentralized controllers are described by Xiong et al (2006). These strategies are as follows: sequential loop closing, independent design, and detuning strategy. Xiong further states that each strategy has its own merits, however they all have the same flaw. Each strategy relies on the steady-state information of the process, resulting in limitations of the controller's performance.

### 2.3.2 Decentralized control categories:

#### 2.3.2.1 Sequential loop closing

The sequential loop closing is regarded as a popular industrial method used to systematically tune MIMO systems, (Choi, Lee, Jung, et al., 2000). For the sequential loop closing method, an initial control loop is designed and closed for the first pair of inputs and outputs. The closed loop then alters the transfer function of the input and output pairing to the second loop. The second loop is then designed using the adjusted transfer function. All the loops are designed in this sequential manner. The ideology behind the sequential loop closing technique is to design a MIMO control system in a sequence of SISO designs. A transfer function is identified at each step between the input and output pairs, (Choi, Lee, Jung, et al., 2000; Choi, Lee & Edgar, 2000). This allows SISO auto-tuning methods used to design each loop.

#### 2.3.2.2 Independent design

The independent loop strategy has each controller designed based on their corresponding open and closed loop transfer functions. This satisfies the imbalances on the process interaction constraints, (Vu & Lee, 2010). The advantage of having an independent loop design is that the failure threshold of the entire control system is automatically guaranteed. However, the drawback is that the interaction of the controllers in the other loop is not considered.

The effective open-loop transfer function is represented as $g_{xx}^{eff}$, and the controllers as gc1. The effective open-loop transfer function differs from the conventional open-loop transfer function through interaction of other loops via the transmission path, (Vu & Lee, 2010). This allows the MIMO system loops to be considered as independent SISO systems and their effective open-loop transfer functions denoted in the equation below.

$$g_{xx}^{eff} = \frac{g_{xx}}{\Lambda_{xx}} \ldots \tag{2.4}$$

Where:

$g_{xx}^{eff}$ = effective open-loop transfer function

$g_{xx}$ = transfer function

$\Lambda_{xx}$ = the diagonal element of the dynamic RGA

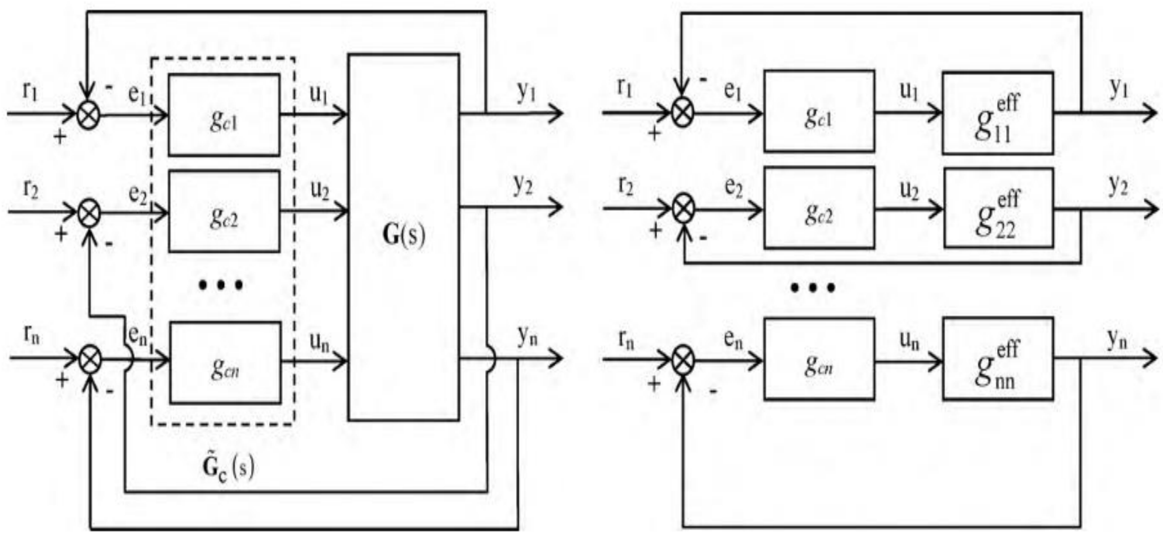


**Figure 2.6:** **Independent loop design with the correspondent EOTFs, (Vu & Lee, 2010).**

#### 2.3.2.3 Detuning

The biggest log-modulus tuning (BLT), strategy is the maximum logarithmic value of a modulus, (Euzebio et al., 2021; Besta & Chidambaram, 2016). The same as RGA, BLT is well known for its consideration of interacting loops of a MIMO system. The controller is designed with the Ziegler-Nichols tuning application for a diagonal transfer function.

To meet the stability criterion of the biggest log-modulus, a detuning factor is introduced. According to authors Besta and Chidambaram (2016), a MIMO system with a loop interaction where $\Lambda_{xx} > 1$, the detuning consists of the reduction of the controller gains and derivative times and addition to the integral times.

Authors often refer to the BLT decentralized controller design approach by Luyben using Internal Model Control (IMC) tuning rules, (Euzebio et al., 2021; Besta & Chidambaram, 2016). The tuning parameter (α) is assumed to be equal to 1, and the IMC settings are calculated using equations 2.5 and 2.6.

$$K_{C,xx-IMC} = \frac{1}{k_{p,xx}}\left[\frac{\tau_{xx}}{\tau_{c,xx}+\theta_{xx}}\right]\ldots \qquad (2.5)$$

Where: $\boldsymbol{\tau_{c,xx} = \alpha\tau_{xx}}$

$$\tau_{I,xx-IMC} = \tau_{xx}\ldots \qquad (2.6)$$

The detuning factor (F) is assumed to be 1.5 for all conditions other than if $\Lambda_{xx} < 1$, then F=0.7. The gains for the diagonal controllers are calculated by equations 2.7 and 2.8.

$$K_{c,xx} = \frac{K_{C,xx-IMC}}{F}\ldots \qquad (2.7)$$

$$\tau_{I,xx} = \tau_{I,xx-IMC}\ \mathrm{X}\ F\ldots \qquad (2.8)$$

The Nyquist plot is used to define the diagonal matrix $G_C$ in equation 2.9 and the closed loop log modulus is defined by equation 2.10. The detuning factor is adjusted until the biggest log modulus LCmax = 2n where n is the order of the system, (Besta & Chidambaram, 2016).

$$W(i\omega) = -1 + \det[I + G(i\omega)G_c(i\omega)]\ldots \qquad (2.9)$$

$$L_{cm}(i\omega) = 20log_{10}\left|\frac{W}{1+W}\right|\ldots \qquad (2.10)$$

### 2.3.3 Control system architecture

There have been numerous publications based on the advancements of control methods over the last 60 to 80 years. One of the earliest forms of advance control was Proportional, Integral, and Derivative (PID). This simple and efficient method of control was considered advanced at the time of its invention. Today the PID is considered a base level with some advanced control methods still being classified under it, (Airikka, 2004). There are various methods used to tune PID controllers, often causing a conflict of which method the designer should use, (Viteckova & Vitecek, 2021).

PID controller tuning methods are either response-based, model-based, or optimal. Response-based tuning method is considered as an experimental approach used in the industry on plants with an extraordinarily complex mathematical model. The Ziegler and Nichols method is known to be popular amongst designers for an experimental approach along with the Cohen and Coon, and relay-based autotuning methods,(Verma & Padhy, 2020). Model-based tuning often uses a frequency-response-based approach or the pole-placement approach. This section aims to explore advanced industrial control strategies.

#### 2.3.3.1 Advance control

Advanced control can be defined as a higher-level control routine that monitors or manages lower-level controllers such as PID and other control loops. In practice, PID would be considered a traditional or classic control. The advance control systems achieve their economic objectives by manipulating the setpoints of these lower-level control loops. This allows the plant to operate closer to its constraints, (Airikka, 2004). According to Airikka, (2004) advance control usually consists of:

- Process model: Generally used to identify process parameters and predict the behaviour of a process.
- Performance criteria: To optimise and evaluate based on process constraints.
- Feedback control

Arikka (2004) also stated that advance control can be categorised into seven control methods, namely:

- Adaptive control
- Multivariable control
- Model-Based Predictive control
- Fuzzy Logic
- Robust control
- Neural network
- Optimal control

#### 2.3.3.2 Adaptive Control method

Adaptive control (AC) is defined as a method used by a controller to alter the controller tuning as changes occur within the dynamics of the process. The control method consists of model reference AC, gain scheduling AC, and auto-tunning AC. Model reference AC matches the closed loop system to a reference model system. This means that the output of the reference model is considered to be the system response. Therefore, the controller can be tuned by adjusting the parameters of the reference model, (Tang et al., 2017).

Auto-tunning AC requires a feedback controller for compensation of the measured process parameters. The auto-tunning process uses the measured control of the feedback controller and process data to create process model parameters. These process model parameters are then used to tune the controller, (Airikka, 2004).

**Table 2.1: Adaptive control advantages and disadvantages**

| Advance control method | Advantages | Disadvantages |
|---|---|---|
| Adaptive control | • A process can operate closer to its constraints for optimal profit. | • Considered more complex as opposed to traditional PID controllers. |
| | • Set different tuning parameters for each setpoint value and adjust them automatically, (gain scheduling). | • Maintenance and repairs can only be done by a technical expert. |
| | • continuously adapt itself to the system behaviour, reducing the need for manual tuning. | • Due to lack of trust AC are limited to the level of direct control over the process itself. |

Adaptive control theory has continued to be a topic of research as it is applicable to numerous industries. A recent study on using a non-linear-L1 adaptive control for a robust flight controller, (Li et al., 2024). Adaptive control has also aided with enhancements of robotic technology, (Liang et al., 2024) Authors Liang et al. (2024) used adaptive dynamic programming control for parallel quadruped robots. Further studies have been conducted with robots for high temperature operations by using adaptive control, (Rudakov et al., 2024). The technology has also found its way into the medical industry. An adaptive control approach of cardiac rhythms for pacemakers has recently been published, (da Silva Lima et al., 2024).

#### 2.3.3.3 Multivariable Control

Multivariable control (MC) is a method with the capability of controlling numerous process inputs and outputs at the same time. These processes are also referred to as multiple-input-multiple-output MIMO systems. This control method contains various control structures and may consist of a combination of control strategies such as PID control with a decoupled matrix. The control can be based on a single compact MC or multiple unit controllers. For the application of multiple unit MC's, compensators are used between unit controllers and process variable inputs. These compensators are used to decouple the interactions between process variables, (Airikka, 2004).

A multivariable process or MIMO process can generally be controlled using decentralized, decoupled, or sparse control method. To determine which control method to select, the interaction between the input and output pairings requires analysis. This can be done by using either a Relative Gain Array (RGA) or Direct Nyquist Array (DNA). RGA identifies the amount of interaction between the input and output pairings using the steady state gains. Whereas DNA determines the dynamic interaction between input and output pairings, (Liu et al., 2019).

**Decentralized control method**

A decentralized control structure is considered as the simplest form of multivariable control due to its diagonal control structure $g_{c,mn}(s)$, as seen in equation 2.11. The diagonal structure allows for easy tuning and closed-loop sequencing. The control structure is based on the control design of a SISO system, where the input and outputs are carefully paired, (Salgado & Conley, 2004).

$$\boldsymbol{G_{Decentralized}(s)} = \begin{bmatrix} \boldsymbol{g_{c1}(s)} & \boldsymbol{0} & \boldsymbol{0} \\ \boldsymbol{0} & \ddots & \boldsymbol{0} \\ \boldsymbol{0} & \boldsymbol{0} & \boldsymbol{g_{c,mn}(s)} \end{bmatrix} \ldots \qquad (2.11)$$

**Decoupled control method**

Decoupled control methodology consists of a full control structure and can be treated as multiple single loops, as seen in equation 2.12. The decoupled control method is generally applied to a centralized controlled MIMO system. The control method can either be static decoupling or dynamic decoupling, (Liu et al., 2019). Static decoupling is developed based on the steady-state gains of the system. The advantage of static decoupling is that the controller can be developed with minimal information. Dynamic decoupling is developed with an accurate process model to improve performance, (Liu et al., 2019).

$$G_{Decoupled}(s) = \begin{bmatrix} g_{c11}(s) & \cdots & g_{c,1n}(s) \\ \vdots & \ddots & \vdots \\ g_{c,m1}(s) & \cdots & g_{c,mn}(s) \end{bmatrix} \ldots \qquad (2.12)$$

**Sparse control method**

A sparse controller structure is an off-diagonal controller, as shown in equation 2.13. The off-diagonal controller, $g_{c,mn}(s)$ allows for improved performance without increasing the structure complexity while maintaining the integrity of the control system, (Shen et al., 2010). The sub controller $K_{mn}$ allows the controller to cope with the coupling effects as opposed to the decentralised controller, (Liao & Sun, 2021).

$$G_{Sparse}(s) = \begin{bmatrix} g_{c1}(s) & \cdots & K_{1n} \\ \vdots & \ddots & \vdots \\ K_{m1} & \cdots & g_{c,mn}(s) \end{bmatrix} \ldots \qquad (2.13)$$

**Table 2.2:** Multivariable control advantages and disadvantages

| Advance control method | Advantages | Disadvantages |
|---|---|---|
| **Multivariable control** | • Exceptional performance for processes with multiple variable interactions. | • Non-adaptable making it susceptible to processes that vary over time. |
| | • Uses more than one control structure, for example, a PID controller with a decoupled matrix. | • Inability to cope with non-linear processes consisting of variable dead time. |
| | • Valid for linear and most nonlinear systems | • The controller is highly sensitive to process modelling errors. |

Multivariable control has made its way into the CNC machine tool industry by enhancing the speed and precision, (Wang & Hsiao, 2024). Authors Wang & Hsiao (2024) proposed a concept for precision control of flexible feed drives using multivariable iterative learning. The theory of multivariable control is applied in Microgrids by decoupling the voltage and current control loops, enhancing transient response and power delivery,(Srikanth et al., 2024). Yu et al. (2024) proposed a cooperative control strategy for multivariable coupled systems.

#### 2.3.3.4 Model Predictive Control

The concept of Model predictive control (MPC) was initially introduced using climate control in 1974, (Martín-sánchez, 2014). A basic block diagram of the MPC concept can be seen in Figure 2.7. Predictive control uses a mathematical model to predict the process output behaviour over a fixed period, this is known as the predictive model. This fixed period is also known as the prediction period, where the controller outputs are required to achieve the predicted process output. The driver block is responsible for generating the desired trajectory for guiding the controller output towards the desired set point without any offsets or oscillations, (Martín-sánchez, 2014).

Based on the method used, process models can be created using either step response, impulse response, or transfer functions. The two most popular methods of MPC's are known as the general predictive control (GPC) or dynamic matrix control (DMC), (Airikka, 2004). For optimal performance of MPC controller dynamic models are often preferred, (Airikka, 2004).

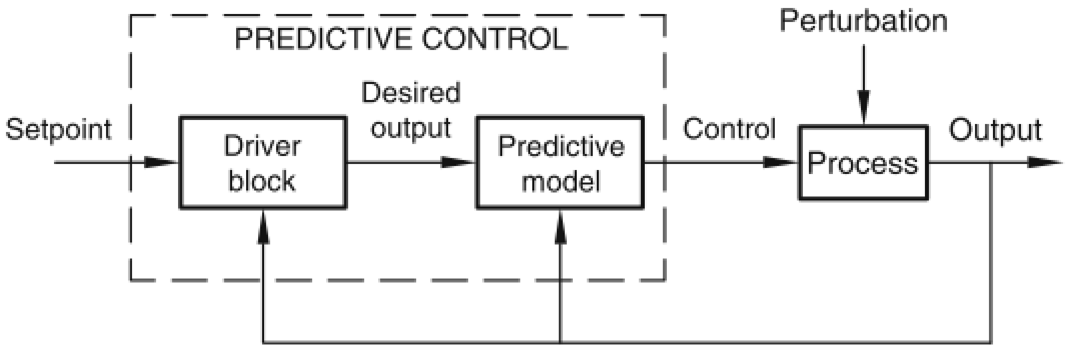


**Figure 2.7:** **Basic MPC block** diagram**, (Martín-sánchez, 2014)**

**Table 2.3:** **MPC advantages and disadvantages**

| Advance control method | Advantages | Disadvantages |
|---|---|---|
| MPC | • The controller can operate closer to constraints | • The controller is susceptible to process modelling errors. |
| | • Multivariable interaction and control | • Poor performance under varying dead-times due to computational load |
| | • Control of dead-time dominant processes and dynamic changes | • Poor performance with non-linear models due to high value of control parameters |

An MPC based control strategy to improve the control of harmonic current in a distribution network was proposed by Jiang et al. (2024). The MPC theory was also implemented in the trajectory tracking control of autonomous vehicles, (J. Zhang et al., 2024). Authors Zhao et al. (2024) proposed a bilinear Koopman MPC for nonlinear dynamic systems. Further enhancements in MPC lead to the preposition of Diffusion MPC by combining multistep action and dynamics for online MPC implementation, (G. Zhou et al., 2024).

#### 2.3.3.5 Fuzzy Logic control

Fuzzy logic (FL) control is a smart control system that mimics human logic, making it a more appropriate solution to control problems. In contrast to Boolean logic, which is either true or false, fuzzy logic represents a range of infinite reasoning. Fuzzification, fuzzy rules, reasoning, and defuzzification are the three stages of control. To produce an FL control signal, the measured process variables are divided into fuzzy logic variables during the fuzzification stage. The integrated process model description is used to perform fuzzy control at the fuzzy rules and reasoning step. The defuzzification stage involves converting the fuzzy control signal into a form that can be understood.

An equalization method for lithium-ion batteries was introduced by authors Wu et al., (2021). The controller inputs were the difference of the state of charge average between two batteries $U_{dif}$ and the state of charge difference of the batteries in equilibrium ΔU. The FLC reduces equalization time and energy loss by dynamically adjusting the equalization current $I_{equ}$.

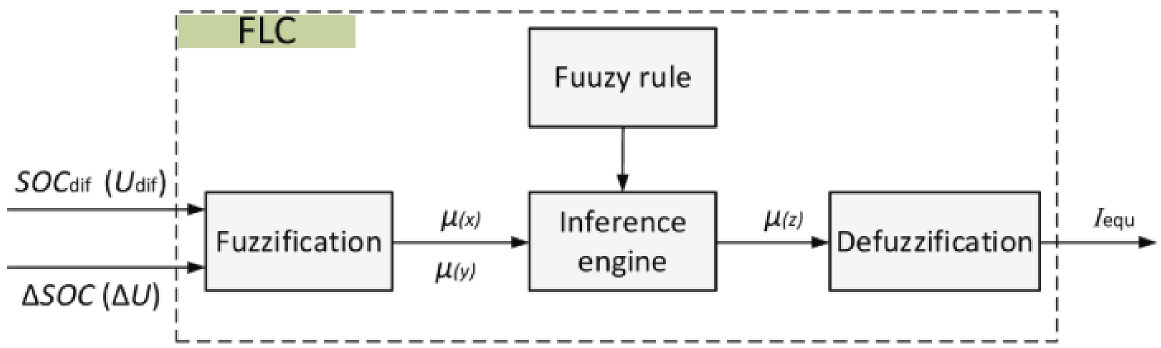


**Figure 2.8:** **FLC of an equalization methodology for lithium-ion batteries, (Wu et al., 2021)**

**Table 2.4:** **Fuzzy Logic advantages and disadvantages**

| Advance control method | Advantages | Disadvantages |
|---|---|---|
| **Fuzzy Logic** | • Good performance for non-linear time-invariant systems. | • Difficult to test and validate. |
| | • Combined with additional controllers. | |

Recent publications on fuzzy logic control have explored its use as an alternative approach in psychological scoring, (Kyriazos & Poga, 2024). The technology has also been explored in the implementation of evaluating the academic progress of students, (Nabiel Algshat, 2024). A study on smart home automation advancements using fuzzy logic systems has been presented by (Ferreira et al., 2024). Authors Sasi et al. (2024) proposed a fuzzy logic controller design of a maximum power point tracker (MPPT) for a Photovoltaic System.

#### 2.3.3.6 Robust control

The control of unknown plants and unclear process dynamics and disturbances is referred to as robust control. In contrast to other advanced control methods, the robust control method leverages these unknown variables or dynamics as controller design parameters. As a result, process modifications that were considered in the design have reliable and robust stability and performance. Robust controls are frequently constructed with the worst-case scenario in mind to maintain a level of acceptance if something goes wrong, (Airikka, 2004).

**Table 2.5:** **Robust control advantages and disadvantages**

| Advance control method | Advantages | Disadvantages |
|---|---|---|
| **Robust** | • Adaptable to process and process dynamic changes | • Mathematically complexed |
| | • Reliable | |
| | • High quality | |

Recent publications have been based on the Robust controller's performance under non-linear conditions. Ahmed et al. (2024) explored the concept of a non-linear robust control application on a six-phase induction machine. A damping parameter has been introduced to manage distributional shifts in robust control and gain scheduling, (Ramadan & Anitescu, 2024). Z. Zhang et al. (2024) proposed a robust control approach using the Smolyak algorithm for implementation on quantum systems subject to uncertainties or disturbances. Another study in quantum systems is the optimal control against detuning error, (Kukita et al., 2024).

#### 2.3.3.7 Neural network control

Neural network control is used as an identification tool for non-linear systems and is rendered ineffective for non-linear and complex system estimation. The most common structure used for neural network controllers is called multi-layer perception. The structure consists of three layers: input; hidden; and output layer. Each layer is linked respectively and comprehends neurons with activation and summing elements, along with weights for the signal that links between layers. The number of neurons used in each layer is dependent on the developer's expertise and process trial and error, (Airikka, 2004).

**Table 2.6:** **Neural network control advantages and disadvantages**

| Advance control method | Advantages | Disadvantages |
|---|---|---|
| Neural network | • Good performance for non-linear systems | • Complex algorithm |
| | • model estimation | • Hardware dependent |
| | • robust due to learning methods | |

Neural network control is explored across numerous disciplines; however, this research will only focus on its engineering applications. A recent publication on the health status prediction of a turbofan engine using artificial neural network, (Szrama, 2024). For geotechnical research a clustered artificial neural network is proposed by Alsamia & Koch (2024) to improve contaminant dispersal prediction. Advancements in biomedical engineering has utilized neural network to forecast the incidence rate of cancer through in-depth learning and oncology,(Y. Liu et al., 2024)

#### 2.3.3.8 Optimal control

Optimal control is defined as the optimization of the performance criteria for the process dynamics over time until the point when the process is optimized. The methods used for optimization and performance criteria may differ. Linear quadratic control attempts to reduce the combination of control actions and errors based on the design parameters. Linear quadratic Gaussian control has a similar control function but is more effective against process disturbance and noise, (Airikka, 2004). Table 2,7 presents the advantages and disadvantages of the Optimal control method.

**Table 2.7: Optimal control advantages and disadvantages**

| Advance control method | Advantages | Disadvantages |
|---|---|---|
| Optimal control | • Used for Multivariable interaction process | • Sensitive to model errors |
| | • Easy to tune based on performance criteria | • Challenging when conducting maintenance |
| | | • Hardware Dependant |

Recent advancements in optimal control technology have seen developments based off implementation of non-autonomous second order stochastic differential equations,(T. Liu et al., 2024). For wind turbine applications authors T. Liu et al. (2024) proposed an optimal controller intended for yaw system vibration and crawling jitter. Authors S. Zhang et al. (2024) explored the method of implementing optimization control on a D-shaped cylinder used in aerospace engineering. A study promoting effective process automation and plant reliability through optimal control is mentioned by Emmanuella Onyinye Nwulu et al. (2023).

The control systems used and put into place during the flotation process are discussed in the section that follows.

## 2.4 Control system applications in the flotation process

This section of the chapter is focused on discussing the available literature for controllers designed specifically for the flotation process. The hardware commonly used in industrial applications of flotation systems is also mentioned. The challenges and limitations of applying a decentralized controller are discussed at the end of this section.

### 2.4.1 Control systems in flotation:

#### Decentralized controller applications in flotation control

The Decentralized control approach is popular amongst researchers to achieve optimal control of a column flotation cell, (Kämpjärvi & Jämsä-Jounela, 2003). The decentralized control approach was applied as a strategy to control the level of a flotation cell by authors Kämpjärvi & Jämsä-Jounela (2003). Kämpjärvi & Jämsä-Jounela further stated that in order to better the performance of a flotation column to the level control. Their research entailed a series of six flotation cells consisting of four different control strategies. The objective of the study was to compare three existing strategies with respect to cell level control and introduce an additional strategy. The three existing strategies were SISO and two MIMO. Special performance indices were used to compare the mentioned control strategies. As a result the SISO strategy which consisted of a feedforward control loop performed against MIMO strategies which were decentralized controllers.

Persechini et al, (2004) presented a decentralized control strategy for a column flotation process. The control technique consisted of three controlled variables which are the froth layer height, air holdup in the collection zone, and bias rate. The manipulated variables were the wash water, air, and non-floated fractional flow rates. By using RGA to determine loop pairings between controlled and manipulated variables. A PI controller was designed based on the RGA analysis. The strategy was validated on a pilot-scaled model of the flotation column.

A decentralized PI controller approach using the decoupling method instead of RGA was proposed by (Tshemese-Mvandaba et al., 2021). The objective of their research was to improve the decentralized PI control design procedure by introducing the decoupling of the interconnecting control loops. The controlled variables are namely the froth layer height and gas holdup in the collection zone. The manipulated variables are the wash water and gas flow rate respectively. The closed-loop responses of both the coupled and decoupled controller design were simulated and analysed using the MATLAB/Simulink environment. As a result, the decoupled decentralised controller designed did show some improvements in steady state error. The interconnecting control loops displayed minimal effect on the transient behaviour.

### Literature table of column flotation control

This section lists a few available works based on column flotation control over the past 20 years. Table 2.8 shows published articles dating back to 2005 relevant to column flotation control. The table can be broken down into the aim or objective of the author's research, the type of processing plant, the control design methodology as well as the findings of the authors' research.

Table 2.8: **Literature table of column flotation control**

| | **Author(s); year; *title*** | **Aim** | **Plant** | **Control design method** | **Results and Findings** |
|---|---|---|---|---|---|
| 1 | Ding Wang, Mingming Ha, Junfei Qiao, Jun Yan & Yingbo Xie; 2020; *Data-based Composite control design with critic intelligence for a wastewater treatment platform* | To achieve an optimal controller capable of critic learning and wastewater verification. | Wastewater treatment | Neural network | The dissolved oxygen concentration and nitrate level can be accurately achieved. However, this control design method requires complex algorithms and high processing power to design and implement. |
| 2 | S. Revollar, R. Vilanova, P. Vega, M. Francisco & M. Meneses; 2020; *Wastewater Treatment Plant Operation: Simple Control Schemes with a Holistic Perspective* | To improve the overall efficiency of a wastewater treatment plant using the control method approach, | Wastewater treatment | Proportional+Intergral | A feasible solution for the optimisation of nitrate elimination and energy consumption. Maximum efficiency requires cascaded control. |
| 3 | Maria M. Papathanasiou, Styliani Avraamidou, Richard Oberdieck, Athanasios Mantalaris, Fabian Steinebach, Massimo Morbidelli, Thomas Mueller-Spaeth, Efstratios N. Pistikopoulos; 2016; *Advanced control strategies for the multicolumn countercurrent solvent gradient purification process* | The development of a control strategy to optimise the efficiency of the multicolumn counter current solvent gradient purification process. | Monoclonal antibody production | MPC-SIMO | The controller is immune to flowrate variation and achieves setpoints without any offsets. |
| 4 | F.B. Sanchotene, G.M. de Almeida & J.L.F. Salles; 2011; *Robust predictive controller of the mold level in a steel continuous casting process* | To reduce the effects of external disturbances and unspontaneous noise on mold level control. | Continuous steel casting process | Hammerstein Generalized Predictive Controller, Type of MPC | Eliminates mold level fluctuations caused by bulging and clogging. Eliminates noise on the signal applied to control valves. However, the controller is tuned by generic |

| | | | | | |
|---|---|---|---|---|---|
| | | | | | algorithms. Fluctuations caused by bulging are only stable between 0,02m to 0,001m |
| 5 | M. Maldonado, A. Desbiens, R. del Villar; 2009; *Potential use of model predictive control for optimizing the column flotation process* | To optimise column flotation control by manipulating the secondary variables such as Froth depth, collection zone gas-holdup and bias rate. | Mineral Processing Flotation | MPC to control local PID loops. | The authors were able to reduce tracking errors of gas-holdup and bias rate without affecting the operating constraints. This is only achieved by not assuming any steady-state conditions for real-time optimisation. |
| 6 | Danny Calisaya, Éric Poulin, André Desbiens, René del Villar, Alberto Riquelme; 2012; *Multivariable Predictive Control of a Pilot Flotation Column* | To achieve control of the hydrodynamic variables of a three-phase column flotation system under industrial conditions | Mineral Processing Flotation | Multivariable control | The controller demonstrated its effectiveness for set-point tracking and disturbance rejection. However, the effectiveness of the controller is dependent on the algorithm's constraints. |
| 7 | Luis G. Bergh & Angélica León R.; 2005; *Simulation of Monitoring and Diagnosis of Flotation Columns Operation Using Projection Techniques* | The demonstration and identification of abnormalities in variable measurements under operating conditions with the use of projection tools. | Mineral Processing Flotation of Copper | DCS using the Principal Component Analysis technique | The technique demonstrates the ability of preserving data quality through mathematical dimension reduction. The limitation of this technique is based off the measurement instruments used to collect the data. |
| 8 | J.D. le Roux; I.K. Craig; 2019; *State controllability of a froth flotation cell* | To maximise the mineral separation process and maintain pulp level stability. | Mineral Processing Flotation | MPC using phenomenological mathematical modelling. | The controller displays clear mathematical relations to the variables and indicates their controllability. However, the model shows no indication of the magnitude, period, or direction of the control action. |
| 9 | Xiaodong Xu, Yahui Tian, Yuan Yuan, Xiaoli Luan ,Fei Liu , Member, and Stevan Dubljevic; 2021; *Output Regulation of Linearized Column Froth Flotation Process* | To investigate the solvability of partial differential equations (PDEs) and ordinary differential equations (ODEs) with time delay. Development of a state feedback and error feedback controller. | Column froth flotation process | Coupled Adaptive Control, philosophical modelling | Successfully designed state feedback and error feedback regulators with satisfactory reference output tracking capabilities. The process however is highly complex consisting of a $6^{th}$ order state space model. |

| | | | | | |
|---|---|---|---|---|---|
| 10 | N. Tshemese-Mvandaba, R. Tzoneva, M. E. S. Mnguni; 2021; *Decentralised PI controller design based on dynamic interaction decoupling in the closed-loop behaviour of a flotation process* | The proposition of an improved strategy for decentralized PI control using the decoupling technique. | Column froth flotation process | Decentralized Decoupled PI control (Multivariable Control) | The design was proven successful in terms of decoupling a multivariable process and easily implementing a PI controller onto the plant. The controller also demonstrates satisfactory setpoint tracking and disturbance rejection. |
| 11 | B. Shean, K. Hadler and J.J Cilliers, 2017; *A flotation control system to optimise performance using peak air recovery* | To develop a Peak Air Recovery controller and implement it using a laboratory flotation cell. | Column froth flotation process | Gathering Set Search Algorithm (GSS) Optimal Control | The GSS controlled system showed that PAR is obtainable and maintained under the conditions that air recovery varies over time. |
| 12 | Tsave P.K, Kostoglou M., Lazaridis N.K., Karapantsios T.D.; 2024; *Hydrodynamic Study of Hybrid Electro-Flotation Column* | To eludicate the characteristics of the gas phase of a hybrid flotation system. | Column froth flotation process | Regulatory Control and Image processing | The study shows that as bubbles decrease in size the closer, they get to the column walls, this leads to an increase in frother concentration proportional to the column fraction increase. The scattered light optical approach used to determine bubble size and quantity detected changes in the energy of the light source as the frother concentration increased. This is due to diffusion over the large quantity of smaller bubbles. |
| 13 | M. Azhin, K. Popli, V. Prasad; 2020; *Modelling and Boundary Optimal Control Design of Hybrid Column Flotation.* | To develop an LQR based Optimal controller design for a hybrid column flotation. | Hybrid Column and Mechanical Flotation Process | Optimal Model based controller (LQR based) | The LQR based controller outperforms conventional PI-based control substantially by achieving a steady state after perturbation in the initial condition. |
| 14 | Alhuseen, Hayder & Abdulrazzaq, Nada & Sedev, Rossen; 2023; *Flotation of Chromium Ions from Simulated Wastewater Using Air Microbubbles.* | To remove chromium ions from simulated wastewater using microbubbles flotation method. | Wastewater treatment | Optimal Control | The results indicated an increase in chromium ion removal from simulated wastewater of up to 95%. The study also concluded that the appropriate pH range can increase the percentage recovery of chromium ions. In addition, the gas flow rate has the potential to increase the recovery ratio by 1:2. |
| 15 | Xu, Xiaodong & Dubljevic, Stevan; 2021; *Robust tracking control of* | To develop a robust regulator for a column flotation process with the | Column flotation process | Robust Controller using phenomenological mathematical modelling. | The hyperbolic partial differential equation is used to set the system boundaries while accounting for the |

| | | | | | |
|---|---|---|---|---|---|
| | *column froth flotation process with an unknown disturbance.* | ability to tolerate unknown disturbances. | | | flotation column's transfer delay to move between the froth and collection zones. The feed flow rate is regarded as the system input, and the concentration of solid particles with air is the system output. The suggested regulator showed resilience by performing adequately in the face of disruptions. |
| 16 | R. Flores-Campos, R. H. Estrada-Ruiz, M. Rodríguez-Reyes, D. Martínez-Carrillo, A. Martínez-Luévanos; 2024*; Concentration of Silver from Recycling of Fine Powder of Wasted Videogame Printed Circuit Boards through Reverse Froth Flotation and Magnetic Separation Processes.* | To use reverse flotation and magnetic separator equipment to recover a concentration of silver. | Recycling of Printed Circuit Boards | Optimal control using mass balance equations | The results showed that preconditioning the pulp with MIBC plus and oleic acid reagents produced the best separation of silver fractions. An increase in dosage led to an increase in recovery because it showed that hydrophilic particles were entangled with hydrophobic particles. |

### 2.4.2 Industrial hardware implementation:

For the past 20 years, researchers have been focused on the development of sensors for measuring the following variables of a flotation column: pulp-froth interface position, the bias rate, the gas holdup, the bubble diameter and distribution, and the bubble surface area flux. According to del Villar et al., (2010) the bubble diameter and distribution, and the bubble surface area flux sensors were developed by researchers from McGill University. Whereas the pulp-froth interface and bias rate sensors were developed by the Université Laval. All 5 sensors are briefly discussed in the following subsection.

**Pulp-froth interface position sensor**

This sensor is commonly used in industrial flotation plants to measure the Froth depth. A float sensor coupled with an ultrasonic sensor is the usual configuration due to its ease of implementation. The dual sensor configuration ensures that no electronic interaction occurs with the pulp. Despite having limited accuracy due to the assumption of the froth and pulp density and the accumulating solids on the float gauges being neglected, the sensor is deemed satisfactory by engineers and practitioners.

The use of pressure gauges is also used to determine the Froth depth. Multiple pressure transducers are used to provide additional information required to estimate the average value of both froth and pulp density. A transducer is placed in the froth zone (upper region of the cell) and another transducer in the collection zone (middle to lower region of the cell), with the assumption that the gravity remains uniform in each zone. This assumption may occasionally lead to incorrect results in froth depth estimation. To address this issue researchers focused on the intensive properties of the pulp, taking into consideration the conductivity and temperature profiles.

**Bias rate sensor**

There are two different strategies by which the bias rate can be estimated in a flotation column. The first strategy utilizes the mass-balance of either zone of the column and measures external flowrates to measure the bias rate. The second strategy uses internal variables measured near the pulp-froth interface for the bias rate estimation. According to del Villar et al., (2010), both strategies of bias rate estimation are dependent on the change in water content of the column’s upper region (Froth zone) resulting in a change in bias rate. For the first strategy, a magnetic flow and gamma-ray density meter are each installed into the column’s feed and tailing streams. Regardless of the expensive instruments used, the estimation accuracy is rendered as poor seeing that the bias rate is a small value calculated by two large quantities (the feed and tailings flow rates). As a result, this strategy is mainly used for calibration or auditing and under cautiously sustained steady-state conditions.

**Gas holdup sensor**

There are three methods available to determine the air/gas holdup in the collection zone of a flotation column. These three methods are based on differential hydrostatic pressure, electrical conductivity, and sound detection. Differential hydrostatic pressure is a technique that requires two hydrostatic pressure measurements at different points in the collection zone. The gas holdup is estimated using the corresponding pressure values, distance, and the pulp's average density between transducers. This method is vulnerable to errors due to the assumption that the feed and tail densities are constant.

The second approach uses Maxwell's equation for a mixture of dispersed air (non-conducting phase) within the pulp (the continuous conducting phase). For this approach, the electrical conductivity is related to either phase concentration. The gas holdup is evaluated using the conductivity of the pulp-to-air mixture and the conductivity of the pulp alone. This method reveals the same concerns as that of the differential hydrostatic pressure method where the measurement of the pulp density is required.

The third approach for gas holdup measurements is known as a sound detection method. This method was initially developed to measure the gas flow rate but evolved into a method of detecting the quantity of air entrained in a slurry pipe. The sonar flow meter measures the volumetric flow rate by detecting turbulence (also known as eddies) within the flow of fluid. This is done by evaluating the speed at which sound would propagate through this fluid. The sensors that are installed on the exterior wall of the tube converts the dynamic tension induced by the "eddies" into electronic signals. These electronic signals are interpreted based on the characteristics of frequency and phase of the "eddies" and the prior processed data to calculate the volumetric flow.

**Bubble size distribution sensor**

The first bubble size distribution sensor was developed at the University of Cape Town, (UCT) in 1989. The sensor pertained to a riser tube and a glass capillary tube placed inside a water reservoir. A portion of the bubbles that reach the reservoir are drawn to the capillary tube using a peristaltic pump. Once in the tube, the bubbles are transformed into cylinders where the length and velocity can be measured using two pairs of photo-transistor LED detectors. The overall volume of gas collected is used to estimate the absolute bubble size. This sensor is however limited to a maximum bubble size due to the diameter of the capillary tube. Modern bubble size distribution sensors now rely on bubble image processing to determine the bubble diameter.

**Superficial gas velocity sensor**

The superficial gas velocity is defined as the ratio between the volumetric gas rate and the cross-sectional area of the device. The purpose of this device is to detect poor gas distribution or sparger malfunctions within flotation cells. The sensor is based on a submerged tube in the aerated pulp and vacuum system to guide gas into a mass flow meter. However, regular commercial flow meters may be configured for these particular measurements within the flotation column to provide sufficient process control.

### 2.4.3 Challenges and limitations in decentralized control

The Decentralized PID control approach is often the preferred approach to feedback control of a flotation column. This is mainly due to the multivariate nature of the flotation process. The process is decentralized by coupling variables as SISO control loops, with one variable manipulated to control the other variable. One drawback mentioned by Hodouin (2011) is the ability to accurately model the system. The author mentions that the empirical method does come with some flaws. The empirical modelling method is dependent on the system measurements which opens the possibility to measurement noise, plant dynamic change, and control loop interactions. Hodouin (2011) uses a grinding circuit which is PID controlled as an example. In this example, Hodouin highlights that the loop interaction could be partially eliminated with the use of decoupling methods applied to the decentralized control architecture. These decoupling methods require further process modelling activities. An additional highlight to this example is to not tune a non-critical variable (Sump level) too strictly and allow it to be more tolerant and waver along the set point.

## 2.5 Emerging technologies and future trends

Prior sections have indicated a substantial amount of work done in academic research and development into sensor technologies and control strategies for the column flotation control process. Despite these improvements, the industrial implementation is quite limited, (del Villar et.al, 2010). According to del Villar et.al (2010), for the industry to benefit from academic advances, a partnership is required between researchers and equipment and service suppliers. These partnerships could improve the current process supervision by making flotation column sensors more practicable and dependable.

### Flotation control and process optimization

A recent trend in developments in flotation process control is directed at the online evaluation and modelling of the bubble size distribution (BSD) within the collection zone, (del Villar et.al, 2010). A key factor of the flotation process is the dispersion properties of gas, or the bubble surface area flux. The bubble surface area flux is directly proportionate to the flotation rate constant, making it a viable control variable for achieving the desired metallurgical result.

Authors H. Zhou et. al (2024), published a paper on the bubble size distribution and its effect in a wide slab caster mold. Their research consists of a three-phase fluidised bed flotation column design in a semi-industrial environment. The flotation column design had a shear effect of a variable liquid velocity and static bed height to assess the creation of bubbles from the shear. The results of the study indicated that the filing bed height has a strong relationship with the strengthening effect of the reduction of bubble size diameter. This is caused by the effect of the filling bed height on the apparent gas velocity, which in turn directly impacts the bubble diameter.

The effect of static pressure on bubble size and contact angle inside a hypothetical flotation column was investigated in research conducted by the authors A.V. Oliveira et.al, (2023). For this study, the hypothetical column flotation cell walls are mimicked by applying a pressure range in contradiction to the bubbles. Their results demonstrated that a decrease in hydrostatic pressure promotes a decrease in contact angle within the collection zone of the cell. In addition, a bubble diameter increases results in a bubble ascending velocity increase. Resulting in a higher rate of coarse particle detachment from the bubbles in the upper region of the hypothetical flotation column. Table 2.9 below shows all the recent publications since 2021 related to bubble size distribution of a flotation column.

**Table 2.9:** **List of recent publications on Bubble Size Distribution**

| | Author | *Title* | Year | Reference |
|---|---|---|---|---|
| 1 | Haichen Zhou; Wenyuan He; Chenxi Ji; Baisong Liu; Xiaoshan Yang; Haibo Li; Wenliang Dong; Liubing Jia | *Mathematical modelling of the effect of SEN outport shape on the bubble size distribution in a wide slab caster mold* | 2024 | (H. Zhou et al., 2024) |
| 2 | Polyxeni Tsave; Margaritis Kostoglou; Nikolaos K Lazaridis; Thodoris D. Karapantsios | *Hydrodynamic Study of a Hybrid Electro-Flotation Column* | 2024 | (Tsave et al., 2024) |
| 3 | Mao Yin; Ning Han; Ting Yang; Yanfeng Li | *Study of a Novel Fluidized Bed Flotation Column with Enhanced Bubble Dispersion* | 2024 | (Yin et al., 2024) |

| | | | | |
|---|---|---|---|---|
| **4** | Claudio Leiva; Claudio Acuña; Saija Luukkanen; Constanza Cruz | *Enhancing bubble bize prediction in flotation processes: a drift flux model accounting for frother type* | 2024 | (Leiva et al., 2024) |
| **5** | Alexandre Oliveira; Jose Tadeu Gouvêa Junior; Thiago Souza; Laurindo Leal Filho | *The Influence of Static Pressure on Bubble Size and Contact Angle of Quartz: Mimicking What May Happen Inside a Hypothetical Flotation Column* | 2023 | (Oliveira et al., 2023) |
| **6** | Polyxeni Tsave; Margaritis Kostoglou; Nikolaos K Lazaridis; Thodoris D. Karapantsios | *Enhancing Fines Recovery by Hybrid Flotation Column and Mixed Collectors* | 2023 | (Tsave et al., 2023) |
| **7** | Xiangning Bu; Shaoqi Zhou; Meng Sun; Muidh Alheshibri; Shakhaoath Khan; Guangyuan Xie; Saeed C. Chelgani | *Exploring the Relationships between Gas Dispersion Parameters and Differential Pressure Fluctuations in a Column Flotation* | 2021 | (Bu et al., 2021) |
| **8** | Rasoul Panjipour; Mohammad Karamoozian; Boris Albijanic | *Bubble size distributions in gas–liquid–solid systems and their influence on flotation separation in a bubble column* | 2021 | (Panjipour et al., 2021) |

An additional field of interest to flotation process control is the correct utilization of frother dosage as a control variable. Authors del Villar et.al (2010), further states that it is proven effective for frother content to affect both the froth and collection zones. In a flotation process frothers are known to alter bubble size in the collection zone and stabilize the froth layer. Thus, considering frother concentration as an adequate secondary control variable.

Authors Celayn et. Al, (2024) recently published an article based on the effects of frother content within a column flotation cell. The focus of the article is to assess the relationship between bubble size and flotation performance with the use of two unique copper ores differing based on their frother dosage. To evaluate the cell's performance, the bubble size was measured in a lab using industrial scales. The researchers concluded with the discovery that the frother is largely responsible for bubble size and copper grade reduction.

One more article published by Zinjenab et.al, (2024) attempts to improve the recovery of ultrafine particles with the use of water containing nanobubbles. These particles are namely zinc and lead minerals. Their theory is to use two separate industrial grade flotation column designs to optimize the volume of water for pulp preparation with nano-bubbled water. Potassium ethyl canthate, potassium amyle xanthate, and frother dosage were also optimized for each concentrate. Their study shows that frother dosage had the most influence in increasing the recovery of both zinc and lead to some degree. Other publications can be seen in Table 2.10 below.

**Table 2.10:** Literature table for frother dosage

| | Author | *Title* | Year | Reference |
|---|---|---|---|---|
| 1 | Adnan Ceylan; Ş. Beste Aydın; Ferihan Göktepe ; Gülay Bulut | *Relation of bubble size, grade and recovery in the copper flotation systems* | 2024 | (Ceylan et al., 2024) |
| 2 | Zahra Taghavi Zinjenab; Ebrahim Azimi; Mahdi Shadman; Mohammad Raouf Hosseini | *Maximization of ultrafine poly-mineral ore sequential flotation recovery through synergistic effect of conventional and nano-size bubble combination* | 2024 | (Taghavi Zinjenab et al., 2024) |
| 3 | Cassandra Austen I; K. Chennakesavulu; G. Ramanjaneya Reddy; N. Vasumathi; Ajita Kumari; Mousumi Gharai; T. Anurag Kumar; T. V. Vijaya Kumar | *Utilizing a sustainable surfactant from Cucurbita pepo seeds for eco-friendly flotation of non-coking coal in sustainable energy applications* | 2024 | (I et al., 2024) |
| 4 | P. Doubra; C. Carelse; D. Chetty; M. Manuel | *Experimental and Modelling Study of Pt, Pd, and 2E+Au Flotation Kinetics for Platreef Ore by Exploring the Influence of Reagent Dosage Variations* | 2023 | (Doubra et al., 2023) |
| 5 | Hao Huang, Xiao Yang, Zhongxian Wu, Bo Qiao, Guangxi Ma, Huaizhi Shao, Dongping Tao, | *An investigation of nanobubble enhanced flotation for fly ash decarbonization* | 2023 | (Huang et al., 2023) |
| 6 | K.C. Syrmakezis, K.G. Tsakalakis, I.P. Sammas | *Valorisation of base metals contained in fine particles of End-of-Life Printed Circuit Boards with the use of column flotation process* | 2023 | (Syrmakezis et al., 2023) |
| 7 | Alsafasfeh, A., Alagha, L. and Al-Hanaktah, A. | *The Effect of Methyl Isobutyl Carbinol "MIBC" on the Froth Stability and Flotation Performance of Low-Grade Phosphate Ore* | 2024 | (Alsafasfeh et al., 2024) |
| 8 | Bilir, Kemal | *Investigation of the Entrainment of Fine-Sized Calcite and Chromite Particles By A Flotation Column With Negative Bias Regime* | 2021 | (BİLİR, 2022) |
| 9 | Ceylan, Adnan & Bulut, Gülay. | *Investigation of the Frother Effect in Two and Three Phases Systems on Bubble Size, Surface tension, Recovery and Grade in Chalcopyrite Flotation.* | 2022 | (CEYLAN, 2021) |

The next section is a brief discussion based on the modern literature available with similarities to the study mentioned in this thesis. More focused on the secondary controlled variables such as froth layer height, gas holdup, and bias rates of the flotation column process. Also identifying the decentralized control processes used to archive flotation control.

## 2.6 Discussion

(Persechini et al., 2004) implemented a decoupling controller consisting of a multivariable system. The authors used a 3x3 transfer function matrix to represent the dynamics of the process. The controlled variables were the froth depth, air holdup in the collection zone, and the bias. The manipulated variables were the wash-water flow rate, air flow rate, and tailing flow rate. A Relative Gain Array (RGA) analysis was used for the steady-state to determine the loop interactions. The RGA method indicated that the best variable pairing for column flotation control are froth depth and wash water; air holdup in the collection zone and the air flow rate; and the bias and the tailings flow rate. This method also demonstrates a relationship between the collection zone height and the bias rate. For high air flow rate application, the froth depth might become unstable and could lessen without any external interference,(Maldonado et al., 2009).

Authors Maldonado et al., (2009) proposed a constrained Model Predictive Control (MPC) with the same variables used by Persechini et al., (2004). Their approach was to use a MIMO 2x2 MPC scheme for the air holdup in the collection zone and the bias rate. The froth depth was controlled by a traditional PI controller due to the lack of loop interaction. The objective was to reduce the tracking error of air holdup and bias rate by maintaining the airflow, wash-water, and bias rate within their operational limits. The MPC strategy may benefit the optimization of the column flotation process if the assumptions of the steady-state conditions in real-time optimization are disregarded. Despite the availability of optimisation control methods, numerous mineral processing plants rely on manual control of lower-level systems by operators or management, (Shean & Cilliers, 2011).

## 2.7 Conclusion

In this chapter, the author reviewed literature based on advanced controller applications as well as the flotation process. The advance controller provided insight into the various control methods applied in practice such as adaptive control, multivariable control, model predictive control, neural network control, and optimal control. Each of these advanced controllers mentioned have their own advantages and limitations. The selection of these controllers should be based on the process model dynamics and control architecture.

Based on the review of the process, column flotation consists of a hierarchy control structure. Maintaining regulatory control of the base level is the focus of obtaining and maximising economic profit. However poor performing controllers often fail to provide base level control autonomously. More recent literature on flotation optimization aims towards the use of chemical reagents to improve concentration grade. The factors that affect flotation control mentioned in section, must be considered for flotation controller development.

A decentralized control mentioned in this literature can provide a solution to base-level control. By choosing the correct input-output pairing using mathematical tools such as RGA or DNA the designed controller limitations are not as restricted. This results in a greater optimal controller performance. The Chapter focuses on discussing different column flotation cell or mechanism including the capability to achieve control over the flotation cell. Theory based on control methods and decentralized control strategies are also discussed in the next chapter.

# CHAPTER 3 : COLUMN FLOTATION CONTROL

## 3.1 Introduction

Column flotation control serves several important purposes in the context of flotation processes. The flotation process involves the regulation and management of column flotation cells to optimize the recovery of valuable minerals and minimize the loss of valuable material. The primary control of a flotation cell is pulp level control, to achieve stability and efficiency. The aim of controlling the flotation system is to increase and optimise the efficiency and performance of the concentration grade and recovery. The additional fundamental controlled variables are known to be the airflow rate, pH, and Reagent addition. Manipulation of these variables can directly affect the concentration grade, tailings grade, and the mass flow rate of the concentrate, (Wills & Finch, 2016). In this chapter, the column flotation cell or mechanism is discussed including the capability to achieve control over the flotation cell. The decentralized control strategies are discussed. The application of decentralized control of flotation columns is mentioned along with the qualities and downfalls. An analysis takes place in the discussion of the decentralized control theory and its application. Thus, concluding the chapter with the controller approach that will be used for the remainder of this research.

## 3.2 Column cell flotation control overview

The flotation process involves several variables that need to be taken into account, based on the three-phase interaction that occurs during this process. Authors Shean and Cilliers (2011) presented the following list of additional variables to consider such as pulp properties, pulp flow rate, froth properties, particle properties, mineral composition of the ore, concentration grade, and recovery and froth wash water rate. Shean and Cilliers (2011), further state that although each of the mentioned variables are to be considered, it would not be necessary to control each variable simultaneously to obtain good process control. This research will only focus on controlling wash-water flow rate and airflow rate.

A column cell can be separated into two regions: the collection zone and the froth zone. The collection zone is in the lower section of the cell and contains less than 30% of air. The froth zone is in the upper section of the cell containing more than 70% of air, (Maldonado et al., 2009; Calisaya et al., 2012). These two regions are seen in Figure

3.1. The success of an industrial column flotation controller is primarily reliant on the accuracy of the measurements taken. It is necessary to have the appropriate actuators and maintain the measurability of both the controlled and manipulated variables, (Le Roux & Craig, 2019). Figure 3.1 demonstrates the process flow diagram of a column flotation cell.

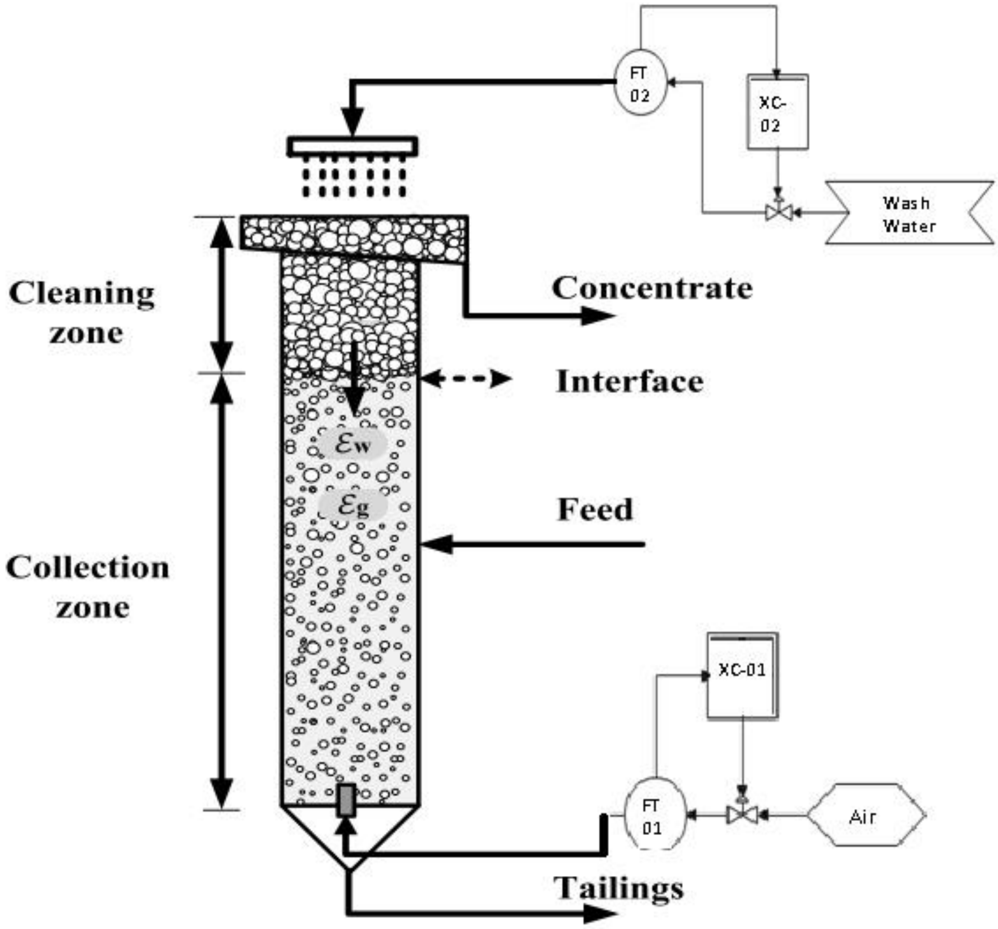


**Figure 3.1:** **Column flotation cell, (Calisaya et al., 2012) with a process flow diagram**

In terms of the manipulated variables, magnetic flow meters are commonly used to measure the tailings flow rate $Q_T$ of the cell. A simple PI controller is used to control an outlet valve that acts as an actuator for the tailings flow rate. The tailings flow rate is manipulated by the PI controller to control the pulp volume. An alternative controller can be developed to monitor all levels of the cell simultaneously. According to Le Roux & Craig (2019), such a controller has already been developed by Mintek known as the FloatStar level stabiliser.

In practice, the column flotation cells occasionally operate in banks to allow the concentrate of one cell to be fed into the next one. This leaves little room for the control of the feed flow rate $Q_{Fd}$. In the instance of the $Q_{Fd}$ into the first cell of the flotation bank, a surge tank with a pump is used to introduce the slurry into the tank. This allows the feed flow rate $Q_{Fd}$ to be manipulated. The pump acts as the actuator and the magnetic flow meter are used to monitor the Feed flow rate $Q_{Fd}$. The air flow rate $J_g$ is often measured using various techniques such as thermal mass flow meters; a differential meter coupled with a venturi tube, or a differential pressure transducer with an annubar tube.

### 3.2.1 Froth Depth ($h_{fz}$)

The froth depth is achieved through the measurement of two separate pressure transducers and is represented by equation 3.1.

$$\rho_{fz} = \frac{P_1(H_2 - h_{fz}) - P_2(H_1 - h_{fz})}{g h_{fz}(H_2 - H_1)} \tag{3.1}$$

Where:

$\rho_{fz}$ = average value of froth zone density

$h_{fz}$ = froth layer height

### 3.2.2 Gas Holdup ($\varepsilon_{gzc}$)

The most conventional method to calculate the gas holdup in the collection zone is to use the difference between the two pressure transducers as seen in equation 3.2.

$$\varepsilon_{gzc} = 1 - \frac{P_2 - P_1}{\rho_{sl} g (H_2 - H_1)} \tag{3.2}$$

### 3.2.3 Bias Rate ($Q_B$)

The bias is defined as the resultant flowrate of water descending beneath the froth region. It is described as the fraction of wash-water beneath the froth zone ($\varepsilon_w$). For a two-phase system froth zone, ($\varepsilon_w$) is estimated using equation 3.3. Where $k_f$ and $k_w$ are the feed and wash-water conductivity, (Calisaya et al., 2012; Maldonado et al., 2009).

$$\varepsilon_w = \left(\frac{k_f - k^*}{k_f - k_w}\right) \tag{3.3}$$

Maldinando et al. (2009), use an empirical relationship in equation 3.4 to relate the fraction of wash-water beneath the froth zone to the bias rate. Calisaya et al. (2012), presented a three-phase system definition in equation (3.5). Where $k_{sgl}$ is the conductivity of the gas-pulp mixture and $\varphi_s$ solid in pulp percentage.

$$Q_B = 0.003966\varepsilon_w - 0.03409 \tag{3.4}$$

$$\varepsilon_w = 100\left(\frac{k_f - k_{sgl}\left(\frac{0.5\varepsilon_g + 1}{1 - \varepsilon_g}\right)}{k_f - k_w(1 - \varphi_s)}\right) \tag{3.5}$$

The pulp level or volume in terms of the controlled variable is measured using a float with a target plate and an ultrasonic transducer. The concentration of minerals at the concentrate and tailings are measured using online X-ray fluorescence analysers. In the case of a column flotation bank, only the concentration grade of the final flotation cell is measured. On rare occasions the concentration grade of the feed, tailings, and intermediate grades are measured, (Le Roux & Craig, 2019).

## 3.3 Challenges with column flotation modelling and control

Flotation process modelling for control is proven to be a challenging task since flotation models are often developed through means of physical parameters that cannot be effectively measured or estimated. The modelling process requires mainly reliable instrumentation. The use of unreliable instrumentation and the sophistication of the flotation process makes it difficult to create an effective model for flotation control purposes that can be calibrated with practical data, (Maldonado et al., 2009; Quintanilla et al., 2021).

The process control of froth flotation is classified as manipulated, controlled, and initial state variables. The classification of these variables does diverge depending on the author's description of what is considered as a controlled or manipulated variable, (Quintanilla et al., 2021). Quintanilla et al (2021) further state that in practice, the PID controller is often used as a conventional controller for regulatory control. However, due to the PID controller not having a process model or constraints it is known to display poor performance under disturbances. In addition to the challenges affecting flotation control is the interaction between process variables. A process such as froth flotation consists of highly complex system dynamics, rendering PID controllers insufficient at maintaining the plants' optimal conditions. This is due to the PID being a SISO control strategy meaning only one controlled variable can control one manipulated variable. Thus, PID overlooks the effects of interaction between other process variables.

## 3.4 Decentralized and decouple control for the column flotation process

A multivariable process or Multi-input Multi-output (MIMO) process can generally be controlled using a decentralized, decoupled, or sparse control method. To determine which control method to select, the interaction between the input and output pairings requires analysis. This can be done by using either a Relative Gain Array (RGA) or Direct Nyquist Array (DNA). RGA identifies the amount of interaction between the input and output pairings using the steady state gains. Whereas DNA determines the dynamic interaction between input and output pairings, (Liu et al., 2019).

The decentralized decoupled control technique is used for this research, with the experimental design that will consist of a 2x2 state-space representation, based on the control structure comparison indicated in Table 3.1. The selection of this control structure is made so that the PI/PID controllers $C_1$ and $C_2$ in the decentralized configuration can be easily tuned, see Figure 3.2. The dynamic model of the experimental flotation cell can be considered as having a coupled structure due to the interconnection of flowrates between control loops. According to Shen et al., (2010) due to the Relative Normalised Gain Array (RNGA) of a 2x2 matrix being symmetric, the preferred control method is either decentralised or decoupled. This is based on the proposed control selection criterion by Shen et al (2010) as an application guideline. However, due to the controlled and manipulated variables already being predetermined, RNGA will not be used for the design.

**Table 3.1:** Control structure comparison

| Control Architecture | Realizability | Stability | Robustness | Implementation |
|---|---|---|---|---|
| Decoupled (Centralized) | A decoupled system is only realizable if the system outputs are not dependent on future inputs. | Most Static and some dynamic decoupling methods are stable. | Seldomly used in industrial applications due to the sensitivity to modelling errors. | Controller parameters require retuning if the system operation changes. |
| Decentralized | A decentralized system is only realizable once suitable input-to-output pairings are achieved. | There is always a controller in the structure that stabilizes the loop. | Widely used in industrial applications despite being sensitive to modelling errors. | Cost-effective control strategy with easy maintenance and tuning. |

| | | | | |
|---|---|---|---|---|
| Sparse | A sparse system is only realizable for a process model with a 3x3 matrix or larger. | The stability exceeds that of the decentralized and decoupled approach due to the addition of sub-controllers. | These are often implemented with MPC and Optimal control strategies. | Reduces the interconnecting data between local controllers using the sub-controllers, at the cost of more complex tuning |

Figure 3.2 is a representation of the proposed control structure that demonstrates the decentralised controller based on the MIMO process model. The diagonal controller $C_1$ will be used to control the froth density by manipulating the wash water flow rate $Q_W$ for the controlled variable $H_f$. Controller $C_2$ will be used to control the air holdup in the collection zone by manipulating the air flow rate $Q_g$. The feedback to the controllers $C_1$ and $C_2$ is used to continuously reduce setpoint error. The transfer functions of the plant are $G_{11}$, $G_{12}$, $G_{21}$, and $G_{22}$ which mathematically share relationships between the two process variables. The Decoupler system is used to decouple the system to allow the two control loops to be independently tuned. The decoupler allows the separation of co-dependant variables allowing the engineer to vary the MIMO system setpoints, (*$H_f$ SP* and *Eg SP*) with the control loops affecting each other.

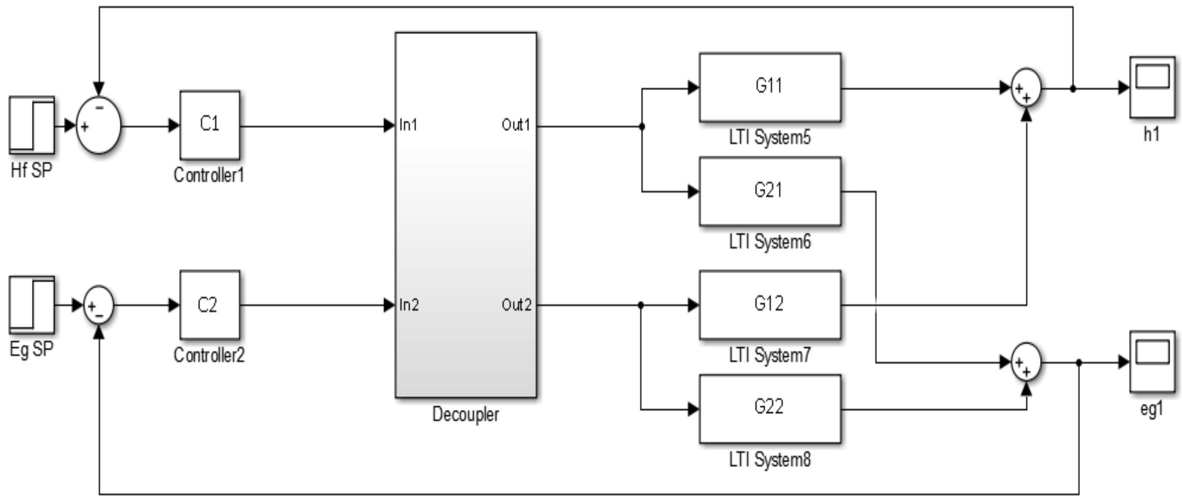


**Figure 3.2:** **Proposed control structure of a decoupled flotation system**

The merits and short comings of the proposed control structure seen in Figure 3.2 are mentioned in the following section.

## 3.5 Advantages and disadvantages of decentralized decoupled control

Below are some of the advantages and disadvantages of decentralized and decoupled control of column flotation mentioned is some of the applied literature.

### 3.5.1 Advantages of decentralized decoupled control in flotation

With decentralized control, implementing different performances to various control loops becomes an easier task, (Desbiens et al., 1997). This is mainly because the individual loop PI controllers can be tuned using SISO strategies. The mode of operation can easily be configured to manual operation if needed. In addition to decentralization, a decoupled approach can be implemented as seen in Kämpjärvi & Jämsä-Jounela (2003) and Tshemese-Mvandaba et al., (2021). The decoupled approach demonstrates the best suitable performance for interconnecting control loops as seen in the flotatoin system.

### 3.5.2 Disadvantages of decentralized decoupled control in flotation

The main downfall of decentralized control implementation in the industry is due to its complexity. The decentralized controller is mainly reliant on the control loop parings. Incorrect control loop parings may result in poor controller performance and major damage to any hardware.

## 3.6 Discussion on decentralized decoupled column cell flotation control

The decentralized control approach is commonly seen applied to a series of cells and occasionally applied to single-cell control. With a process consisting of many interconnecting loops, decentralized control theory applications to column flotation are few. Authors Kämpjärvi & Jämsä-Jounela (2003), study shows that the performance of the decoupled control strategy is more successful as opposed to the SISO strategy.

The decentralized decoupled strategy proved to be successful once again with the study conducted by Tshemese-Mvandaba et al., (2021). The decentralized decoupled PI design demonstrated improved performance in steady state error and stability. However, both studies never conducted experiments to monitor the decoupled controller behaviour under disturbances. For this study, the flotation cell presented in Figure 3.1 will be modelled and simulated using the MATLAB/Simulink environment. The selected flotation cell will be decentralized and decoupled within the MATLAB/Simulink environment for controller design and implementation. The decentralized and decoupled control design will be tested against setpoint tracking and disturbance control.

## 3.7 Conclusion

This chapter discusses the method of decentralized and decoupled control, the Column cell flotation control. Based on the proposed model, the two mentioned control loops clearly illustrate dependence and interaction with each other. This has been a concern for flotation control and numerous Multi-In Multi-Out systems. A decoupled approach is proposed to simplify the controller design by reducing the interaction between control loops. The following chapter will display the coupling relationship between interconnecting control loops.

# CHAPTER 4 : DEVELOPMENT AND SIMULATION OF THE FLOTATION COLUMN PROCESS

## 4.1 Introduction

The purpose of this chapter is to demonstrate the effects of process variable interactions within the column flotation system. This chapter comprises of an open-loop flotation system evaluation. The pilot column will be modelled using system dynamic equations that will be used for the simulation. The transfer functions are written and stored using MATLAB and the system dynamic equations are modelled in the Simulink environment. The step-response of each controlled variable, (for the purpose of this research is froth depth and gas holdup in the collection zone) are analysed to monitor the control loop interactions. A decoupled open-loop flotation system is introduced and evaluated against the performance of the open-loop coupled system. Based off the results of the open-loop simulations one case study is selected for the design of an advanced decoupled controller.

## 4.2 Flotation system development

The research of Nasseri et al, (2020) is used for the final case study. Their pilot flotation column consisted of two peristaltic pumps and rotary encoders to monitor and control the feed and tailings flowrate. To manipulate the wash water, a diaphragm pump is used. The air is supplied using a compressor and airflow control is done using an airflow meter and a stepper motor. An ultrasonic sensor is used to measure the pulp level within the column and two pressure sensors are located at P1 and P2 in Figure 4.1 below.

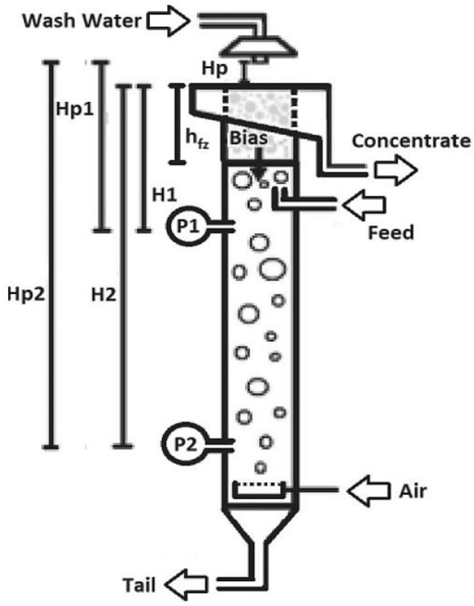


**Figure 4.1:** **Pilot flotation column for a case study, (Nasseri et al., 2020)**

Nasseri et al, (2020) used a similar methodology to Maldonado et al., (2009) to obtain the dynamic model of the system. The step responses of the three secondary variables were obtained by manipulating the input variables (wash water, airflow, and tailings flow rate). The feed flow rate is considered as a constant, for the entire process. The input variables were tested individually with the remaining two kept constant for the duration of the input test. A system identification toolbox was used in MATLAB to obtain the models, with a sample time of 2 seconds. Nasseri et al, (2020) further states that due to the nature of the system, the peristaltic pump used to control the tailings flow rate provided some instability when modelling the bias rate. Due to the bias rate constantly changing with respect to the tailings flow rate the bias rate model was removed from their research.

## 4.3 Mathematical modelling of the flotation process

The mathematical modelling of a flotation cell is divided into two categories: Empirical and Phenomenological modelling. Empirical Modelling relies on the use of static models to relate to input and output plant data. The relationships between dependant and independent variables for predictive model control are established through measurements of a physical system. Phenomenological modelling is based on the understanding of froth flotation physics. These models can further be classified as kinetic, population balance, and probabilistic based modelling, (Shean and Cilliers, 2011). Authors J Le Roux and I Craig (2019) proposed a non-linear state space phenomenological, using mass balance equations. To control the froth flotation process, a two-phase dynamic model is developed to represent the relationship between controlled and manipulated variables of the experimental model. The model is identified as follows:

$$\begin{bmatrix} h \\ \varepsilon_g \end{bmatrix} = \begin{bmatrix} G_{11} & G_{12} \\ G_{21} & G_{22} \end{bmatrix} \begin{bmatrix} Q_W \\ Q_g \end{bmatrix} \tag{4.1}$$

Where $G_{11}$, $G_{12}$, $G_{21}$, $G_{22}$ signify transfer functions and $Q_W$ represents the wash water flowrate and $Q_g$ the Gas flowrate.

The signify transfer functions of the considered model are:

$$G_{11} = \frac{-(0.065058)}{(s+0.0114)} \tag{4.2}$$

$$G_{12} = \frac{-0.2022(s-0.0161)}{(s+0.0063)(s+0.054)} \tag{4.3}$$

$$G_{21} = \frac{-0.0031}{(s+0.0038)} \times e^{-18s} \tag{4.4}$$

$$G_{22} = \frac{0.1448(s+0.0097)}{(s+0.0069)(s+0.062)} \times e^{-1.1s} \tag{4.5}$$

The plant model is true under the following conditions:

- $Q_F$ is constant.
- 0.2 L/min < $Q_T$ < 0.8 L/min
- 0.2 L/min < $Q_w$ <0.9 L/min
- 3 L/min < $Q_g$ < 7 L/min
- 12% < $\varepsilon_g$ < 15%
- 4 cm < $h_f$ < 60 cm

An empirical model is used based on the two-phase system mentioned above. This method relies on the measurements recorded by authors Persechini et al., (2000). Phenomenological modelling relies on differential equations based on process kinetics. The phenomenological modelling method would result in a higher order model and will reach beyond the scope of this research. Hence, considered an empirical model for this research.

### 4.3.1 Height

The 2X2 model is defined in equation 4.1, and the froth layer height in the Laplace domain, is defined in equation 4.6.

$$h(s) = G_{11}Q_w(s) + G_{12}(s)Q_g(s)\ldots \qquad (4.6)$$

### 4.3.2 The air hold-up zone.

Based on the 2X2 model defined in equation 4.1, the gas-holdup in the collection zone is defined by equation 4.7.

$$\varepsilon_g(s) = G_{21}Q_w(s) + G_{22}(s)Q_g(s)\ldots \qquad (4.7)$$

### 4.3.3 The Bias zone

According to Nasseri et al., (2020) the bias rate constantly changed with respect to the tailings flowrate. This is due to the peristaltic pump being unstable while controlling the tailings flow rate. As a result, the bias rate model was not considered for their research. Due to the nature of this research, the bias rate model is of little significance, hence not considered.

## 4.4 Data collection, simulation results and analysis

The Identified 2x2 dynamic model presented by Nasseri et al., (2020) is analysed in this section. This is done to monitor the effects of the interacting loops between the controlled and manipulated variables. The 2x2 model is then decoupled and evaluated against the coupled system.

### 4.4.1 Simulation of the coupled flotation system

This sub-section focuses on the open-loop simulation of the coupled flotation system. The aim is to study the natural behaviour of the considered flotation model. To model the multivariable column flotation system the following Figure 4.2 is developed in MATLAB/Simulink by incorporating equations (4.2 - 4.4).

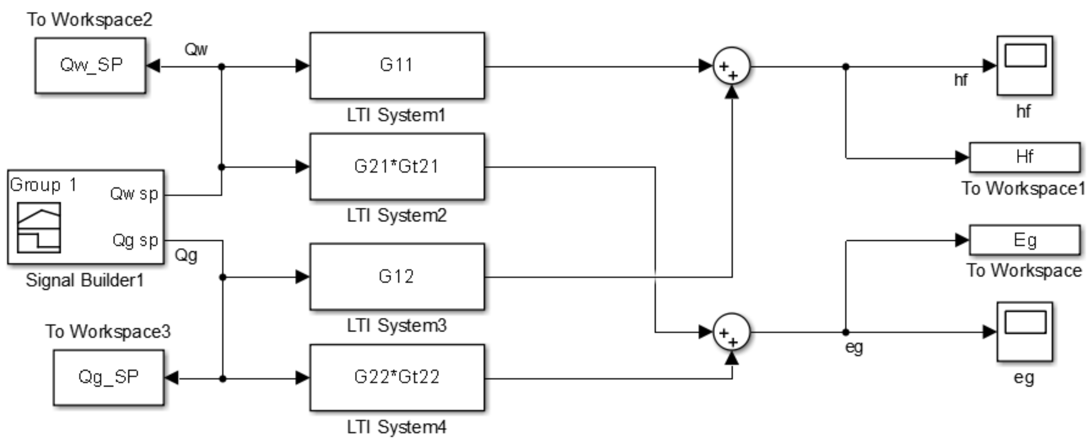


**Figure 4.2:** **Coupled flotation plant under test.**

The above model, figure 4.2 is then subjected to the setpoint changes. The characteristic of each response is created by implementing a signal from the signal's builder Qw sp and Qg sp to Figure 4.2. The flowrate setpoint values per test case are defined in Table 4.1 below.

**Table 4.1:** **Coupled Simulation Setpoint Variations per Test Case**

| **Cases** | **Hf** | | **Eg** | | **Description** |
|---|---|---|---|---|---|
| | **Qw Setpoints** | **Time (kilo-sec)** | **Qg Setpoint** | **Time (kilo-sec)** | |
| **1** | 0.4-0.6-0.8-0.3-0.4 ($cm^3/s$) | 0-1-2-3-4 | 5 (%) | 0-1-2-3-4 | The Qw setpoint is varied over time with the Qg setpoint remaining constant. Both the Qw and Qg setpoints are within the given model constraints. |
| **2** | 0.45 ($cm^3/s$) | 0-1-2-3-4 | 4-5.5-7-3-4 (%) | 0-1-2-3-4 | The Qg setpoint is varied over time with the Qw setpoint remaining constant. Both the Qw and Qg setpoints are within the given model constraints. |
| **3** | 1-5-3-4 (cm) | 0-1-2-3 | 1-8-5-5 (%) | 0.5-1.5-3-4 | This case simulated four changes made to the setpoint pulse signal. As indicated in the height loop, the changes are made from 1,5,3, and 4 at different times. On the air-loop the changes. |

**Case 1:**

To monitor the effect of the wash water flow rate ($Q_w$) on the froth depth ($h_f$) and the gas holdup in the collection zone ($\varepsilon_g$), the gas flowrate remains constant, and the wash water flow rate is altered every 1000 seconds. Refer to Table 4-1 Case 1 for flowrate setpoint values.

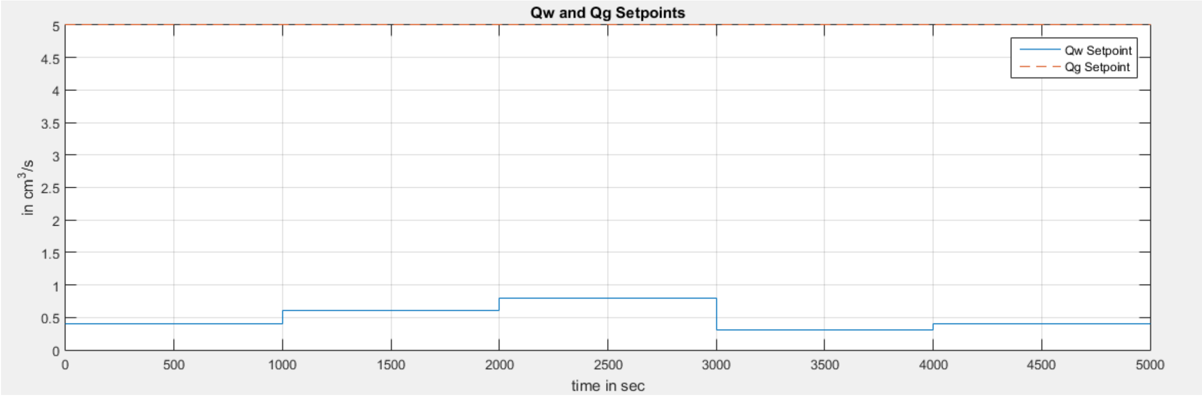


**Figure 4.3:** Flowrate Qw and Qg Setpoint changes

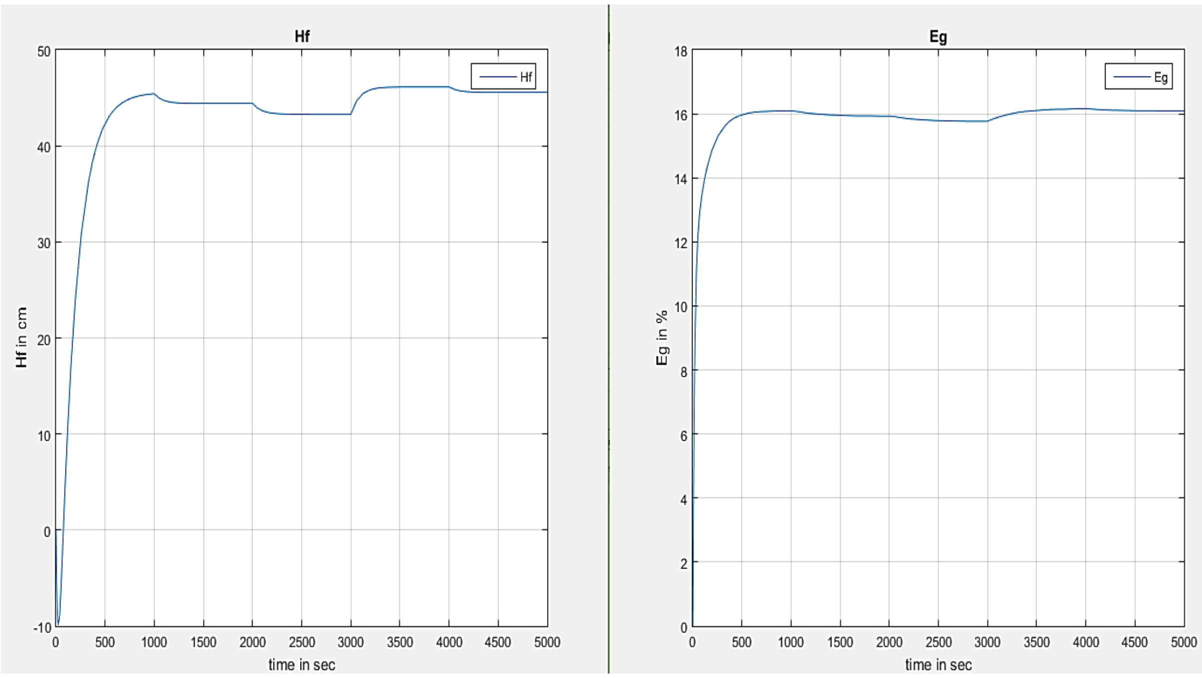


**Figure 4.4:** Froth Height (Hf) and Gas Holdup (Eg) response to changes in Qw

By observation, it can be seen in Figure 4.4 that the setpoint variation in wash water flow rate $Q_w$ at time intervals of 1 kilo-second affects both the Froth Height (Hf) and Gas Holdup in the collection zone (Eg). However, wash water more variation effect is seen on the froth height (Hf) results at each interval.

**Case 2:**

To monitor the effect of the gas flowrate ($Q_g$) on the froth depth ($h_f$) and the gas holdup in the collection zone ($\varepsilon_g$), the wash water flowrate remains constant, and the gas flow rate is altered every 1000 seconds. Refer to Table 4.2 Case 2 for flowrate setpoint values.

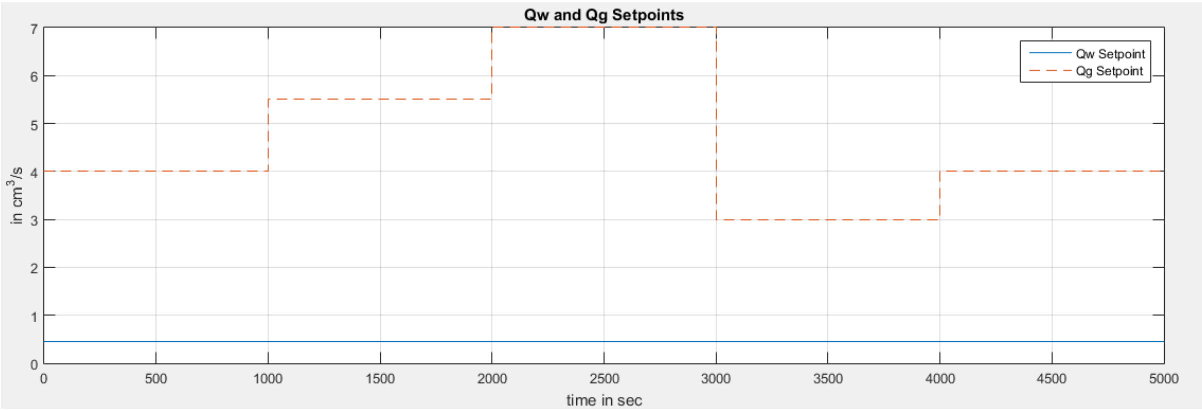


**Figure 4.5:** **Flowrate Qw and Qg Setpoint changes**

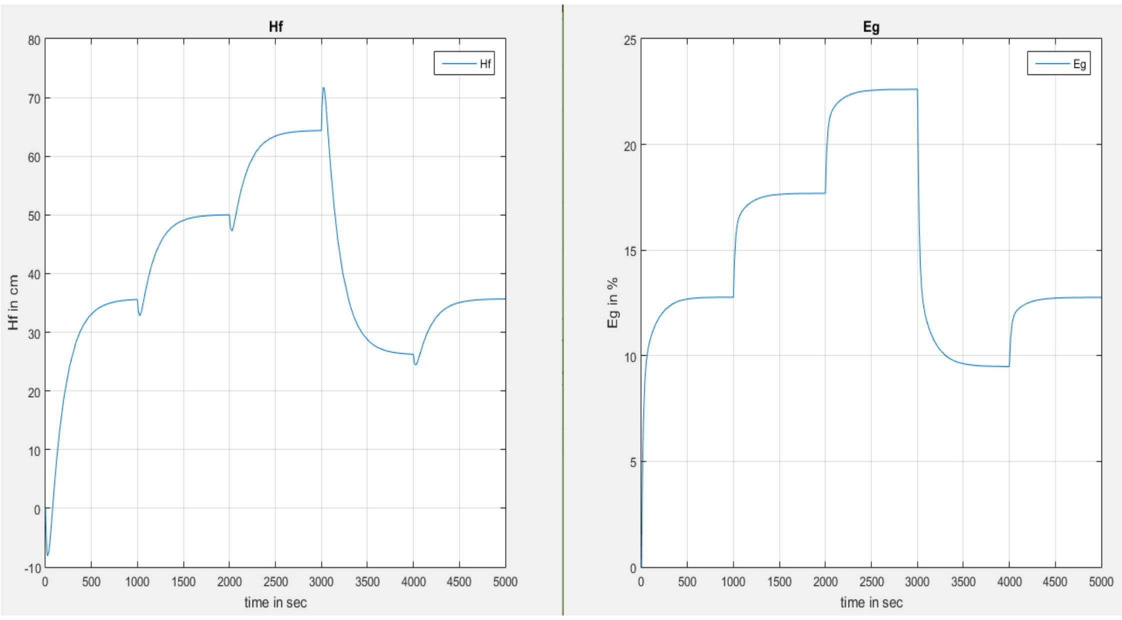


**Figure 4.6:** **Froth Height (Hf) and Gas Holdup (Eg) response to changes in Qg**

As presented in Figure 4.6, it is realised that the setpoint variation in gas flow rate $Q_g$ at time intervals of 1 kilo-second effects both the Froth Height (Hf) and Gas Holdup in the collection zone (Eg).

### Case 3:

To observe the flotation system's setpoint tracking capabilities, both the wash water flow rate (Qw) and gas flow rate (Qg) are altered at different periods of time. The Qw setpoints will be varied every 1 kilo-seconds and the Qg setpoint will be varied every 0.5 kilo-seconds. See table 4.1 Case 3 for setpoint values.

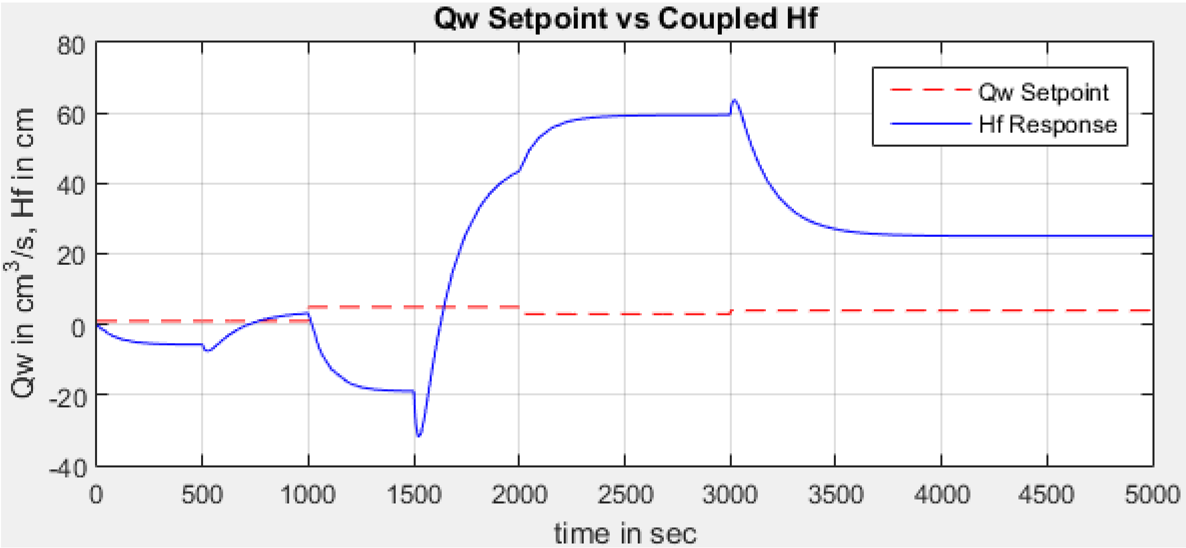


**Figure 4.7:** Setpoint Tracking of Coupled Froth Height

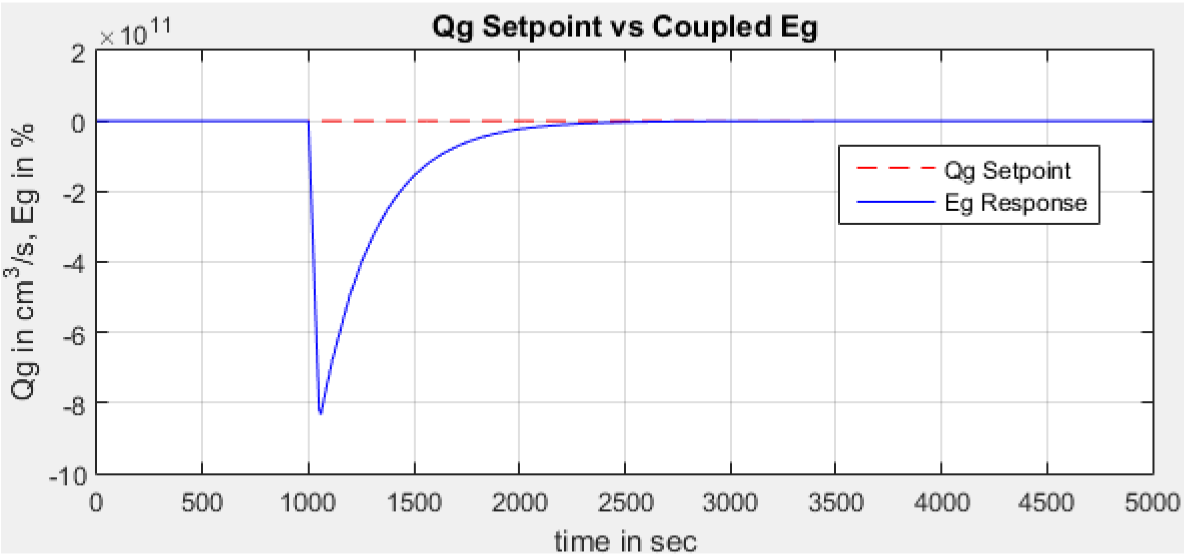


**Figure 4.8:** Setpoint tracking of Coupled Gas holdup in the collection zone

It can be seen from figure 4.7 and figure 4.8 that the coupled response of both the Froth Height (Hf) and Gas holdup (Eg) are affected by setpoint changes to both the Qw and Qg. It is also evident in figure 4.8 that at t = 1 kilo-sec the Eg response displays a negative response with an amplitude large enough to render the Qg setpoints not visible. This is due to a wash water (Qw) setpoint change applied at 1 kilo-sec, therefore, the increase in Qw has resulted to a negative response in the gas hold up loop. The next step is to decouple the system to minimise the control loop interactions.

### 4.4.2 Development and evaluation of a decoupled flotation system

Considering the Decoupled system to be *T(s)* and defined by equation 4.8.

$$T(s) = \begin{bmatrix} T_{11} & 0 \\ 0 & T_{22} \end{bmatrix} = \begin{bmatrix} G_{11} & G_{12} \\ G_{21} & G_{22} \end{bmatrix} \begin{bmatrix} D_{11} & D_{12} \\ D_{21} & D_{22} \end{bmatrix} \quad (4.8)$$

Where:

$$D_{12} = \frac{-G_{12}}{G_{11}} \quad (4.9)$$

$$D_{21} = \frac{-G_{21}}{G_{22}} \quad (4.10)$$

$$D_{11} = D_{22} = 1$$

The decoupling process is completed as follows:

$$\begin{bmatrix} \mathrm{T}_{11} & 0 \\ 0 & \mathrm{T}_{22} \end{bmatrix} = \begin{bmatrix} \mathrm{G}_{11}\mathrm{D}_{11} + \mathrm{G}_{12}\mathrm{D}_{21} & \mathrm{G}_{11}\mathrm{D}_{12} + \mathrm{G}_{12}\mathrm{D}_{22} \\ \mathrm{G}_{21}\mathrm{D}_{11} + \mathrm{G}_{22}\mathrm{D}_{21} & \mathrm{G}_{21}\mathrm{D}_{21} + \mathrm{G}_{22}\mathrm{D}_{22} \end{bmatrix} \dots \quad (4.11)$$

Using equation 4.8, multiply the flotation plant and decoupled matrices ($G_{xx}$ * $D_{xx}$), that have led to equation 4.11. Where $T_{11}$ is also known as the systems froth height, ($H_f$) and $T_{22}$ is also known as the gas holdup in the collection zone ($\varepsilon_g$).

Then substitute equations 4.9 and 4.10 into 4.11, which resulted to equation 4.13.

$$\begin{bmatrix} H_f & 0 \\ 0 & \varepsilon_g \end{bmatrix} = \begin{bmatrix} G_{11} + G_{12}\left(\frac{-G_{21}}{G_{22}}\right) & G_{11}\left(\frac{-G_{12}}{G_{11}}\right) + G_{12} \\ G_{21} + G_{22}\left(\frac{-G_{21}}{G_{22}}\right) & G_{21}\left(\frac{-G_{12}}{G_{11}}\right) + G_{22} \end{bmatrix} \dots \quad (4.12)$$

$$\begin{bmatrix} H_f & 0 \\ 0 & \varepsilon_g \end{bmatrix} = \begin{bmatrix} G_{11} + G_{12}\left(\frac{-G_{21}}{G_{22}}\right) & 0 \\ 0 & G_{21}\left(\frac{-G_{12}}{G_{11}}\right) + G_{22} \end{bmatrix} \quad (4.13)$$

The control loops can now be represented as two independent SISO systems where:

$$H_f = G_{11} + G_{12}\left(\frac{-G_{21}}{G_{22}}\right) \quad (4.14)$$

$$\varepsilon_g = G_{22} + G_{21}\left(\frac{-G_{12}}{G_{11}}\right) \quad (4.15)$$

Using the Case study 3 plant model parameters ($G_{11}$; $G_{12}$; $G_{21}$ and $G_{22}$), the following open loop transfer functions were achieved:

$$H_f = \frac{-0.060729\ (\mathrm{s} + 0.05322)\ (\mathrm{s} + 0.008991)\ (\mathrm{s}\hat{}2\ +\ 0.01227\mathrm{s}\ +\ 3.977\mathrm{e} - 05)}{(\mathrm{s} + 0.054)\ (\mathrm{s} + 0.0114)\ (\mathrm{s} + 0.0097)\ (\mathrm{s} + 0.0063)\ (\mathrm{s} + 0.0038)}$$

$$\varepsilon_g = \frac{0.15443\ (\mathrm{s} + 0.05465)\ (\mathrm{s} + 0.01007)\ (\mathrm{s} + 0.006596)\ (\mathrm{s} + 0.00189)}{(\mathrm{s} + 0.062)\ (\mathrm{s} + 0.054)\ (\mathrm{s} + 0.0069)\ (\mathrm{s} + 0.0063)\ (\mathrm{s} + 0.0038)}$$

### 4.4.3 Evaluation of a decoupled open-loop flotation system

To evaluate the effectiveness of the designed decoupled model. A decoupled system was developed based on equations 4.14 and 4.15 in Simulink to monitor the effectiveness of the system. Figure 4.9 presents the SIMULINK model of the decoupled open-loop system.

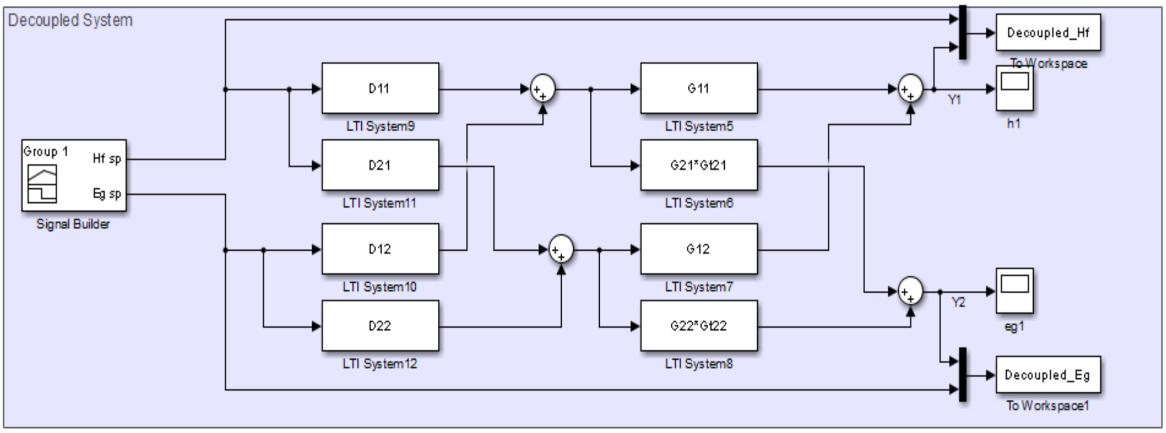


**Figure 4.9:** Decoupled system used for setpoint tracking

The response of $H_f$ for both the setpoint and decoupled systems are displayed in Figure 4.910 showing the effects of the setpoint changes based on case 1 described in Table 4.2. The expected outcome of the decoupled system is that the setpoint changes of $H_f$ should not have any effect on the air holdup loop of $\varepsilon_g$.

**Table 4.2:** Decoupled simulation setpoint changes

| Cases | Hf | | Eg | | Description |
|---|---|---|---|---|---|
| | Setpoints | Time (kilo-sec) | Setpoint | Time (kilo-sec) | |
| **1** | 1-5-3-4 | 0-1-2-3 | 1-8-5-5 (%) | 0.5-1.5-3-4 | This case simulated four changes made to the setpoint pulse signal. As indicated in the height loop, the changes are made from 1,5,3, and 4 at different times. On the air loop the changes occur 500 seconds later than that of the froth layer height. |

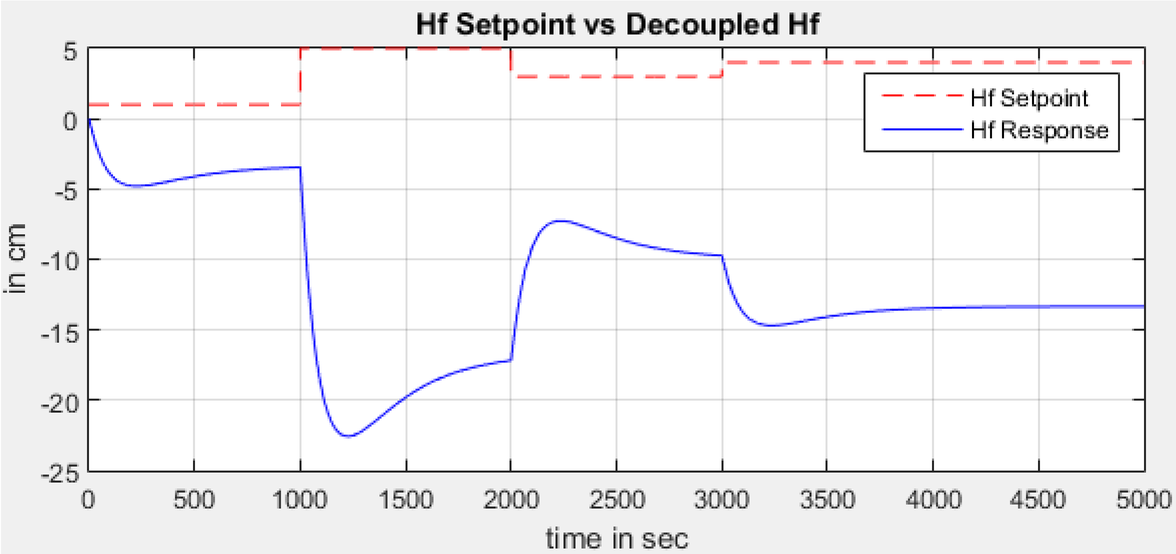


**Figure 4.10:** **Hf Setpoint vs Decoupled Hf response**

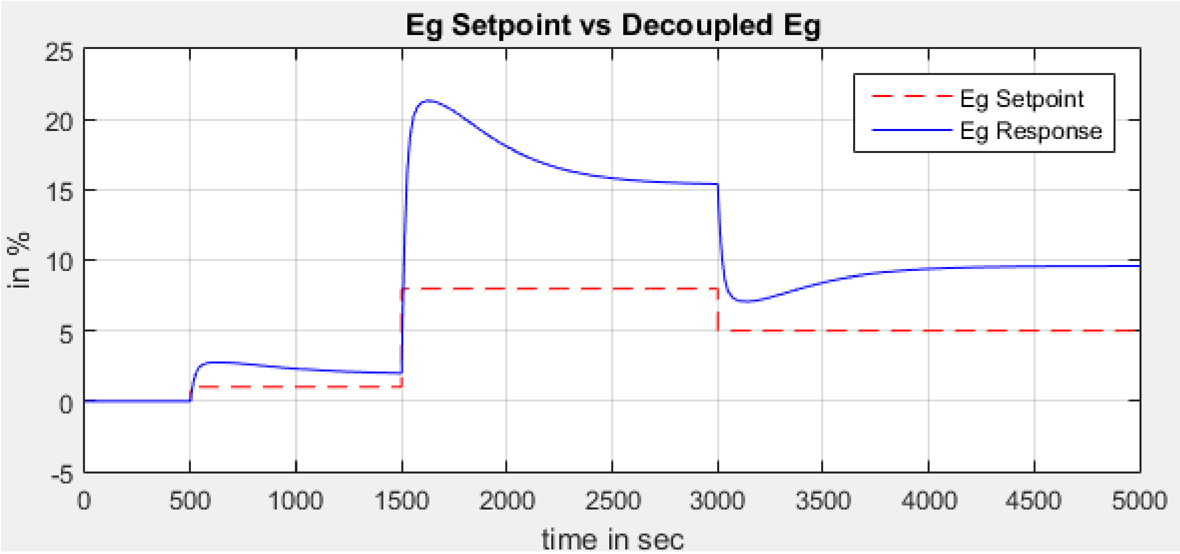


**Figure 4.11:** **Eg Setpoint vs Decoupled Eg response**

It can be noted that in Figure 4.10, the decoupled $H_f$ does not respond to the changes seated in the setpoint of the gas holdup ($\varepsilon_g$) at 500 seconds. Figure 4.11 displays the response of $\varepsilon_g$ for both the setpoint and decoupled system. The decoupled $\varepsilon_g$ shows no response to change in the $H_f$ setpoint variations. Therefore, the gas holdup and froth height loops can be considered as effectively decoupled proving that the decoupled design is effective. However, both the decoupled froth height and gas holdup demonstrates poor setpoint tracking performance. Hence motivating the additional requirements of a controller. The next sub-section focuses on the comparison analyses based on the open-loop behaviour of the coupled and decoupled flotation system.

### 4.4.4 Summary of the coupled and decoupled open-loop behaviour of the flotation system under different values of the inflow rates

Both the coupled and decoupled systems were subjected to the setpoint changes as seen in Table 4.1 and Table 4.2. The open-loop coupled flotation system was subjected to three individual cases of setpoint variations as seen in Table 4.1. The first and second cases were used to monitor the behaviour of the froth height and gas holdup based on the wash water flowrates and gas flowrates. As a result, the relationship between the respective flowrates and process variables was monitored. The third case in Table 4.1 is used to determine the behaviour of the open-loop flotation system setpoint tracking performance. The open-loop coupled flotation system demonstrated poor setpoint tracking performance and instability due to interacting control loops. A decoupled system is designed and evaluated using Table 4.2 under the same setpoint changes as the coupled flotation system in Table 4.1 Case 3. The decoupled system is seen to be more stable than the coupled system for both the froth height and gas holdup. The following table declares the characteristic performance of the system.

**Table 4.3:** **Flotation Coupled and Decoupled step response characteristics**

| Flotation Model | | RiseTime: | SettlingTime: | Overshoot: | Peak: | PeakTime: | Ess: |
|---|---|---|---|---|---|---|---|
| Coupled System | Hf | 8.7120e+03 | 1.0672e+04 | 4.1469e-10 | -3.3292 | 3.9319e+09 | 0.86622836 |
| | Eg | 8.7120e+03 | 1.0672e+04 | 1.7141e-09 | 1.9153 | 6.1053e+09 | 1.06465546 |
| Decoupled system | Hf | 219.0005 | 1.86e+03 | 3.862e-10 | -3.8622 | 2.00e+03 | 2.862 |
| | Eg | 8.4094 | 1860 | 1.6140 | 2.6140 | 259.0005 | 1.614 |

The characteristics of the decoupled system in Table 4.3 demonstrates loop independence between the froth height (Hf) and gas hold up (Eg) loops. It also shows a large settling time and steady state error (Ess). The coupled system shows an improved Ess however the rise time and settling time vary due to the dependence on the interactions of manipulated variables (Qw and Qg). With the use of PI and PID controller tuning the Ess and settling time problem of the decoupled flotation system can be easily resolved.

## 4.5 Observation and discussion

The purpose of this subsection is to discuss and compare the simulated results between the coupled and decoupled flotation systems. The discussion will be based on the relationship between each control loop of the mentioned case studies.

### 4.5.1 The effect of wash water on froth depth

In this scenario the wash water flow rate of the system was manipulated within the respective model constraints. The gas flow rate remained constant within the given pilot model constraints. By observation, the coupled system and decoupled system presented different behaviour to the changes in setpoints. The coupled system displays an increase in froth depth as the wash water flowrate increases. For the decoupled system an increase in the wash water flow rate displayed a minor decrease in the froth depth. This effect can be seen in Figures 4.4 and 4.10.

### 4.5.2 The effect of wash water on gas holdup

This scenario uses the same concept as the above-mentioned test method, where the gas flow rate remained constant as the wash water flow rate was manipulated. The coupled system behaviour displays minor increases and decreases proportional to the wash water flowrate, refer to Figure 4.4. The decoupled system shows no response as the effect was considered negligible, as seen in Figure 4.11.

### 4.5.3 The effect of gas flow rate on froth depth

In this scenario the gas flow rate of each case study was manipulated within the respective model constraints. The wash water flow rate remained constant within the given pilot model constraints. The coupled system response shows an increase in gas flow rate, resulting in an increase in froth depth. However, the decoupled system response demonstrates no effect to the gas flow rate setpoint changes. Refer to figures 4.6 and 4.10 for the coupled and decoupled system responses respectively.

### 4.5.4 The effect of gas flow rate on gas holdup

For this scenario the test method is the same as the one mentioned above where the gas flow rate of each case study was manipulated within the respective model constraints. The wash water flow rate remained constant for the duration of the simulation. Both the coupled and decoupled systems presented similar behaviour with the step-response being directly proportional to the changes in the gas flow rate. These results can be seen in Figures 4.6 and 4.11.

### 4.5.5 Decoupled flotation process

By observation of Figure 4.10 and Figure 4.11, has no interconnection between variables as either set point is altered. It is noted that the set points are varied at different amplitudes at different intervals to investigate the interconnection between the control loops. As a result, the loops demonstrated their independence from one another under the described conditions. However, even though the system is decoupled, an unstable loop can still cause instability to the decoupled loop. This is due to a closed loop pole of $H_f$ being on the RHS of the imaginary (jω) axis. To analyse the closed loop natural response of the $\varepsilon_g$ in SIMULINK, the $H_f$ control loop had to be left as an open loop circuit so that $\varepsilon_g$ can remain stable.

## 4.6 Conclusion

The simulation results of this chapter present the interaction between process loops. To reduce the interaction between these loops a system decoupler was introduced. The decoupler allows the system to react like a SISO system making the flotation system PI controllers easier to tune. It is also established in the decoupler performance evaluation that the decoupled system provides more stability by suppressing the process loop interaction. The decoupled flotation process model developed in this chapter presents good potential for controller development. The controller should produce an improved performance in setpoint tracking as opposed to just the decoupled system. The following chapter suggests an implementation of a PI control method for a decoupled flotation system.

# CHAPTER 5 : DECENTRALIZED DECOUPLED CONTROLLER DESIGN AND SIMULATION

## 5.1 Introduction

This chapter will focus on a decentralized decoupled design procedure for the flotation system. A brief description of Multi-input Multi-output control is introduced in this chapter. The MATLAB/Simulink environment is utilized as the design and evaluation platform for the work presented in this chapter. The decoupled system is designed to formulate a proportional-integral (PI) controller, with its parameters fine-tuned through the utilization of the pole placement technique as presented in section 5.2. The PI controller setpoint tracking is analysed to determine the controller's capabilities. The analysis of the simulation results of the entire chapter is discussed along with the challenges and limitations of selecting the PI control method, as presented in section 5.4 and section 5.5.

## 5.2 Design of decentralized decoupled controllers

The pole placement or pole-assignment technique is a closed-loop design strategy whereby the closed-loop poles of the plant are assigned to calculated locations on the s-plane. The closed loop poles are placed strategically so that the dominant poles contain the desired damping ratio $\zeta$ and undamped natural frequency $\omega_n$. The pole placement approach often raises the order of the system by 1 or 2 depending on pole-zero cancellation. The approach is dependent on the dominant poles, and it is assumed that non-dominant poles have a negligible effect on the transient response.

### 5.2.1 Desired closed-loop pole location

In this subsection, the process of designing the closed-loop poles is presented. For this research, the assumption is made that the system has 2$^{nd}$ order dominant poles. This simplifies the determination of the desired closed-loop poles by using the second-order characteristic equation (5.1) below.

$$G(s) = \frac{{\omega_n}^2}{s^2+2\zeta\omega_n s+{\omega_n}^2} \tag{5.1}$$

For specific response, the 2$^{nd}$ order characteristic equation is used to determine the Rise Time ($t_r$), Settling time ($t_s$), Percentage overshoot (%OS), peak time ($t_p$), and time delay ($t_d$). In this example, a Percentage overshoot of 10% and a settling time of 500 sec are used. With the desired %OS given as 10% the desired damping ratio $\zeta$ and undamped natural frequency $\omega_n$ can be determined by the following equations 5.2 and 5.3.

$$\zeta = \sqrt{\frac{ln\left(\frac{\%Os}{100}\right)^2}{\pi^2 + ln\left(\frac{\%Os}{100}\right)^2}} \tag{5.2}$$

$$\omega_n \approx \frac{4}{\zeta t_s} \tag{5.3}$$

Where:

$\zeta = 0.5912$ and $\omega_n = 0.0135$

Thus, substituting the desired $\zeta$ and $\omega_n$ results into 2nd order characteristic equation 5.1.

$$G(s) = \frac{{\omega_n}^2}{s^2 + 2\zeta\omega_n s + {\omega_n}^2} \tag{5.1}$$

Therefore, the following desired closed loop characteristic equation is achieved:

$$G(s) = \frac{0.0001831}{s^2 + 0.016\, s + 0.0001831} = \frac{0.0001831}{(s + 0.0080\ +\ 0.0109i)(s + 0.0080\ -\ 0.0109i)}$$

$$G(s) = \frac{0.0001831}{s^2 + 0.016\, s + 0.0001831} = \frac{0.0001831}{(s + 0.0080\ +\ 0.0109i)(s + 0.0080\ -\ 0.0109i)} \tag{5.4}$$

Due to the flotation closed loop poles being a 4th order system, 2 non-dominant poles ($P_1$ and $P_2$) are added to the desired characteristic equation where $P_1$ and $P_2$ are real and 5 times greater than the desired dominant closed loop poles.

$$G(s) = \frac{0.0001831(P_1)(P_2)}{(s + 0.0080 + 0.0109i)(s + 0.0080 - 0.0109i)(s + P_1)(s + P_2)}$$

Where:

$P_1 = 5+0.0080$

$P_2 = 5+P_1$

Resulting in the following desired closed-loop transfer function, presented in the following equation. 5.5:

$$G(s) = \frac{0.009194}{s^4 + 15.04\, s^3 + 50.44\, s^2 + 0.806\, s + 0.009194} \tag{5.5}$$

The resulting closed-loop transfer function is then modelled and simulated in Simulink under a step input. The response of the desired closed loop system G(s) is shown in Figure 5.1.

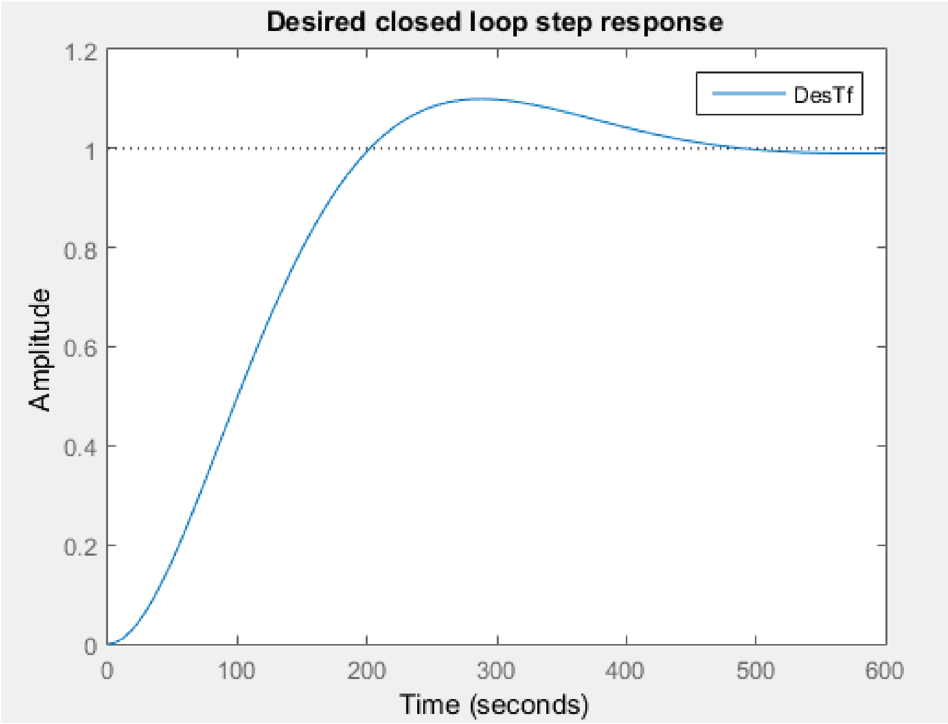


**Figure 5.1**: **Desired closed-loop step response of G(s)**

Table 5.1 presents the characteristics behaviour of the system's step response. The settling time of the desired closed loop system G(s) is approximately equal to 500 seconds with an overshoot of 10%.

**Table 5.1: Desired closed-loop step response characteristics**

| **Characteristics** | **DesTF** |
|---|---|
| **RiseTime (sec):** | 135.5199 |
| **SettlingTime (sec):** | 438.1913 |
| **Overshoot (%):** | 9.9999 |
| **Peak:** | 1.1000 |
| **PeakTime (sec):** | 287.8231 |

This information can be used as a reference for the Decoupled PI controller design. G(s) will be used as the desired closed-loop poles for PI parameter tuning.

## 5.3 System modelling description and design

In this section, the dynamic model of the system is described and the process of developing the decentralized decoupled PI controller is discussed. The section is partitioned in such a way that the controller tuning is conversed for each control loop (Froth Layer Height and Gas Holdup).

### 5.3.1 Decentralized decoupled flotation model

At this point, the system is assumed to be successfully decentralized and decoupled based on the results of the previous chapter. The froth height ($H_f$) and gas holdup ($\varepsilon_g$) are considered the controlled variables of the flotation column model. Whereas the process variables are the wash-water flowrate ($Q_w$) and gas flowrate ($Q_g$). The transfer function of the decoupled flotation column can now be defined by equation 5.6.

$$\begin{bmatrix} T_{11} & 0 \\ 0 & T_{22} \end{bmatrix} = \begin{bmatrix} G_{11} + G_{12}\left(\frac{-G_{21}}{G_{22}}\right) & 0 \\ 0 & G_{21}\left(\frac{-G_{12}}{G_{11}}\right) + G_{22} \end{bmatrix} \tag{5.6}$$

Where:

$T_{11}$ and $T_{22}$ are the transfer functions for froth height and Gas holdup respectively.

It can be seen from equation 5.6 that both control loops now act as two independent SISO systems. Thus, reducing the complexity of tuning a PI controller for each loop. The next step is to design the PI controller for each controlled variable.

### 5.3.2 Decentralized decoupled PI controller design for the froth layer height process

This subsection focuses on the decoupled PI design for the froth layer height ($H_f$). equation (5.7) can be used to describe a closed loop transfer function with unity feedback as seen in Figure 5.2.

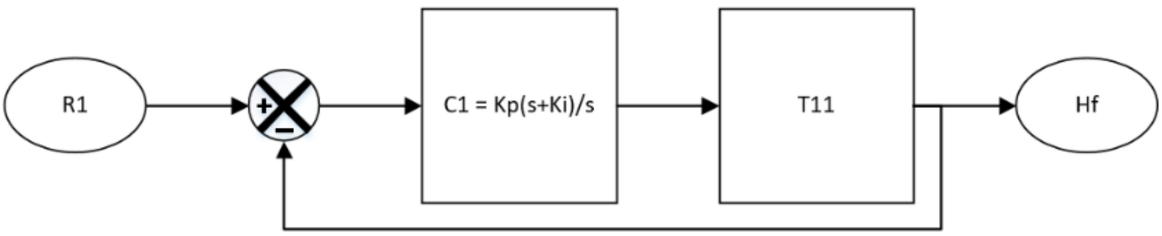


**Figure 5.2:** **Decentralized decoupled PI controller design concept for froth layer height**

Figure 5.2 is used to model the PI controller design for the height loop $H_f$.

$$\frac{H_f}{R_1} = \frac{C_1 T_{11}}{1 + C_1 T_{11}} \tag{5.7}$$

Where:

$$\boldsymbol{C_1 = \frac{K_p(s+K_i)}{s}} \tag{5.8}$$

$$R_1 = Setpoint\ for\ Washwater\ flowrate$$

And

$$T_{11} = \frac{-0.060729\,(s+0.05322)\,(s+0.008991)\,(s^2 + 0.01227s + 3.977e{-}05)}{(s+0.054)\,(s+0.0114)\,(s+0.0097)\,(s+0.0063)\,(s+0.0038)} \quad (5.9)$$

Using pole-zero cancellation on the decoupled open loop transfer function ($T_{11}$), the poles $(s + 0.054)\,(s + 0.0097)$ and zeros $(s + 0.05322)\,(s + 0.008991)$ are eliminated to obtain the following ($T_{11}$) open loop transfer function.

$$T_{11} = \frac{-0.060729\,(s^2 + 0.01227s + 3.977e{-}05)}{(s+0.0114)\,(s+0.0063)\,(s+0.0038)} \quad (5.10)$$

Thus, the closed loop response is given by the following equation (5.11):

$$\frac{H_f}{R_1} = \frac{[-0.06073s^2 - 0.0007451s - 2.415e{-}06]K_{p1}(s+K_{i1})}{s[s^3+0.0215s^2+0.0001391s+2.729e{-}07]+[-0.06073s^2-0.0007451s-2.415e{-}06]K_{p1}(s+K_{i1})}$$

... (5.11)

The closed loop characteristic equation can be represented as a polynomial with the $K_p$ and $K_i$ being the unknown variables. Refer to equation 5.11.

$$s^4 + [0.0215 - 0.06073K_{p1}]\,s^3 + [0.0001391 - 0.0007451K_{p1} - 0.06073K_{p1}\,K_{i1}]\,s^2 + [2.729e-07 - 2.415e-06K_{p1} - 0.0007451K_{p1}K_{i1}]s - 2.415e-06KpK_{i1} = 0\ldots \quad (5.12)$$

To determine the closed loop poles of the system the appropriate values for Kp and Ki need to be determined. The parameters of the PI controller can be used to achieve the desired poles. This is done by comparing the process characteristic equation with the desired characteristic equation, see equation 5.12.

$$s^4 + [0.0215 - 0.06073K_{p1}]\,s^3 + [0.0001391 - 0.0007451K_{p1} - 0.06073K_{p1}K_{i1}]\,s^2 + [\,2.729e-07 - 2.415e-06K_{p1} - 0.0007451K_{p1}K_{i1}]s - (2.415e-06)K_{p1}K_{i1} = s^4 + 15.04\,s^3 + 50.44\,s^2 + 0.806s + 0.009194\ldots \quad (5.13)$$

By comparison of coefficients in equation 5.13, the PI controller parameters are found using the following:

$$K_{p1} = -\frac{15.04 - 0.0215}{0.06073} = -247.3500$$

$$K_{i1} = \frac{0.009194}{(2.415e-06)Kp} = 3.6913e{+}05$$

### 5.3.3 Decentralized decoupled PI controller design for the gas holdup process

The focus of this subsection is based on the decoupled PI design for the Gas holdup in the collection zone ($\varepsilon_g$). The PI controller design can be represented in Figure 5.3.

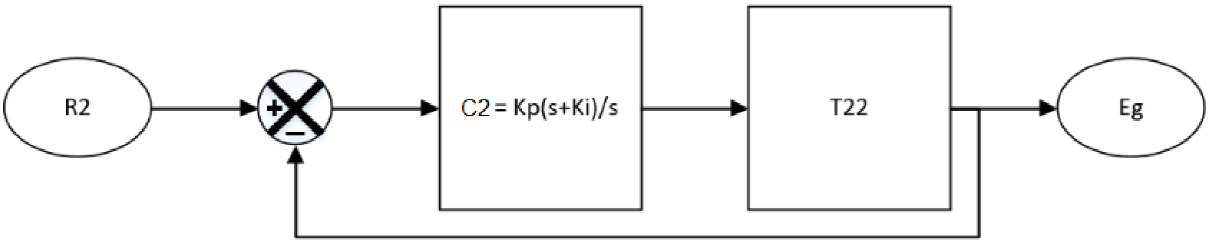


**Figure 5.3:** **Decentralized decoupled PI controller design concept for gas holdup**

The design procedure is the same as the PI design for the froth layer height loop $H_f$ where the closed loop transfer function of $\varepsilon_g$ can be determined by the following:

$$\frac{\varepsilon_g}{R_2} = \frac{C_2 T_{22}}{1 + C_2 T_{22}} \tag{5.14}$$

Where:

$$\boldsymbol{C_2} = \frac{\boldsymbol{K_{p2}(s+K_{i2})}}{\boldsymbol{s}} \tag{5.15}$$

$$R_2 = Setpoint\ for\ the\ Gas\ flowrate$$

And

$$T_{22} = \frac{0.15443\ (\mathrm{s} + 0.05465)\ (\mathrm{s} + 0.01007)\ (\mathrm{s} + 0.006596)\ (\mathrm{s} + 0.00189)}{(\mathrm{s} + 0.062)\ (\mathrm{s} + 0.054)\ (\mathrm{s} + 0.0069)\ (\mathrm{s} + 0.0063)\ (\mathrm{s} + 0.0038)}$$

Using pole-zero cancellation on the decoupled open loop transfer function ($T_{11}$), the following poles and zeros are eliminated $(\mathrm{s} + 0.054)\ (\mathrm{s} + 0.0063)$ and $(\mathrm{s} + 0.05465)\ (\mathrm{s} + 0.006596)$ to obtain the following ($T_{22}$) open loop transfer function.

$$T_{22} = \frac{0.15443\ (\mathrm{s} + 0.01007)\ (\mathrm{s} + 0.00198)}{(\mathrm{s} + 0.062)\ (\mathrm{s} + 0.0069)\ (\mathrm{s} + 0.0038)}$$

Thus, the closed loop transfer function is given by the following:

$$\frac{\varepsilon_g}{R_2} = \frac{[0.1544s^2 + 0.001861\mathrm{s} + 3.079\mathrm{e}-06]K_{p2}(\mathrm{s} + K_{i2})}{\mathrm{s}[s^3 + 0.0727s^2 + 0.0006896\mathrm{s} + 1.626\mathrm{e}-06] + [0.1544s^2 + 0.001861\mathrm{s} + 3.079\mathrm{e}-06]K_{p2}(\mathrm{s} + K_{i2})}$$

The closed loop characteristic equation can be expressed as:

$$s^4 + [0.0727 + 0.1544K_{p2}]s^3 + [0.0006896 + 0.001861K_{p2} + 0.1544K_{p2}K_{i2}]s^2 + [1.626\mathrm{e}-06 + 3.079\mathrm{e}-06K_{p2} + 0.001861K_{p2}K_{i2}]\mathrm{s} + (3.079\mathrm{e}-06)K_{p2}K_{i2} = 0$$

Comparing the process characteristic equation with the desired characteristic equation

$$s^4 + [0.0727 + 0.1544K_{p2}]s^3 + [0.0006896 + 0.001861K_{p2} + 0.1544K_{p2}K_{i2}]s^2 + [1.626\mathrm{e}-06 + 3.079\mathrm{e}-06K_{p2} + 0.001861K_{p2}K_{i2}]\mathrm{s} + (3.079\mathrm{e}-06)K_{p2}K_{i2} = s^4 + 15.04\,s^3 + 50.44\,s^2 + 0.806s + 0.009194$$

By comparison of coefficients the PI controller parameters are found using the following:

$$K_{p2} = \frac{15.04 - 0.0727}{0.1544} = 96.9583$$

$$K_{i2} = \frac{0.009194}{(3.079\mathrm{e}-06)K_{p2}} = 9.4793e - 05$$

The design procedure for the decoupled PI controllers is accomplished following the flowchart presented in Figure 5.4.

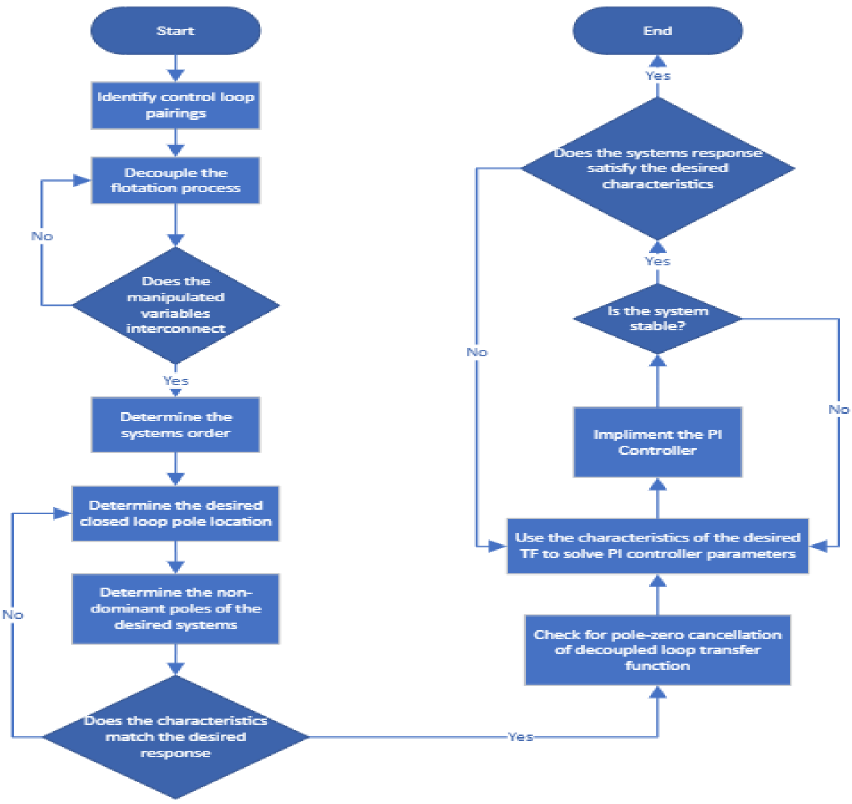


**Figure 5.4:** Decoupled PI design procedure flow diagram

The initial stage of the design is to develop a decoupled system. If the controlled variables of the plant are still dependent on the manipulated variables aside from the chosen control pair, the decoupling process needs to be assisted. Determining the order of the system is important to determine the number of non-dominant closed loop poles the system requires. It is then important to measure the system's non-dominant poles against the desired response. The system's characteristics are used to tune the PI parameters of the controller. If the system is unstable or doesn't perform as required, the PI parameters need to be tuned once more by adjusting the placement of the desired closed-loop poles.

The following section is an evaluation of the flotation controller designs mentioned in this section. With the use of the flow diagram in Figure 5.4 the individual PI controllers for each control loop of the flotation column can be examined.

## 5.4 Results analysis

This section is used to evaluate the designed Decoupled PI controller performance against the natural closed loop system. A series of four test cases will be used to test the controlled variables (froth height and gas holdup) both with and without the PI controller engagement. The following table best describes each test case to be performed.

**Table 5.2:** Decoupled PI Flotation Controller Test Cases

| Cases | Hf | | Eg | | Description |
|---|---|---|---|---|---|
| | Setpoints (cm) | Time (kilo-sec) | Setpoint (%) | Time (kilo-sec) | |
| 1 | 0-1 | 0 | 0-1 | 0 | A step input is implemented at 0 seconds to observe the characteristics of both Simulink models mentioned in Figure 5.6 and Figure 5.5. The aim is to compare the closed loop performance of the system with and without the designed controller. |
| 2 | 1-5-3-4 | 0-1-2-3 | 1-8-5-5 (%) | 0.5-1.5-3-4 | This case simulates four changes made to the setpoint pulse signal. As indicated in the height loop, the changes are made from 1,5,3, and 4 at different times to the air-loop changes. |
| 3 | 0-1 | 0 | 0-1 | 0 | An impulse response is modelled into the system as a disturbance for both the froth height and gas holdup control loops. This case aims to observe the system's stability as the disturbances are applied to the respective controlled variables. |
| 4 | 0-1 | 0 | 0-1 | 0 | An impulse response is modelled into the system as a disturbance for both the froth height and gas holdup control loops. The aim of this case is to observe the controller's stability as the |

| | | | | | |
|---|---|---|---|---|---|
| | | | | | disturbances are applied to the flotation plant flow rates. |

### Case 1: Step response

To investigate the performance and effects of the decoupled PI controller design of the flotation process, the closed loop systems are monitored and compared against the given set point variation. The flotation plant is modelled in MATLAB/SIMULINK for closed-loop analysis. Figure 5.5 is modelled to monitor the flotation plant's natural closed-loop system without any form of control. Declare cases that will be used for the evaluation of the closed-loop system’s performance. Whereas Figure 5.6 is modelled to be the closed-loop decoupled PI controller for performance monitoring and behavioural analysis. The objective of this test case is to demonstrate the closed loop performance of the flotation plant with and without the implementation of a PI controller.

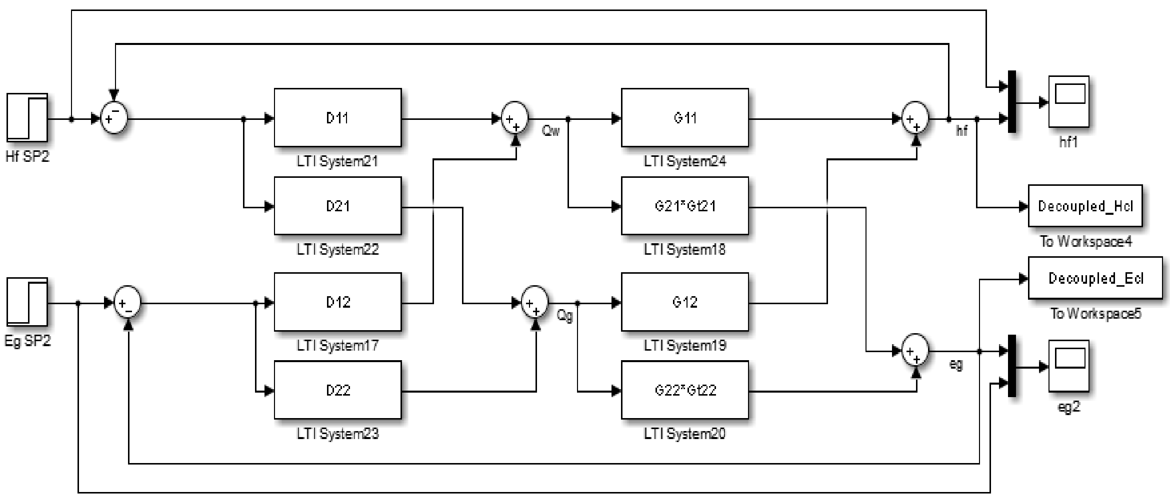


**Figure 5.5**: **Closed loop natural flotation system with unity feedback**

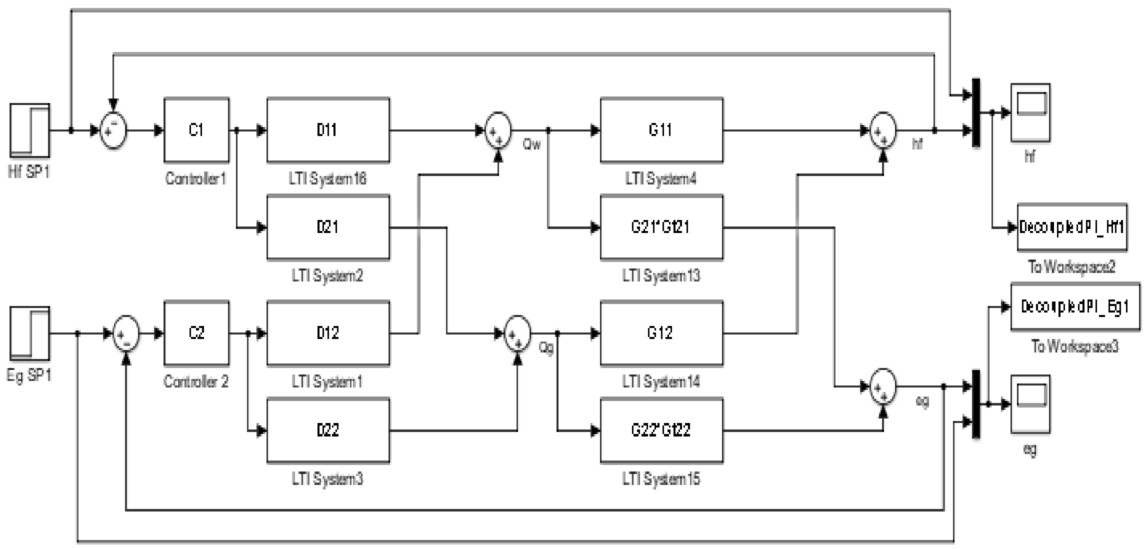


**Figure 5.6:** **Closed loop Decoupled PI flotation Simulink model**

A step input is introduced into both systems, meaning that Hf SPx and Eg SPx both experience a change in set-point of an amplitude of 1 at 0 sec. The Hf SPx and Eg SPx are the froth height setpoint and gas holdup setpoints respectively, where the 'SPx' represents either SP1 or SP2. These setpoints are in relation to figures 5.5 and 5.6. The output characteristics can be displayed in Table 5.3 and the step response of the decoupled PI controllers (Hfcon and Egcon) are compared to the step responses of the closed loops with unity feedback (hcl and Ecl). The Hfcon and Egcon are the closed loop froth height and gas holdup responses with the decoupled PI control action implemented. Whereas the hcl and Ecl are the decoupled closed loop froth height and gas holdup responses without any control action implemented.

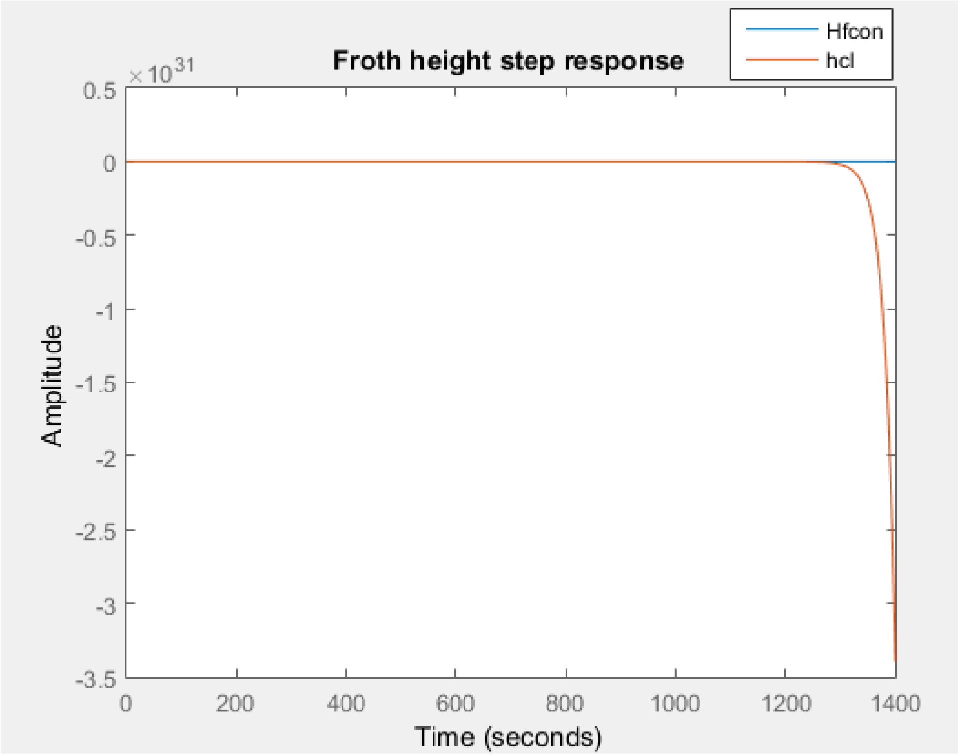

**Figure 5.7:** **Froth height step response comparison of PI (Hfcon) and no controller (hcl)**

Figure 5.7 demonstrates the system's transient behaviour to a step input variation in the setpoint of the froth height. The response labelled as Hcl represents the decoupled froth Height closed-loop system without any controller included as presented by the SIMULINK model in Figure 5.5. The step input is applied to the system the closed-loop response becomes unstable as time tends to infinity. The response labelled as Hfcon represents the decoupled froth height closed-loop system with the PI control implementation. The Hfcon response shows an improvement in stability over time.

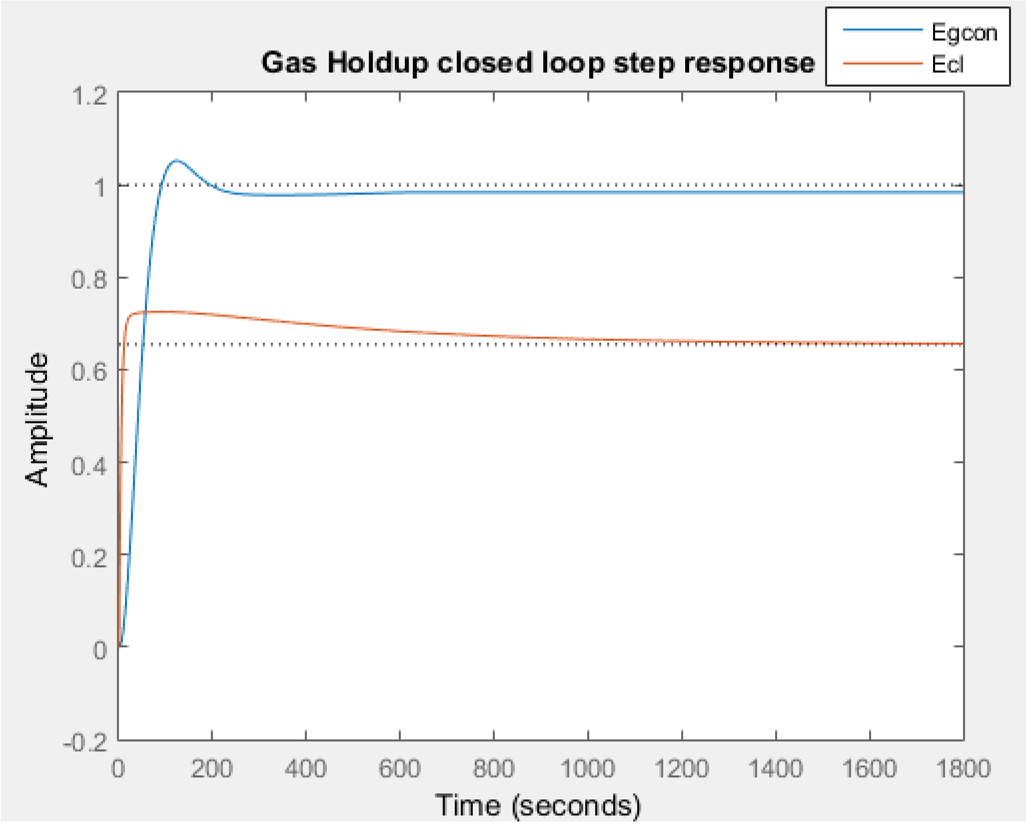


**Figure 5.8:** **Gas holdup step response of a PI (Egcon) and no controller (Ecl)**

Figure 5.8 reveals the system's transient behaviour to a step input variation in the setpoint of the gas holdup. The response Ecl represents the decoupled gas holdup closed-loop system without any control action applied. It can be noted that the Ecl response undershoots and has a large steady-state error. The Egcon response is a representation of the decoupled gas holdup closed-loop system with the PI control action. As a result, the steady-state error is largely reduced, due to the involvement of the designed PI controller.

**Case 2: Setpoint tracking**

This case simulates multiple changes made to the setpoint pulse signal over a given period. As per Table 5.2 case 2, the four changes made to the setpoint pulse signal of both the decoupled PI controlled system seen in Figure 5.10, and the decoupled system without the PI controller seen in Figure 5.9. This case aims to observe the setpoint tracking performance of the decoupled PI controlled system and measure the performance against a system without any control action applied.

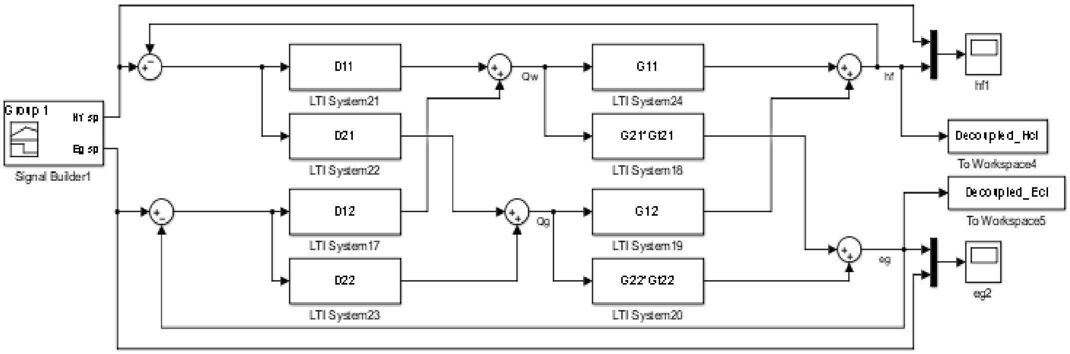


**Figure 5.9:** Decoupled closed loop Setpoint Tracking Model

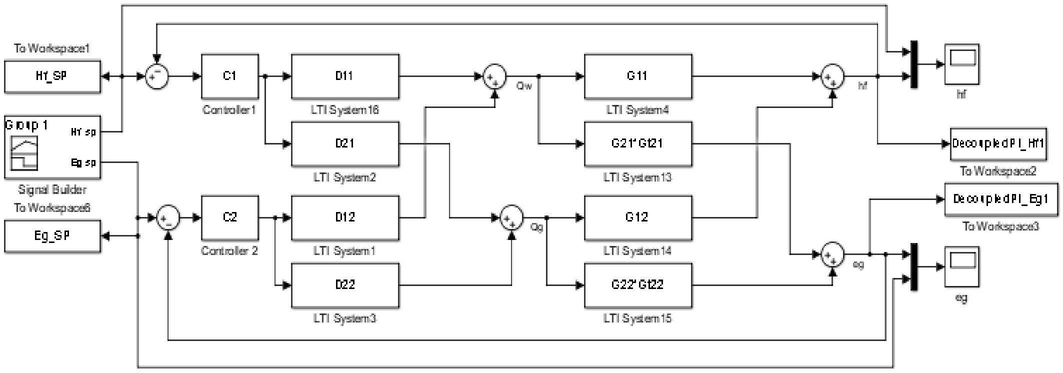


**Figure 5.10:** Decoupled PI controlled Setpoint Tracking Model

The signal builders seen Figure 5.10 and Figure 5.9 are used to create the pulse amplitude variations at different times to simulate the variations in setpoints. The output of both modelled systems is measured against the desired setpoints.

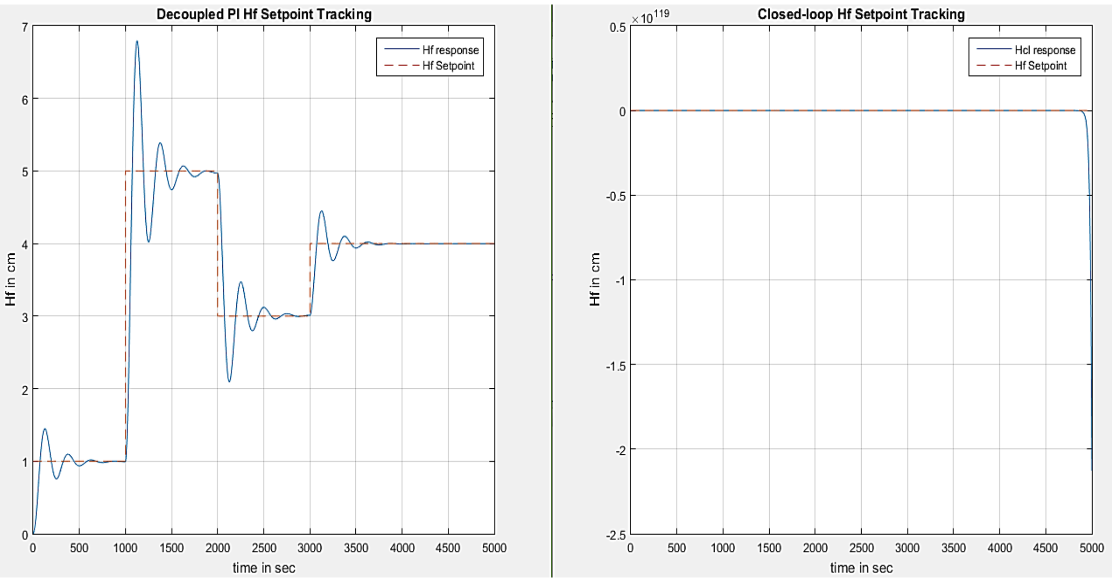


**Figure 5.11:** Setpoint Tracking Response of Decoupled froth height (Hf) Closed-loop response with PI (Left) and without a controller (Right)

The froth height setpoint tracking is displayed in Figure 5.11. The response titled Decoupled PI has the decoupled PI controller implemented along with the froth height setpoint changes. The plot titled Closed-loop Hf has only the decouple implementation and no PI control action. By observation of Figure 5.11, the decoupled closed-loop Hf demonstrates instability and oscillations over time. However, with the implementation of the PI control action the Hf maintains some form of stability. This allows the Hf to adjust to multiple setpoint changes despite the high overshoot.

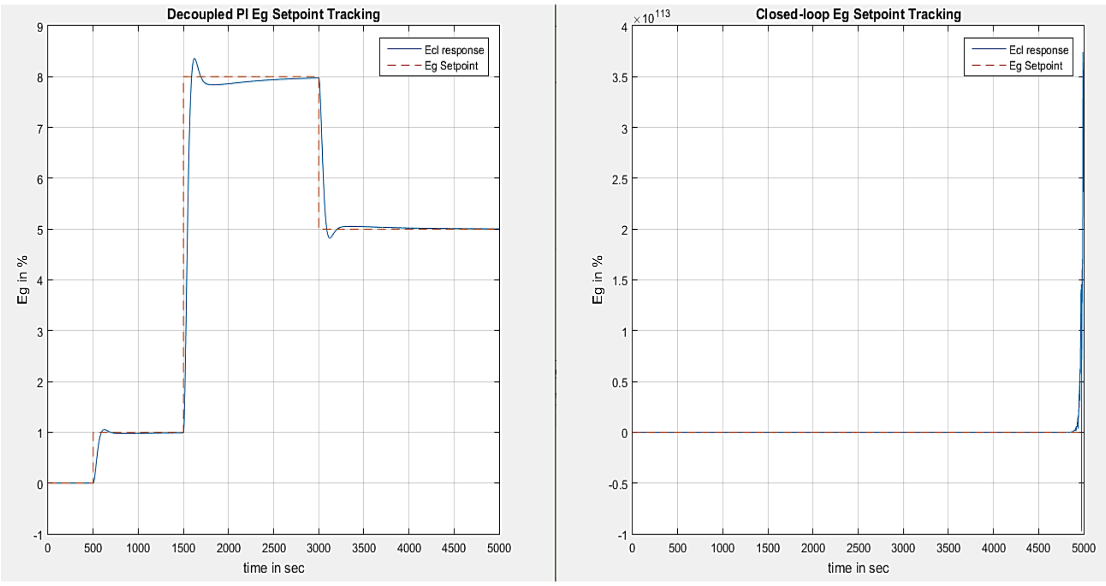


**Figure 5.12: Eg Setpoint Tracking Response of Decoupled PI (Left) and Closed-loop natural response (Right)**

The gas holdup setpoint tracking is displayed in Figure 5.12. The response titled Decoupled PI Eg has the decoupled PI controller implemented along with the gas holdup setpoint changes. The plot titled Closed-loop Eg has only the decouple implementation and no PI control action. By observation of Figure 5.12, the decoupled closed-loop Eg demonstrates instability and oscillations over time. However, with the application of the PI control action the Eg maintains its stability. This allows the Eg to adjust to multiple setpoint changes with the desired overshoot and damping ratio.

### Case 3: Disturbance scenario 1

This test case introduces impulse responses as disturbances to the output response of each loop. The decoupled PI controlled model in Figure 5.14 and the decoupled model without the PI controller in Figure 5.13 are both subjected to these disturbances. The aim of this case is to monitor the effectiveness of the decoupled PI controlled model's ability to suppress a disturbance when imposed onto the froth height (hf) or the gas holdup (eg). The derivative blocks help to create the effect of an impulse response with a sample time of 10 sec.

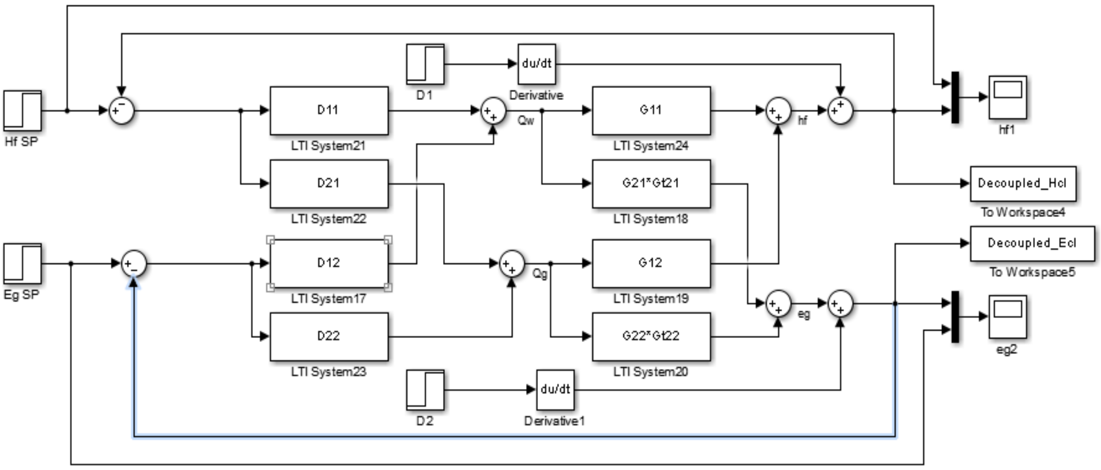


**Figure 5.13:** **Disturbance Scenario 1 Closed loop natural flotation system with unity feedback**

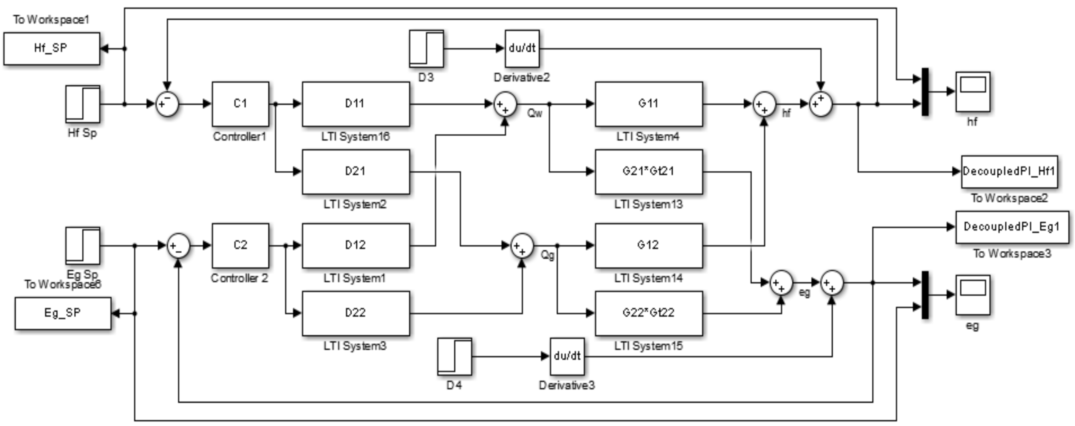


**Figure 5.14:** **Disturbance Scenario 1 Decoupled PI controlled flotation system with unity feedback**

A step response with an amplitude of 1 is added to Hf and Eg of both models in Figure 5.14 and Figure 5.13 when t = 0 seconds. The system is given time to settle until a disturbance D1-D4 is added to both the froth height and gas holdup control loops at t = 1200 seconds. The amplitude of the disturbances was set to 0.001.

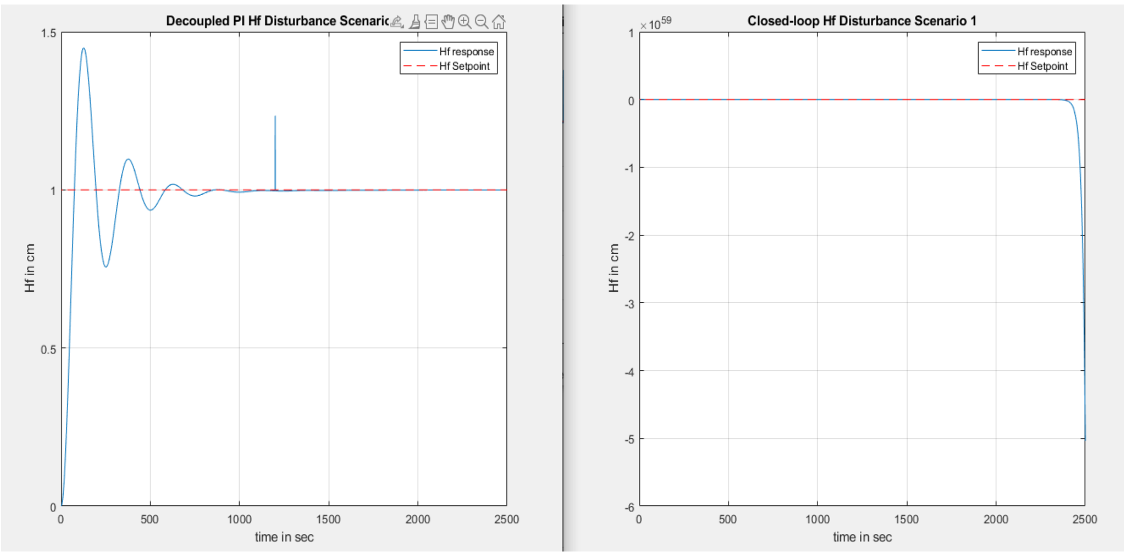


**Figure 5.15:** **Disturbance Scenario 1 Decoupled closed-loop Hf response with PI controller (Left) and without a controller (Right)**

The results of the froth height disturbance scenario 1 are displayed in Figure 5.15. The response titled Decoupled PI Hf has the decoupled PI controller implemented along with the froth height step response and disturbance imposed. The plot titled Closed-loop Hf has only the decouple applied and no PI control action. By observation of Figure 5.15, it can be seen that the decoupled closed-loop Hf demonstrates instability and oscillations over time at magnitudes too great to witness the effect of the disturbance. However, with the application of the PI control action, the Hf maintains minimal stability with little to no disturbance dominance.

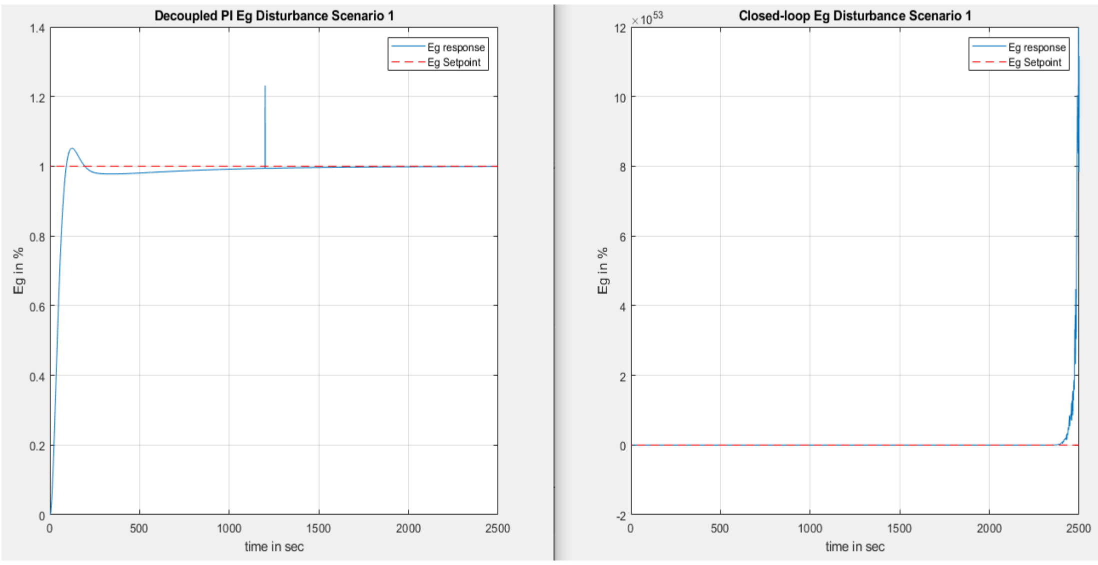


**Figure 5.16:** **Disturbance Scenario 1 Decoupled closed-loop Eg response with PI controller (Left) and without a controller (Right)**

The gas holdup disturbance scenario 1 is displayed in Figure 5.16. The response titled Decoupled PI Eg has the decoupled PI controller implemented along with the froth height step response and disturbance imposed at the output side of the system. The plot titled Closed-loop Eg has only the decouple applied and no PI control action. By observation of Figure 5.16, it can be seen that the decoupled closed-loop Eg demonstrates instability and oscillations over time at magnitudes too great to witness the effect of the disturbance. However, with the implementation of the PI control action the Eg maintains minimal stability with little to no effect of the disturbance.

**Case 4: Disturbance scenario 2**

This test case introduces disturbances at the input stage of the flotation system for each loop. The decoupled flotation system without the PI controller is shown in Figure 5.17 and the decoupled PI controlled model in Figure 5.18, both models will be subjected to these disturbances. The aim of the case is to monitor the effectiveness of the decoupled PI controlled model's ability to suppress a disturbance when imposed onto the wash water flowrate (Qw) or the gas flow rate (Qg). The derivative blocks help to create the effect of an impulse response with a sample time of 10 sec.

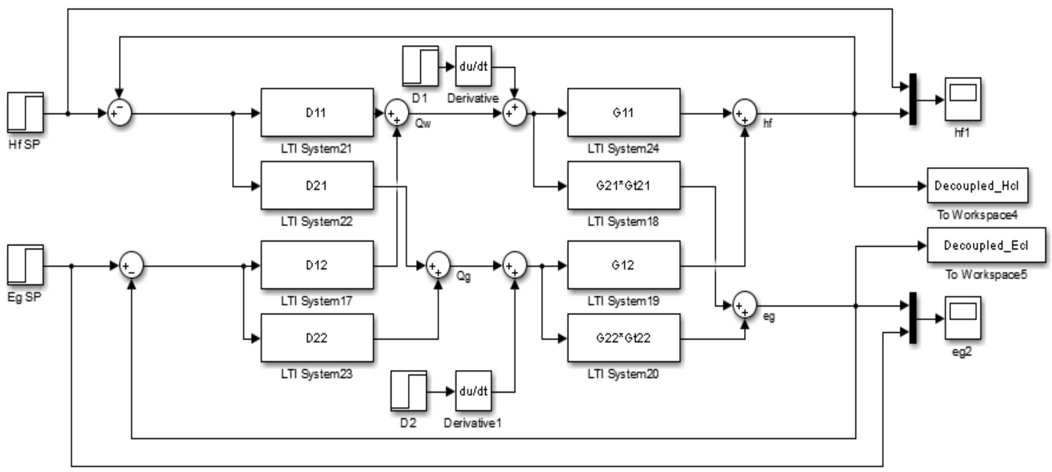


**Figure 5.17:** **Closed loop Decoupled flotation system with unity feedback**

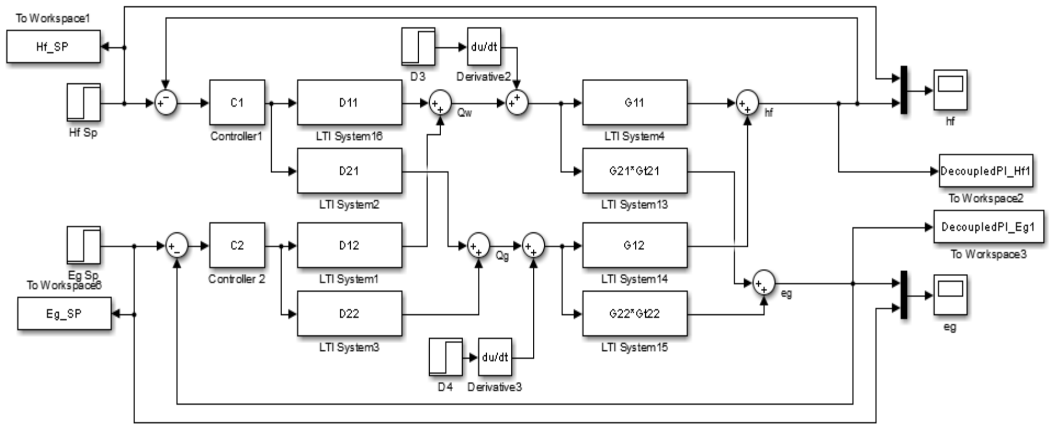


**Figure 5.18:** **Closed-loop-Decoupled and PI controlled flotation system with unity feedback**

A step response with an amplitude of 1 is added to Hf and Eg setpoints of both models in Figure 5.18 and Figure 5.17 when t = 0 seconds. The system is given time to settle until the disturbances D1-D4 are added to both the wash water flowrate and gas flowrate of the froth height and gas holdup control loops at t = 1200 seconds. The amplitude of the disturbances was set to 0.001. The next step is to observe the response of the flotation system under case 4.

The results of the froth height under the disturbance scenario 2 are displayed in Figure 5.19. The response titled Decoupled PI Hf has the decoupled PI controller applied along with the froth height step response and disturbance imposed. The plot titled Closed-loop Hf has only the decouple implementation and no PI control action.

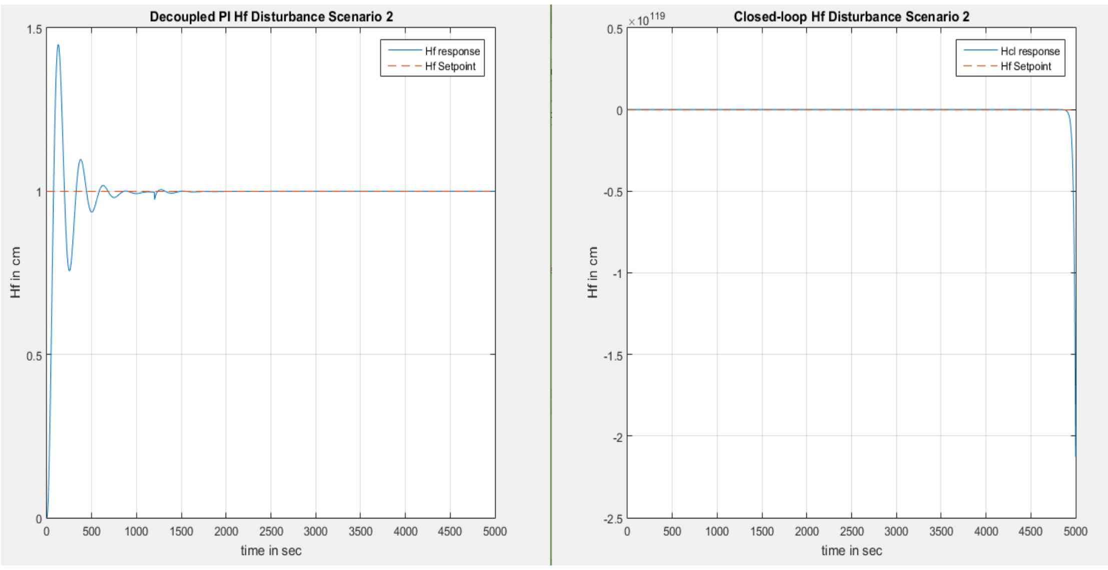


**Figure 5.19:** **Disturbance Scenario 2 Decoupled closed-loop Hf response with a PI controller (Left) and without a controller (Right)**

By observation of Figure 5.19, it can be seen that the decoupled closed-loop Hf demonstrates instability and oscillations over time at magnitudes too great to view the effect of the disturbance. However, with the application of the PI control action the Hf maintains stability with a high overshoot. The disturbance does show visibility, and the controller is seen to provide some disturbance suppression.

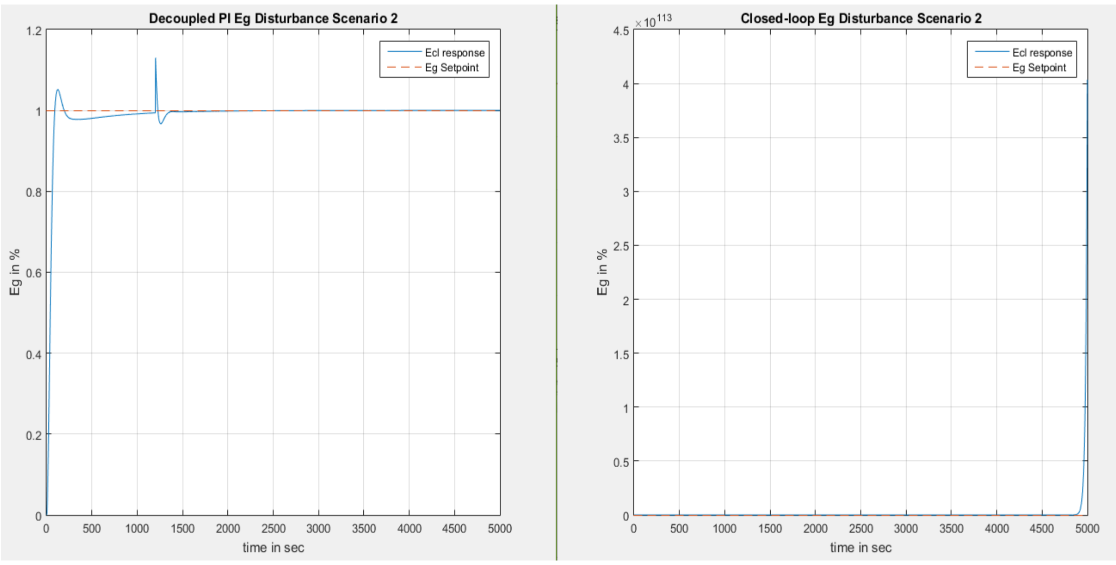


**Figure 5.20:** **Disturbance Scenario 2 Decoupled PI controlled (Left) and closed-loop (Right) Eg response**

The gas holdup disturbance scenario 2 is displayed in Figure 5.20. The response titled Decoupled PI Eg has the decoupled PI controller implemented along with the froth height step response and disturbance imposed. The plot titled Closed-loop Eg has only the decouple implementation and no PI control action. By observation of Figure 5.20, it can be seen that the decoupled closed-loop Eg demonstrates instability after t=0 seconds and tends to infinity over time at magnitudes too great to witness the effect of the disturbance. However, with the implementation of the PI control action the Eg maintains minimal stability with minimal disturbance suppression.

### Test case characteristics

A summary of the test case results characteristics can be found in Table 5.3 below. In case 1, the reference of a step input is used to determine whether the decoupled PI controller performed as designed. The gas holdup control loop (Egcon) performed as per desired specification (Overshoot = 10% and Settling time = 500 seconds). However, the froth height control loop (Hfcon) presented a greater overshoot (55.96%) and longer settling time (850.39 seconds). The froth height control loop did however provide stability as opposed to the decoupled control loop (Hcl). Case 2 shows no change in control structure other than the application of signal builders, hence the characteristics being the same as that of case 1.

For cases 3 and 4, Table 5.3 shows that the peak values are seen when the disturbances are applied at 1200 seconds. The table also indicates that both the froth height and gas holdup control loops settle after 1200 seconds. The decoupled gas holdup control loop (Ecl) for Cases 3 and 4 contains a peak time of 5000 seconds, meaning that the response becomes unstable over time.

**Table 5.3:** **Closed-loop step response characteristics of a flotation process**

| Case: | Control loop | RiseTime (s): | SettlingTime (s): | Overshoot (%): | Peak: | PeakTime (s): | Ess: |
|---|---|---|---|---|---|---|---|
| **1** | Hfcon | 50.6268 | 850.3920 | 55.9666 | 1.5597 | 131.8340 | -0.004 |
| | Hcl | NaN | NaN | NaN | Inf | Inf | Inf |
| | Egcon | 58.6045 | 474.8497 | 5.2085 | 1.0521 | 122.4387 | 0.0102 |
| | Ecl | 7.5288 | 938.7823 | 10.7805 | 0.7250 | 90.6538 | 0.866228355 |
| **2** | Hfcon | 50.6268 | 850.3920 | 55.9666 | 1.5597 | 131.8340 | -0.004 |
| | Hcl | NaN | NaN | NaN | Inf | Inf | Inf |
| | Egcon | 58.6045 | 474.8497 | 5.2085 | 1.0521 | 122.4387 | 0.0102 |
| | Ecl | 7.5288 | 938.7823 | 10.7805 | 0.7250 | 90.6538 | 0.866228355 |
| **3** | Hfcon | 74 | 1200 | 99.69 | 1.9969 | 1200 | 0.0031 |
| | Hcl | NaN | NaN | NaN | Inf | Inf | Inf |
| | Egcon | 91 | 1200 | 99.41 | 1.9941 | 1200 | 0.0102 |
| | Ecl | 213 | 4957 | NaN | 4.0359e+113 | 5000 | -3.6019e+112 |
| **4** | Hfcon | 74 | 1200 | 99.69 | 1.9969 | 1200 | 0.0031 |
| | Hcl | NaN | NaN | NaN | Inf | Inf | Inf |
| | Egcon | 91 | 1296 | 0.1302 | 1.1302 | 1202 | 0.0209 |
| | Ecl | 213 | 4957 | NaN | 4.0359e+113 | 5000 | -3.6019e+112 |

## 5.5 Performance evaluation and discussion

For this section, the MATLAB/Simulink results of the Decoupled PI controllers are analysed and discussed. The performance of each decoupled PI controller is measured against the performance of the decoupled flotation system without the control action applied. The first case is the evaluation of a step response. The second case was to evaluate the setpoint tracking. The third and final case was to evaluate the controller's performance to induced disturbances.

### 5.5.1 Decoupled PI controller for froth height ($H_f$)

The %OS for the system is beyond the desired value of 10% as seen in Table 5.3. This also includes the settling time. However, compared to the natural closed loop feedback response the decoupled PI controller does demonstrate a form of stability. The decoupled PI does show some degree of success by having a steady state error (Ess) of approximately 0. The designed PI controller does provide improved setpoint tracking and disturbance suppression if imposed to the wash water flowrate. However, the disturbance mentioned in test case 3 shows clear evidence despite the system maintaining its stability, as seen in Figure 5.15. Using separate desired system characteristics might help improve the system's performance.

### 5.5.2 Decoupled PI controller for gas holdup ($\varepsilon_g$)

The $\varepsilon_g$ loop PI controller presented itself as less challenging to analyse having no right-hand side (RHS) poles, making the natural closed loop response stable. As seen in Table 5.3, the %OS also differs from the desired response, but the settling time almost matches the desired characteristics. However, when measuring the decoupled PI response against the natural response it is observed that the decoupled PI-controlled system has a better steady-state error (Ess). The designed PI controller does provide improved setpoint tracking and minimal disturbance suppression if imposed to the gas flowrate. The disturbance mentioned in test case 3 shows clear evidence despite the system maintaining its stability, as seen in Figure 5.16.

## 5.6 Challenges and limitations

The froth flotation process is renounced for the interconnecting control loop, rendering the controller design and tuning quite challenging. Initially, the decoupled design had to be revisited on numerous occasions due to its ineffectiveness to separate the froth height control loop from the gas holdup control loop. The developed decoupler does however show separation of control loops but demonstrates poor set point tracking capabilities. Hence the need for a controller.

The decoupled plant presented a higher-order system, resulting in the use of non-dominant poles and pole-zero cancelation being necessary to design and tune the PI controller. The froth height loop shows a lack of disturbance suppression when induced onto the froth height and a greater overshoot and settling time than that of the desired system.

## 5.7 Conclusion

In this chapter, a flotation decoupled PI controller was presented. The decoupled design presented no interconnection and resulted in success with the separation of the two control loops. The P and I parameters were tuned using the pole placement method. The decoupled PI controllers were modelled in SIMULINK and analysed against their desired performance and the decoupled closed loop natural performance. As a result, the decoupled PI demonstrated exceptional performance with regard to steady state error but does leave some room for improvement.

# CHAPTER 6 : ADVANCE CONTROLLER DESIGN

## 6.1 Introduction to model adaptive control

In this chapter, A Model Reference Adaptive Controller (MRAC) is designed as an advanced controller. The purpose of this advanced controller is to fulfil the limitations of the decoupled PI controller mentioned in the previous chapter. The objective of this chapter is to develop the adaptive controller and to analyse its performance based on predetermined test conditions. A brief explanation of the functionality of the adaptive controller is given. With the flotation system still decoupled, the model reference adaptive controller is developed. The MRAC controller is then simulated using MATLAB/Simulink and the result analysed based on the given criteria. The controller design challenges and limitations are also noted towards the end of this chapter.

An adaptive control system automatically compensates for changes in system dynamics by adjusting the controller characteristics so that the overall system performance remains the same, or relatively maintained at an optimum level. This control system considers any degradation in plant performance with time. The benefit of using Model Reference Adaptive Control (MRAC) is that it provides quick adaptations for the defined inputs. Therefore, model-reference controllers are added, due to their adaptation mechanism. Model Reference Adaptive Control (MRAC) theory is designed to adjust the controller parameters in a way that the actual plant output would track the output of a reference model using the same respective inputs, (Jain & M.J, 2013).

This chapter contains a brief overview of the methodology behind Model Reference Adaptive Control. The Massachusetts Institute of Technology (MIT) theory of MRAC is then applied to the decentralized decoupled flotation process, this can be seen in section 6.2 of the current chapter. The reference model is primarily generated, followed by the decentralized decoupled controller design. The result of the design is then evaluated under the MATLAB/Simulink environment in section 6.3. The results analysis, challenges, and limitations are mentioned in sections 6.4 and 6.5 respectively.

## 6.2 Reference model development and adaptation rule

The MRAC design consists of a reference model, controller, and adjustment mechanism. The reference model is used to get the desired response. The controller or control law parameter $\theta$ is described as a collection of adjustable parameters, but mainly dependent on the adaptation gain (ɣ). The adjustment mechanism alters the controller parameters to track the response of the reference model. For this design, we will be using the Massachusetts Institute of Technology (MIT) rule presented in (Jain & M.J, 2013) as the controller adjustment mechanism.

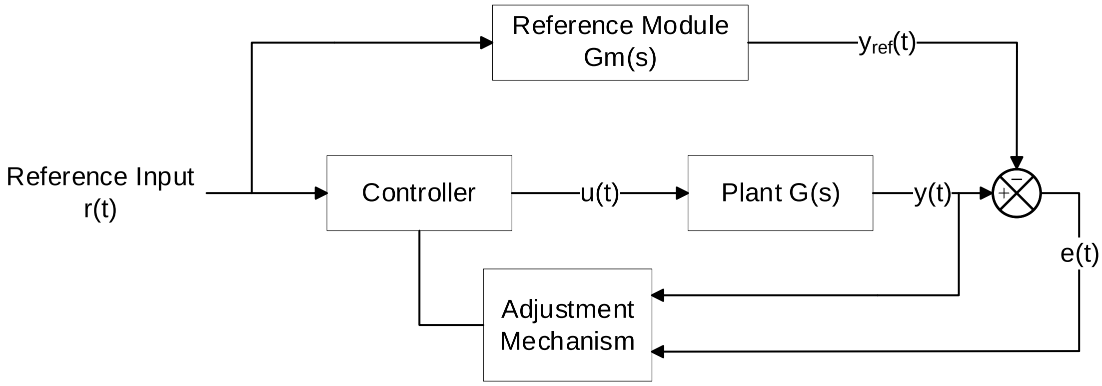


**Figure 6.1:** **MRAC system, (Jain & M.J, 2013)**

### 6.2.1 Reference model development

The development of a reference model is to achieve the desired response of the reference input. For the decoupled system each control loop consists of a reference model. A second-order system is used to obtain the desired response. For this research, the assumption is made that the plant parameters are unknown. When designing a reference model, these are general assumptions to be made. This assumption simplifies the determination of the desired closed-loop poles by using the second-order characteristic equation below.

$$G(s) = \frac{\omega_n{}^2}{s^2+2\zeta\omega_n s+\omega_n{}^2} \qquad (6.1)$$

To achieve the desired characteristics, the second-order characteristic equation is used to determine the Rise Time ($t_r$), Settling time ($t_s$), Percentage overshoot (*%OS*), peak time ($t_p$), and time delay ($t_d$). To emphasize this, a Percentage overshoot of 10% and a settling time of 500 sec was used. The percentage overshoot and settling time values are chosen based on the decoupled PI controller design. This will reduce the complexity of comparing the PI controller and MRAC controller design. With the desired %OS given as 10% the desired damping ratio $\zeta$ and undamped natural frequency $\omega_n$ can be determined by the following equations (6.2) and (6.3).

$$\zeta = \sqrt{\frac{\ln\left(\frac{\%Os}{100}\right)^2}{\pi^2+\ln\left(\frac{\%Os}{100}\right)^2}} \qquad (6.2)$$

$$\omega_n \approx \frac{4}{\zeta t_s} \qquad (6.3)$$

Where:

$\zeta = 0.5912$ and $\omega_n = 0.0135$

Thus, substituting the desired $\zeta$ and $\omega_n$ results into our second-2nd order characteristic equation 6.4 the following desired open loop characteristic equation is achieved:

$$\boldsymbol{Gm(s)} = \frac{\mathbf{0.0001831}}{\boldsymbol{s^2+0.016\,s+0.0001831}} \tag{6.4}$$

The Simulink model that represents the reference model can be seen in Figure 6.2 below.

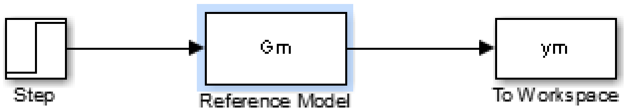


**Figure 6.2: Simulink block diagram**

Once the reference model is achieved, the Adaptation rule can now be applied to the system.

### 6.2.2 Adaptation rule

The adaptation rule known as the sensitivity model or the MIT rule is derived by the selection of a quadratic performance criteria to minimise the set point tracking error over a given period. The criteria can be defined by the following integral, also known as the cost function, (J. Candy, 2021):

$$\boldsymbol{J(t+T) = \frac{1}{2}\int_t^{t+T} e^2(\tau;\theta)\,d\tau} \tag{6.5}$$

For:

$$\boldsymbol{e(t;\theta) = x_p(t) - x_m(t)} \tag{6.6}$$

Where:

$e(t;\theta)$ = tracking error

$x_p(t)$ = Process/Plant Model

$x_m(t)$ = Reference Model

With $\theta_i$ being the unknown parameters of $x_p(t)$ and $x_m(t)$ over the tracking error period $T$. Based on the decreasing criterion seen in equation 6.5, these parameters are updated as follows:

$$\boldsymbol{\theta(t+T) = \theta(t) - \gamma \frac{\partial J}{\partial \theta} = \theta(t) - \gamma \int_t^{t+T} e(\tau;\theta) \frac{\partial e(\tau;\theta)}{\partial \theta} \partial \tau} \tag{6.7}$$

Thus,

$$\boldsymbol{\frac{\theta(t+T)-\theta(t)}{T} = -\frac{\gamma}{T} \int_t^{t+T} r(\tau;\theta) \frac{\partial x_p(t;\theta)}{\partial \theta} \partial \tau} \tag{6.8}$$

Where:

$$\boldsymbol{\frac{\partial e(\tau;\theta)}{\partial \theta} = \frac{\partial x_p(t;\theta)}{\partial \theta}} \tag{6.9}$$

As $lim_{T\rightarrow 0}$ the change in parameters are as follows

$$\boldsymbol{\frac{\partial \theta(t)}{\partial t} = -\gamma \times e(t;\theta) \times \frac{\partial x_p(t;\theta)}{\partial \theta}} \tag{6.10}$$

The sensitivity to changes in the state parameters is known as the sensitivity derivative. In practice, this technique is occasionally known as the gradient technique or the MIT rule. It is also stated that the technique does not always guarantee system stability, (Candy, 2021). The next subsection is based on the decoupled MRAC design for the flotation process, aiming to design a decoupled controller for both the froth height and gas holdup.

### 6.2.3 Decoupled MRAC design for the flotation process

The decoupled MRAC controller is designed in Simulink using the MIT rule. The objective is to design a decoupled controller for both the froth height and gas holdup with the ability to track their respective reference models. Working in the s-domain, the error can be defined by the following equation.

$$\boldsymbol{E(s) = K_T T(s) U(s) - K_m Gm(s) Uc(s)} \tag{6.11}$$

Where:

T(s) = Decoupled flotation process

Gm(s) = Reference model transfer function

$K_T$ = Decoupled flotation process gain

$K_m$ = Reference model gain

Uc(s) is used to define the control law:

$$u(t) = \theta * u_c(t) \tag{6.12}$$

With partial differentiation:

$$\frac{\partial E(s)}{\partial \theta} = K_T T(s) Uc(s) = \frac{K_T}{K_m} Y_m(s) \tag{6.13}$$

Resulting in a sensitivity derivative of:

$$\frac{\partial \theta(t)}{\partial t} = -\gamma\, e \frac{K_T}{K_m} y_m = -\gamma' e\, y_m \tag{6.14}$$

The law mentioned in equation 6.14 above is used for adjusting the parameters of $\theta$. The law is applicable to both decoupled control loops (froth height and gas hold-up) resulting in the Simulink model presented in Figure 6.3. The Reference Model 1 (RM1) and Reference Model 2 (RM2) blocks are the reference model transfer functions of the respective froth height and gas hold-up. The control law is implemented by Product 2 and Product 6 (which can be seen highlighted in Figure 6.3). For this model, the adaptive gains (Gama1 and Gama2) are chosen to be +0.005 and -0.005 respectively. The adaptation gain can be any real value > 0. Equation 6.14 is used to design the Model Reference Adaptive controller shown in Figure 6.3.

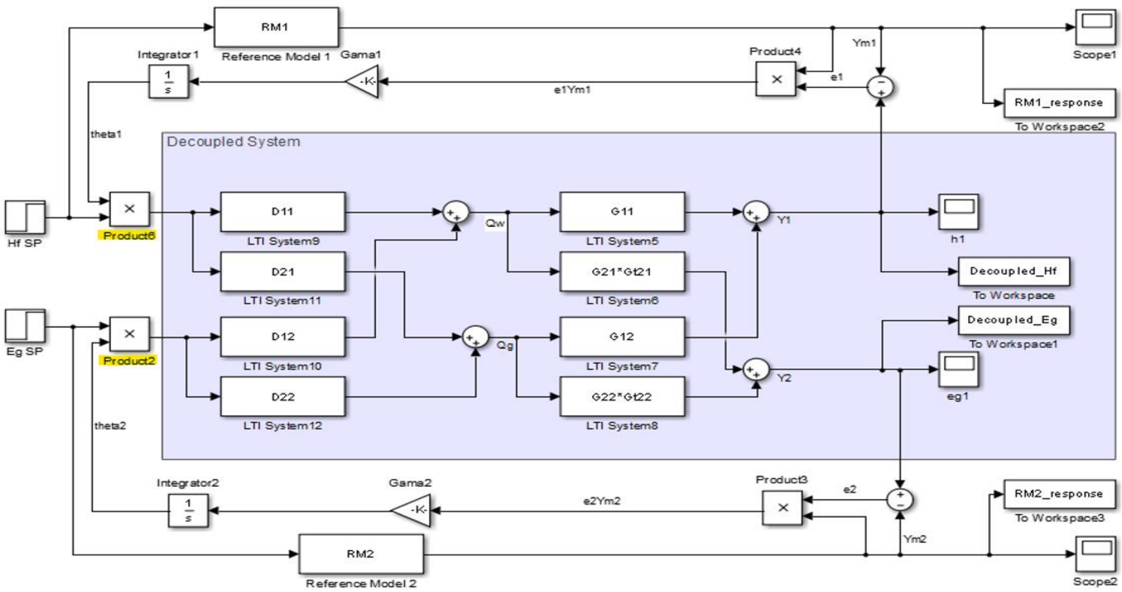


**Figure 6.3:** **MRAC MIT rule of a decoupled flotation process**

The next section is based on the analysis of the decoupled MRAC of the flotation process.

### 6.3 Decoupled model reference adaptive controller design analysis

In this section, the design analysis is separated into three test cases. The first case is the characteristic analysis of the controlled system. The second case is the setpoint tracking analysis and the third case is the controlled system reaction against disturbance. The conditions of these test cases can be seen in Table 6.3 below.

**Table 6.1:** **Test Case Conditions of the designed MRAC**

| Cases | Hf | | Eg | | Description |
|---|---|---|---|---|---|
| | Setpoints (cm) | Time (kilo-sec) | Setpoint (%) | Time (kilo-sec) | |
| **1** | 0-1 | 0 | 0-1 | 0 | A step input is implemented at 0 seconds to observe the characteristics of the Simulink model mentioned in Figure 6.1. The aim is to compare the MRAC performance of the system with the desired reference model. |
| **2** | 1-5-3-4 | 0-1-2-3 | 1-8-5-5 (%) | 0.5-1.5-3-4 | This case simulates four changes made to the setpoint pulse signal. As indicated in the height loop, the changes are made from 1,5,3, and 4 at different times to the air-loop the changes. The aim is to observe MRAC controller performance under numerous setpoint changes. |
| **3** | 0-1 | 0 | 0-1 | 0 | A disturbance is introduced into the system for both the froth height and gas holdup control loops. This case aims to observe the designed controller's ability to maintain the stability of the system as the disturbances are applied to the froth height and gas holdup. |
| **4** | 0-1 | 0 | 0-1 | 0 | A disturbance is introduced into the system through the wash water flow rate and gas flow rate. The aim of this case is to observe the controller's stability as the disturbances are applied to the flotation plant flow rates. |

To investigate the performance and properties of the decoupled MRAC design of the flotation process, the controlled variables are monitored and measured against the reference model. This method is used to determine the controller's performance to reference model tracking. The flotation plant is developed in MATLAB/SIMULINK for closed-loop performance monitoring and behavioural analysis of the controlled process when subjected to various setpoint adjustments as shown in Figure 6.4.

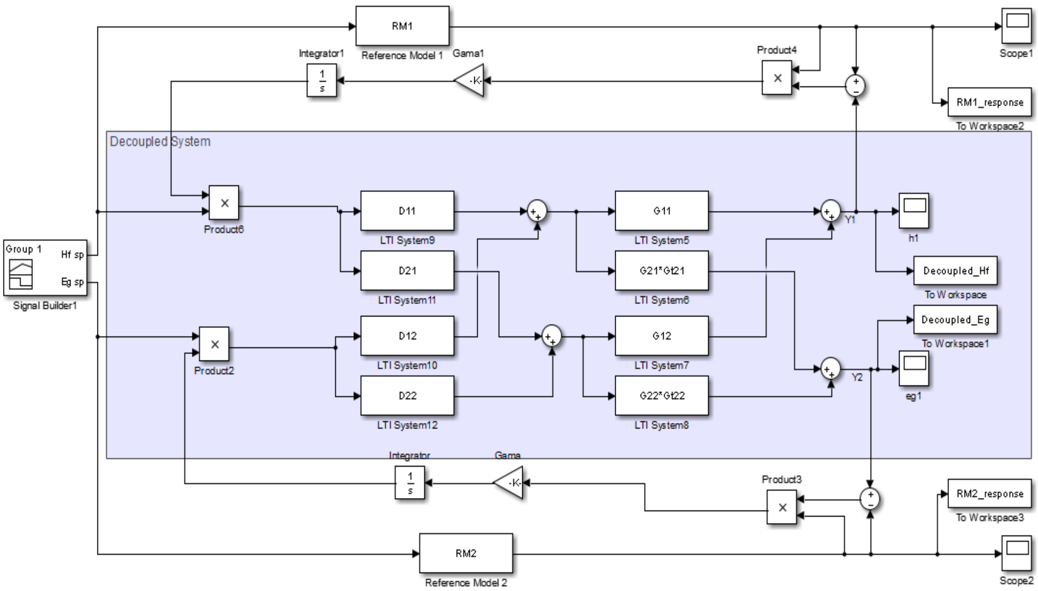

**Figure 6.4:** **MRAC Simulink analysis model of the flotation process**

### 6.3.1 Model reference adaptive control step response analysis

#### Case 1: Test description

A step input is introduced into both systems, meaning that the froth height setpoint (Hf SP) and gas holdup setpoint (Eg SP) both experience a change in set-point of amplitude of 1 at 0 sec. The output characteristics can be displayed in Table 6.2 and the step response of the decoupled MRAC controllers (Hf response and Eg response) are compared to the step responses of the reference models (RM1 and RM2 response) in Figure 6.5.

#### Case 1: Test results

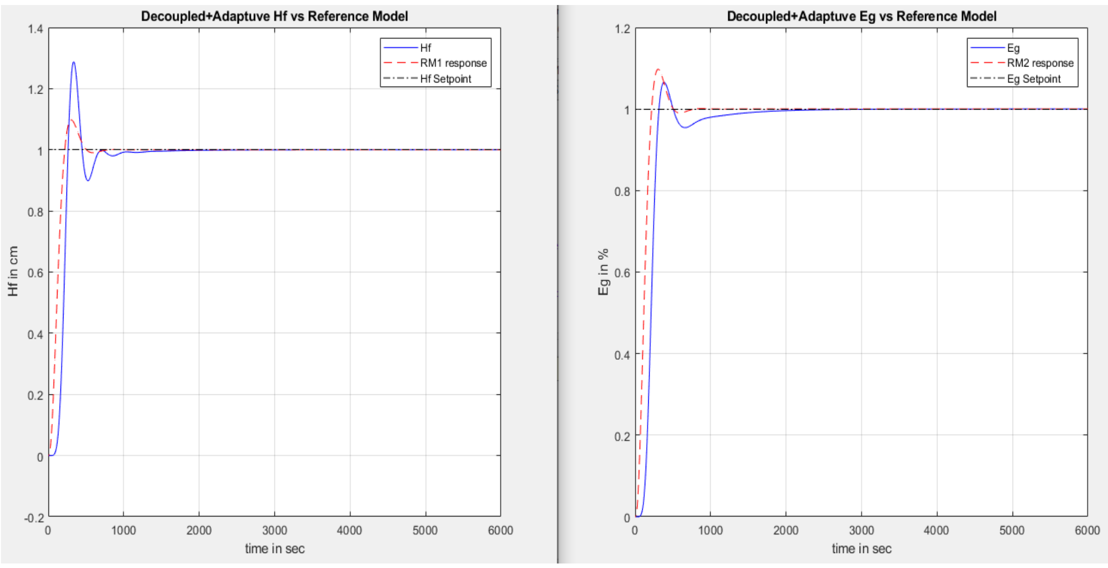


**Figure 6.5:** **MRAC decoupled controller step response gamma = 0.005**

Figure 6.5, presents the step response of the decoupled MRAC system for both controlled variables. The Froth height (Hf) is displayed on the left-hand side and the Gas holdup (Eg) to the right-hand side. Analysing the froth height step response, the controlled loop response (Hf) has a higher overshoot and longer settling time as opposed to the gas holdup (Eg). The controlled variables (Froth height and Gas holdup) responses are seen to have a slight time delay when measured against the reference models RM1 and RM2. This is due to the natural time delay in the flotation plant transfer function.

**Table 6.2:** **MRAC design characteristics to a step response**

| Characteristics | Hf (cm) | RM1 | Eg (%) | RM2 |
|---|---|---|---|---|
| RiseTime (sec): | 244.6465 | 135.5231 | 284.9500 | 135.5231 |
| SettlingTime (sec): | 523.6977 | 437.8855 | 500.0000 | 437.8855 |
| Overshoot (%): | 29.1733 | 10.0000 | 6.7557 | 10.0000 |
| Peak: | 1.292 | 1.1000 | 1.0674 | 1.1000 |
| PeakTime (sec): | 328.3780 | 287.8231 | 361.1478 | 287.8231 |

### 6.3.2 Model reference adaptive control setpoint tracking analysis

#### Case 2: Test description

The MRAC Simulink model in Figure 6.4 is then subject to several setpoint variations best described in Table 6.3. This is to monitor the MRAC controller performance under different adaptation gains or gamma $\gamma$ settings.

**Table 6.3:** **Set point variations for MRAC simulation.**

| Hf | | Eg | |
|---|---|---|---|
| Setpoint | Time (sec) | Setpoint | Time (sec) |
| 1 | 0 | 1 | 500 |
| 5 | 1000 | 8 | 1500 |
| 3 | 2000 | 5 | 3000 |
| 4 | 3000 | 5 | 4000 |

**Case 2: Test results**

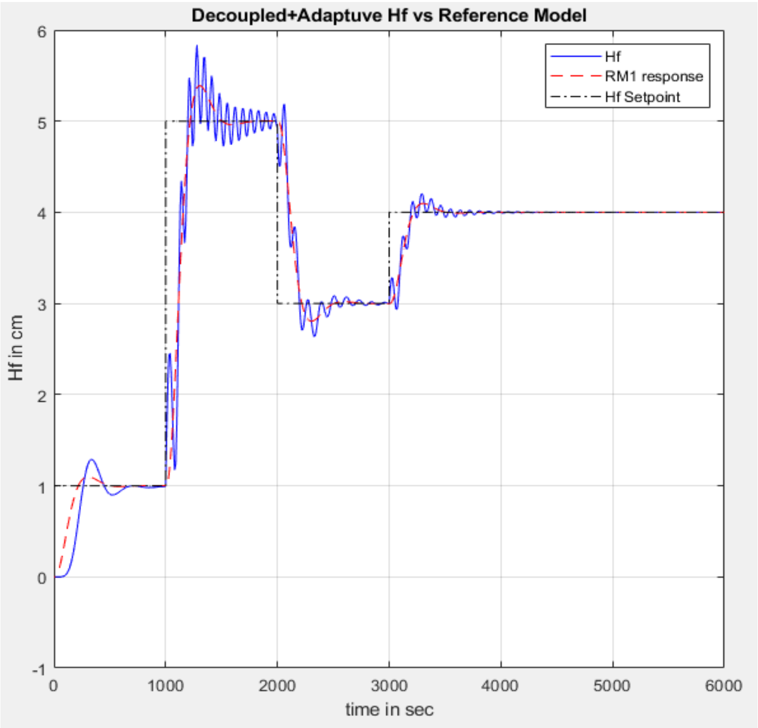


**Figure 6.6:** **MRAC response of froth height with gamma = 0.005**

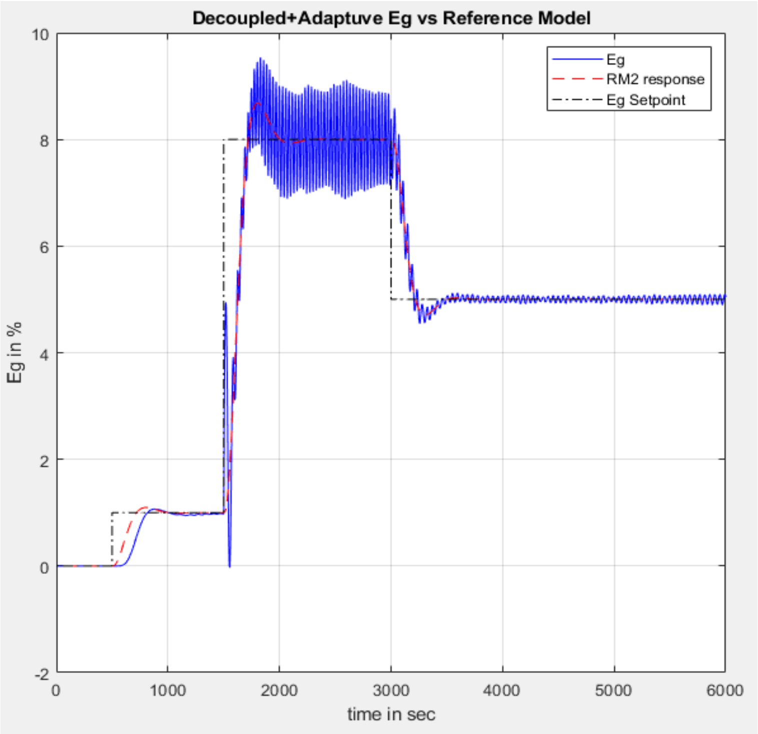


**Figure 6.7:** **MRAC response of gas holdup with gamma = 0.005**

It can be seen from Figure 6.6 and Figure 6.7 that the Model Reference Adaptive controller responds positively to minor setpoint variations. However, despite the setpoint tracking still being evident, setpoint variations at a larger magnitude will result in instability and oscillations. This can be fixed by reducing the gamma value for the Adaptive controller.

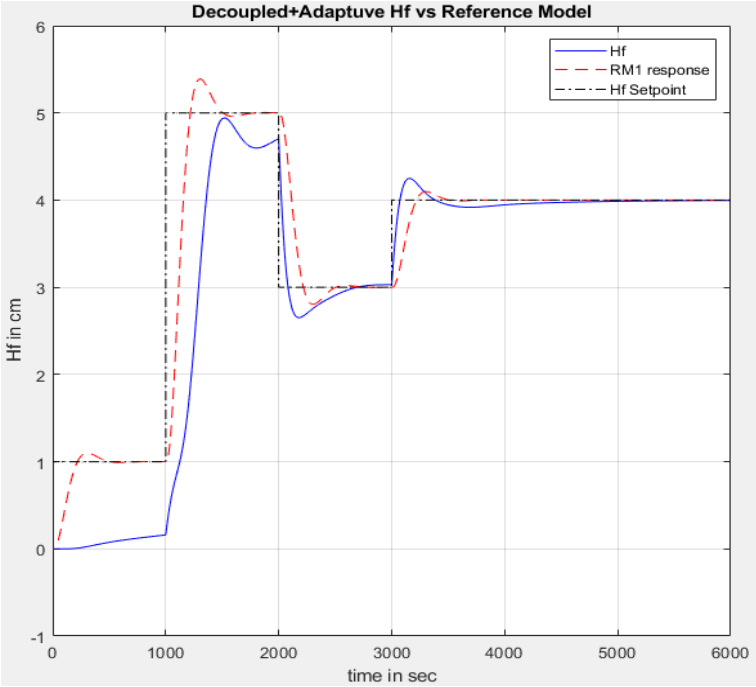


**Figure 6.8:** MRAC response of froth height with gamma = 0.00005

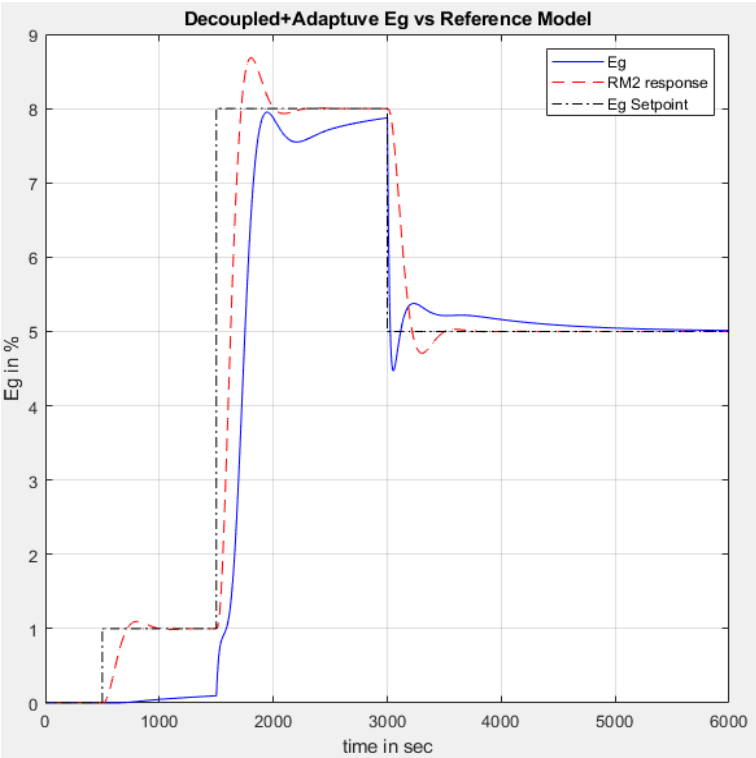


**Figure 6.9:** MRAC response of gas holdup with gamma = 0.00005

Figure 6.8 and Figure 6.9 shows the setpoint tracking of the adaptive controller design. The gamma values for both adaptive controllers are reduced to manage larger setpoint variations. The settling time and rise time have noticeably increased when minor setpoint changes occur. Resulting in the controller becoming less responsive to these minor setpoint changes.

### 6.3.3 Model reference adaptive control evaluation against disturbance

In this subsection, the designed Decoupled MRAC is measured against disturbances induced before and after the plant. The procedure is separated into two scenarios based on where the disturbances occur. The first scenario introduces the disturbance at the output of each loop, whereas the second scenario introduces the disturbance to the flotation plant flow rates.

#### 6.3.3.1 Case 3: Disturbance scenario 1

Impulse responses (D1 and D2) are added to the output response of each loop (y1 and y2) in Figure 6.10, this is done to evaluate the effectiveness of the system to disturbance rejection imposed onto the froth height (y1) or the gas holdup (y2). The derivative blocks assist in creating the effect of an impulse response with a sample time of 10 sec. The purpose of this scenario is to monitor the effects of the system and controller under the disturbance of the plant outputs (froth height and gas holdup in the collection zone).

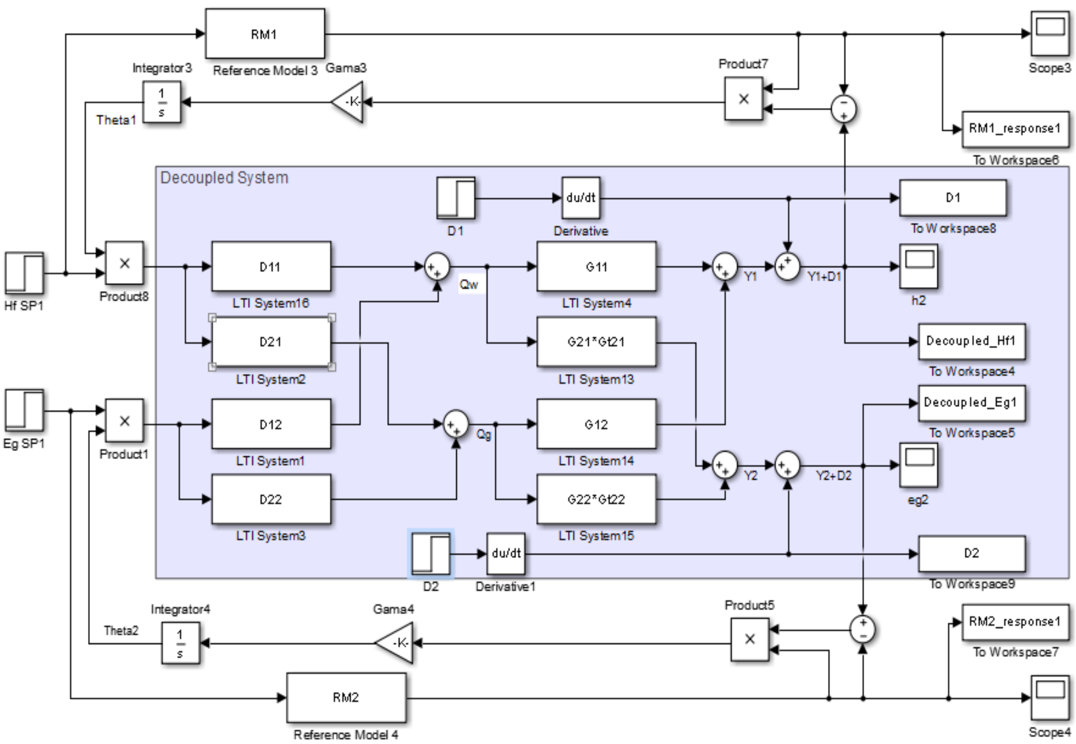


**Figure 6.10: Decoupled MRAC with disturbance scenario 1**

The test conditions (TC) are defined in Table 6.4 below, indicating the setpoint changes in froth height and gas holdup. The gamma is varied to compensate for the larger amplitude setpoint variations in test conditions C and D. As well as the disturbances induced at the given time in columns 4 and 5 of the following Table 6.4.

**Table 6.4:** **Scenario 1 Test conditions**

| Gamma = 0.005 | | | | |
|---|---|---|---|---|
| **TC** | **Setpoint of Hf & Eg** | **Time (sec)** | **D1 & D2** | **Time (sec)** |
| **A** | 1 | 0 | 0.01 | 1200 |
| **B** | 1 | 500 | 0.1 | 200 |
| **Gamma = 0.00005** | | | | |
| **C** | 0-10 | 0 | 0.01 | 200 |
| **D** | 0-10 | 500 | 0.1 | 1200 |

### Test condition A:

The simulation based on the Test condition A values described in Table 6.4 were used in the SIMULINK diagram displayed in Figure 6.10. The setpoints of the froth height (Hf) and gas hold up (Eg) were changed to 1 at a time of T=0 sec. The step response settles well until the disturbance is implemented at a time of T=1200 sec. The controller response is plotted against its respective reference models in Figure 6.11. The aim of this test condition is to monitor the controlled system stability when a disturbance occurs after a minor change in setpoint.

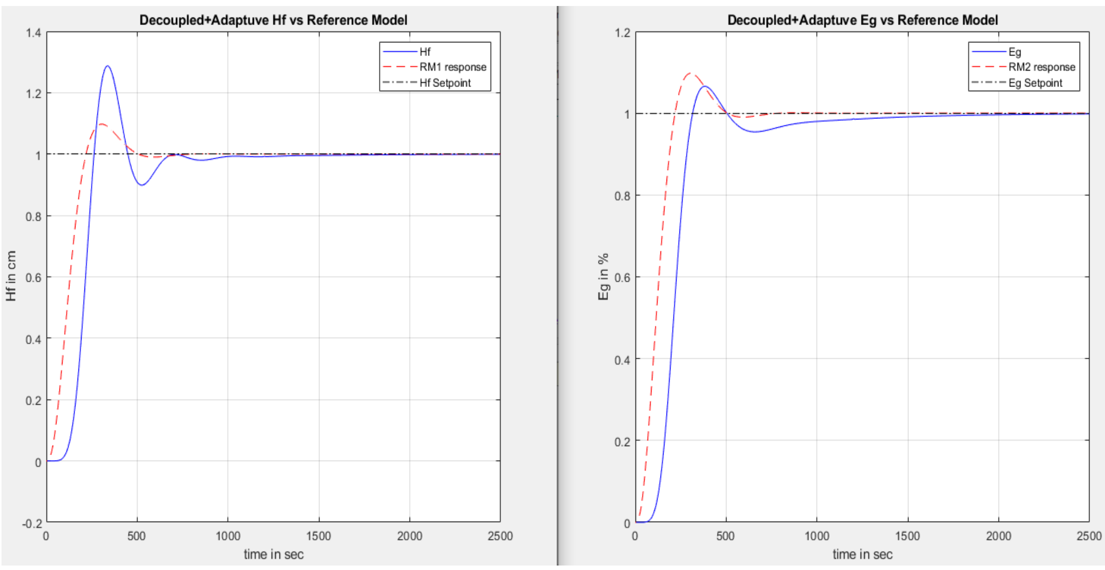


**Figure 6.11:** **Decoupled MRAC Scenario1 Test Condition A response**

Comparing the reaction of the system for both loops with and without the reference model, it can be noted that the response with reference model rejected well and effectively managed the disturbance. The disturbances of D1 and D2 are shows no clear sign of visibility to the output responses of Hf and Eg respectively. However, the system maintained its stability.

**Table 6.5:** Scenario 1 Test condition A response characteristics

| Characteristics | Hf (cm) | RM1 | Eg (%) | RM2 |
|---|---|---|---|---|
| **RiseTime (sec):** | 260 | 210 | 310 | 210 |
| **SettlingTime (sec):** | 750 | 450 | 1200 | 450 |
| **Overshoot (%):** | 28.7764 | 9.75 | 8.45 | 9.75 |
| **Peak:** | 1.2878 | 1.097 | 1.0850 | 1.097 |
| **PeakTime (sec):** | 350 | 300 | 310 | 300 |

### Test condition B:

The simulation based on the Test condition B values described in Table 6.4 is considered and used at this point, this condition is applied in the SIMULINK diagram displayed in Figure 6.10. The setpoints of the froth height (Hf) and gas hold up (Eg) are settled to stay at zero until a step change of 1 is applied at a time of *T=500 sec*. The disturbance impulse occurred at a time of *T=200 sec* before the occurrence of a step input into their respective setpoints. The aim of this test condition is to monitor the controlled system stability when a disturbance occurs before a minor change in setpoint. Hence if an anomaly occurs while measuring the controlled variables the system shall remain stable. The closed-loop controlled system response is plotted against its respective reference models in Figure 6.12.

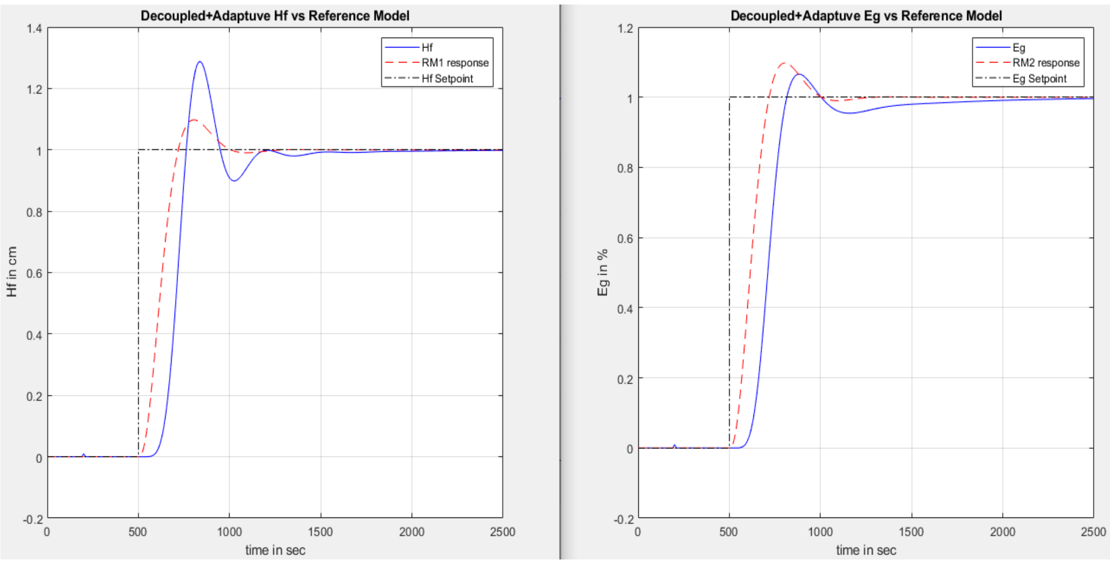


**Figure 6.12:** Decoupled MRAC Scenario1 Test Condition B response

The step response of the MRAC design for test case 3 scenario 1 can be seen in Figure 6.12. The controlled variable responses Froth height (Hf) and gas holdup (Eg) are compared to their respective reference model responses. The disturbances of D1 and D2 are visible at T=200 sec to the output responses of Hf and Eg respectively. However, the system still maintains its stability when the reference model control is used. The controller maintained the stability of both the froth height and gas holdup after a setpoint change.

**Table 6.6:** **Scenario 1 Test condition B response characteristics**

| Characteristics | Hf (cm) | RM1 | Eg (%) | RM2 |
|---|---|---|---|---|
| **RiseTime (sec):** | 760 | 710 | 810 | 710 |
| **SettlingTime (sec):** | 850 | 950 | 880 | 950 |
| **Overshoot (%):** | 28.7764 | 9.75 | 6.5757 | 9.75 |
| **Peak:** | 1.2878 | 1.0975 | 1.0658 | 1.0975 |
| **PeakTime (sec):** | 760 | 800 | 850 | 800 |

### Test condition C:

The simulation based on the Test condition C values described in Table 6.4 were used in the SIMULINK diagram displayed in Figure 6.10. The setpoints of the froth height (Hf) and gas hold up (Eg) were changed to 10 at a time of T=0 sec. To accommodate a setpoint change of 10, the gamma value is reduced to 0.00005. The step response is allowed to settle until an impulse response occurs at a time of T=1200 sec. The controller response is plotted against its respective reference models in Figure 6.13. The aim of this test condition is to monitor the controlled system stability when a disturbance occurs after a major change in setpoint, hence the reduction in gamma is necessary.

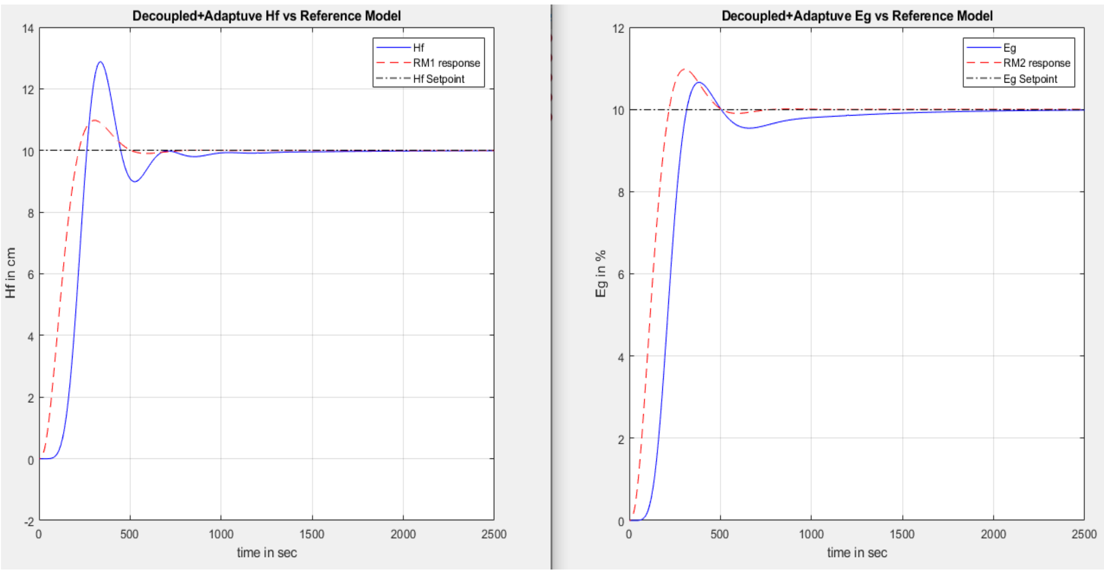


**Figure 6.13:** **Decoupled MRAC Scenario1 Test Condition C response**

Comparing the reaction of the system under study for both control loops, it can be noted that the response shows minimal evidence of the disturbance at t = 1200 seconds. Resulting in effectively suppressing and management of the disturbance imposed onto the froth height and gas holdup. The controller maintained the stability of both the froth height and gas holdup.

**Table 6.7:** **Decoupled MRAC Scenario1 Test Condition C Response Characteristics**

| Characteristics | Hf (cm) | RM1 | Eg (%) | RM2 |
|---|---|---|---|---|
| **RiseTime (sec):** | 140 | 48.1284 | 210 | 48.1284 |
| **SettlingTime (sec):** | 780 | 955.4955 | 880 | 450 |
| **Overshoot (%):** | 28.878 | 9.765 | 6.5757 | 9.765 |
| **Peak:** | 12.8776 | 10.9764 | 10.658 | 10.9764 |
| **PeakTime (sec):** | 350 | 306.9682 | 850 | 306.9682 |

### Test condition D:

The simulation based on the Test condition D values described in Table 6.4 were used in the SIMULINK diagram displayed in Figure 6.10. The setpoints of the froth height (Hf) and gas hold up (Eg) were changed to 10 at a time of T=500 sec. The step disturbances D1 and D2 are introduced at a time of T=200 sec. The controller response is plotted against its respective reference models in Figure 6.14. The aim of this test condition is to monitor the controlled system stability when a disturbance occurs after a minor change in setpoint.

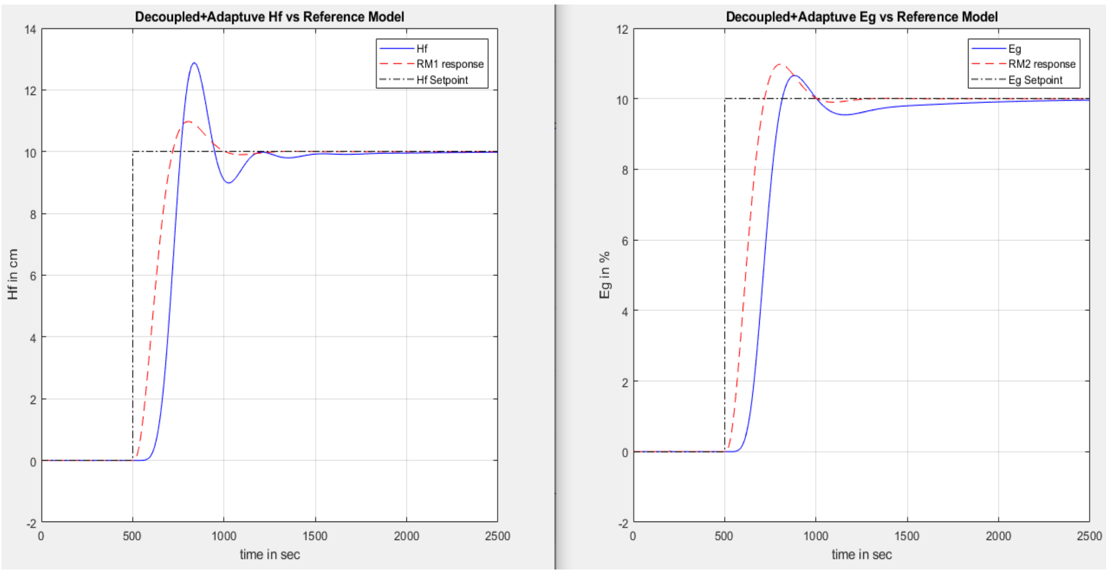


**Figure 6.14:** **Decoupled MRAC Scenario1 Test Condition D response**

Comparing the transient response for both adaptive control loops in Figure 6.14. It can be noted that the gamma was decreased to 0.0005 to accommodate the large setpoint change. The responses are compared to their respective reference model responses. The disturbances of D1 and D2 are visible in the output responses of Hf and Eg respectively. The controller maintained the stability of both the froth height and gas holdup after a setpoint change. The disturbance is seen to be effectively reduced upon the reduction of gamma.

**Table 6.8:** **Scenario 1 Test condition D response characteristics**

| Characteristics | Hf (cm) | RM1 | Eg (%) | RM2 |
|---|---|---|---|---|
| **RiseTime (sec):** | 640 | 546.6975 | 630 | 546.6975 |
| **SettlingTime (sec):** | 1750 | 951.8277 | 2230 | 951.8277 |
| **Overshoot (%):** | 28.878 | 9.78 | 6.57697 | 9.78 |
| **Peak:** | 12.8776 | 10.977 | 10.6577 | 10.977 |
| **PeakTime (sec):** | 850 | 803.8980 | 880 | 803.8980 |

#### 6.3.3.2 Case 4: Disturbance scenario 2

Two Impulse disturbances (D1 and D2) are added to the input of the plant and the decoupler of each loop to check the effectiveness of disturbance rejection imposed onto the froth height (y1) or the gas holdup(y2). The derivative blocks help to create the effect of an impulse response with a sample time of 10 sec. The purpose of this scenario is to monitor the effects of the system and controller under the disturbance of the plant inputs (wash water flowrate and gas flowrate).

The test conditions are the same as scenario 1 which is described in Table 6.4, indicating the setpoint changes in froth height and gas holdup. The gamma is varied to compensate for the larger amplitude setpoint variations in rows C and D. As well as the disturbances induced at the given time in columns 4 and 5. For this scenario the flow rates Qw and Qg experience disturbances D1 and D2 respectively to simulate irregularities that may occur with the flow rates of the flotation plant.

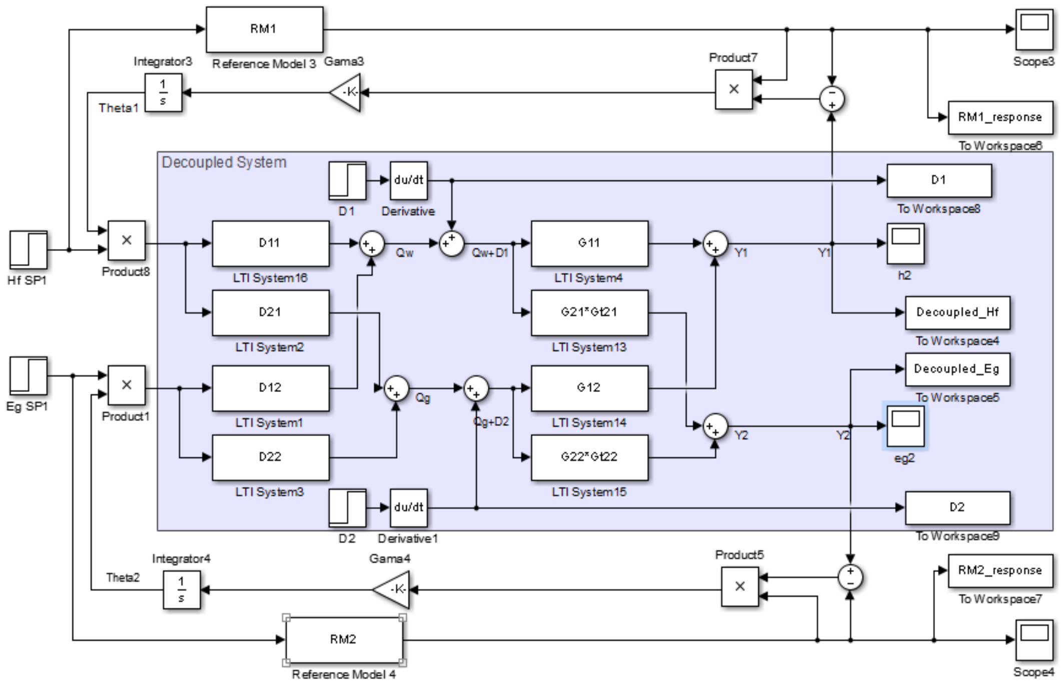


**Figure 6.15:** Decoupled MRAC with disturbance scenario 2

**Test condition A:**

The simulation based on the Test condition A values described in Table 6.4 were used in the SIMULINK diagram displayed in Figure 6.15. The setpoints of the froth height (Hf) and gas hold up (Eg) were changed to 1 at a time of T=0 sec. The step response is allowed to settle until an impulse response occurs at a time of T=1200 sec. The controller response is plotted against its respective reference models in Figure 6.16. The aim of this test condition is to monitor the controlled system stability when a disturbance occurs after a minor change in setpoint.

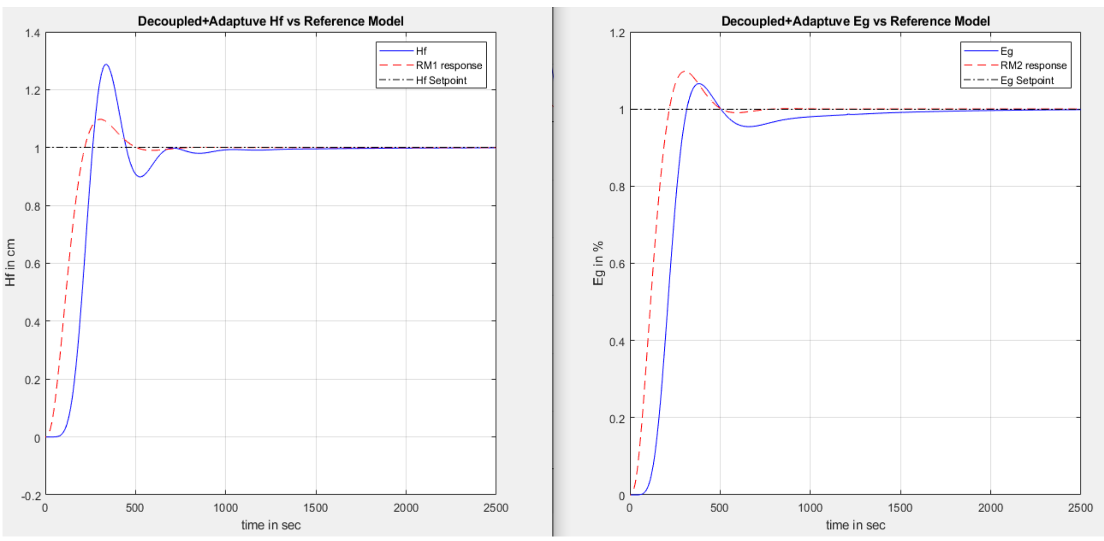


**Figure 6.16:** Decoupled MRAC Scenario 2 Test Condition A response

Comparing the reaction of the system for both loops with and without the reference model, it can be noted that the response with the reference model rejected well and effectively managed the disturbance. The disturbance of D2 shows clear visibility on the output response of Eg when induced onto gas flow rate Qg as opposed to being induced into the wash water flow rate Qw on the output response of Hf. However, the system still maintains its stability and no oscillations occur. While the gas holdup control loop shows evidence of the disturbance at t = 1200 seconds. The controller maintained the stability of both the froth height and gas holdup.

**Table 6.9:** Scenario 2 Test condition A response characteristics

| Characteristics | Hf (cm) | RM1 | Eg (%) | RM2 |
|---|---|---|---|---|
| **RiseTime (sec):** | 260 | 210 | 310 | 210 |
| **SettlingTime (sec):** | 850 | 450 | 1330 | 450 |
| **Overshoot (%):** | 28.7764 | 9.75 | 8.0547 | 9.75 |
| **Peak:** | 1.2878 | 1.097 | 1.0805 | 1.097 |
| **PeakTime (sec):** | 350 | 300 | 380 | 300 |

### Test condition B:

The simulation based on the Test condition B values described in Table 6.4 were used in the SIMULINK diagram displayed in Figure 6.15. The setpoints of the froth height (Hf) and gas hold up (Eg) were changed to 1 at a time of T=500 sec. The impulse responses occur at a time of T=200 sec before the occurrence of a step input into their respective setpoints. The controller response is plotted against its respective reference models in Figure 6.17. This test condition aims to monitor the controlled system stability when a disturbance occurs before a minor change in setpoint.

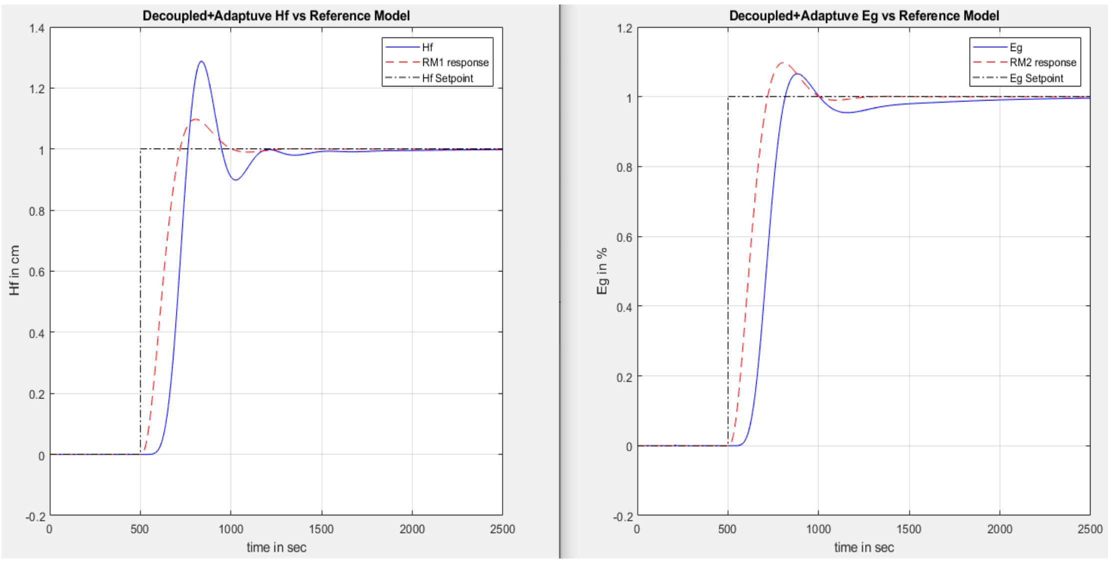


**Figure 6.17:** Decoupled MRAC Scenario 2 Test Condition B response

The transient response of the MRAC design for test case 3 scenario 2 can be seen in Figure 6.17. The responses are compared to their respective reference model responses. The disturbance of D2 shows clear visibility on the output response of Eg when induced onto gas flow rate Qg as opposed to being induced into the wash water flow rate Qw on the output response of Hf. The response of both systems displays no disturbance at t = 200 seconds. The controller maintained the stability of both the froth height and gas holdup after a setpoint change demonstrating the reference model tracking capabilities.

**Table 6.10:** **Scenario 2 Test condition C response characteristics**

| Characteristics | Hf (cm) | RM1 | Eg (%) | RM2 |
|---|---|---|---|---|
| **RiseTime (sec):** | 760 | 710 | 810 | 710 |
| **SettlingTime (sec):** | 1350 | 950 | 1.5000e+03 | 950 |
| **Overshoot (%):** | 28.7764 | 9.75 | 6.5812 | 9.75 |
| **Peak:** | 1.2878 | 1.0975 | 1.0658 | 1.0975 |
| **PeakTime (sec):** | 350 | 800 | 880 | 800 |

**Test condition C:**

The simulation based on the Test condition C values described in Table 6.4 were used in the SIMULINK diagram displayed in Figure 6.15. The setpoints of the froth height (Hf) and gas hold up (Eg) were changed to 10 at a time of T=0 sec. The step response is allowed to settle until an impulse response occurs at a time of T=1200 sec. The controller response is plotted against its respective reference models in Figure 6.18. This test condition aims to monitor the controlled system stability when a disturbance occurs after a major change in setpoint, hence the reduction in gamma.

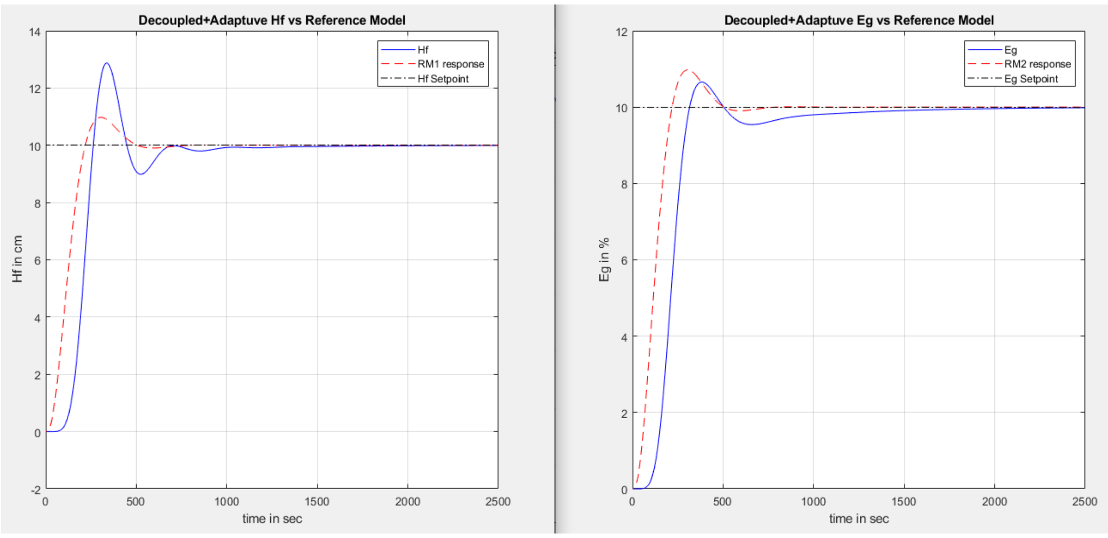


**Figure 6.18:** **Decoupled MRAC Scenario 2 Test Condition C response**

The comparison of the reaction of the system for both control loops, it can be noted that the response shows minimal evidence of the disturbance at t = 1200 seconds. The disturbance of D2 shows low visibility on the output response of Eg when induced onto gas flow rate Qg as opposed to being induced into the wash water flow rate Qw on the output response of Hf. However, the system still maintains its stability and no oscillations occur. Resulting in effectively suppressing and management of the disturbance imposed onto the froth height and gas holdup. The controller maintained the stability of both the froth height and gas holdup.

**Table 6.11:** **Scenario 2 Test condition C response characteristics**

| Characteristics | Hf (cm) | RM1 | Eg (%) | RM2 |
|---|---|---|---|---|
| **RiseTime (sec):** | 140 | 710 | 130 | 710 |
| **SettlingTime (sec):** | 850 | 950 | 2160 | 950 |
| **Overshoot (%):** | 28.7764 | 9.75 | 6.5769 | 9.75 |
| **Peak:** | 12.8776 | 1.0975 | 10.6577 | 1.0975 |
| **PeakTime (sec):** | 350 | 800 | 380 | 800 |

**Test condition D:**

The simulation based on the Test condition D values described in Table 6.4 were used in the SIMULINK diagram displayed in Figure 6.15. The setpoints of the froth height (Hf) and gas hold up (Eg) were changed to 10 at a time of T=0 sec. The step response is allowed to settle until an impulse response occurs at a time of T=1200 sec. The controller response is plotted against its respective reference models in Figure 6.19. The disturbance of D2 shows minimum to no visibility on the output response of Eg when induced onto gas flow rate Qg as opposed to being induced into the wash water flow rate Qw on the output response of Hf. However, the system still maintains its stability and no oscillations occur. The aim of this test condition is to monitor the controlled system stability when a disturbance occurs after a major change in setpoint, hence the reduction in gamma.

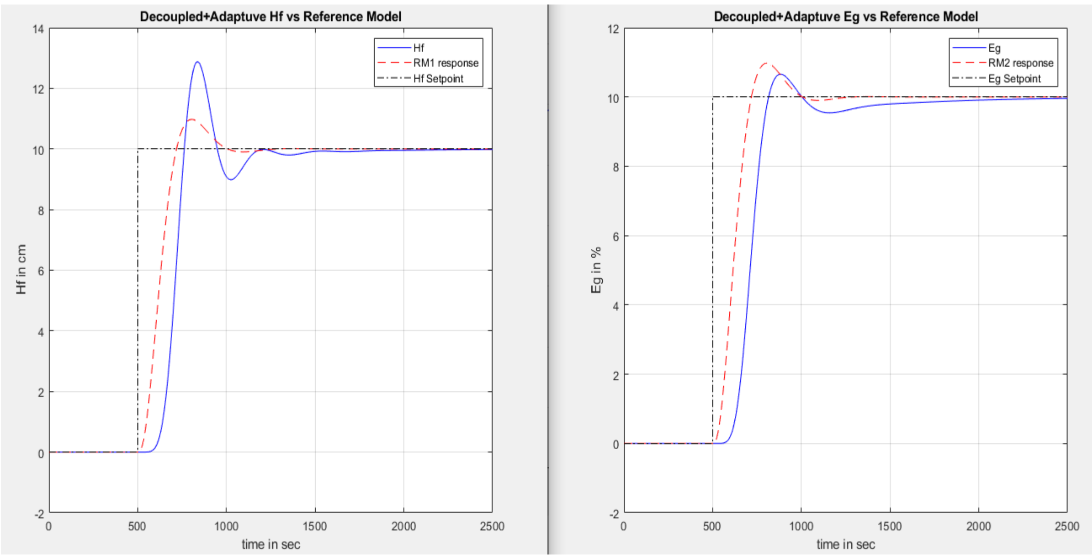


**Figure 6.19:** **Decoupled MRAC Scenario 2 Test Condition D response**

Comparing the transient response for both adaptive control loops in Figure 6.20. It can be noted that the gamma was decreased to 0.0005 to accommodate the large setpoint change. The responses are compared to their respective reference model responses. The response of both system displays the disturbance at t = 200 seconds and maintains system stability. The controller maintained the stability of both the froth height and gas holdup after a setpoint change. The disturbance is seen to be effectively reduced upon the reduction of gamma. The transient response characteristics can be seen in

Table 6.12 below.

**Table 6.12:** **Scenario 2 Test condition D response characteristics**

| **Characteristics** | **Hf (cm)** | **RM1** | **Eg (%)** | **RM2** |
|---|---|---|---|---|
| **RiseTime (sec):** | 640 | 546.6975 | 630 | 546.6975 |
| **SettlingTime (sec):** | 2160 | 951.8277 | 2160 | 951.8277 |
| **Overshoot (%):** | 28.7764 | 9.78 | 6.5769 | 9.78 |
| **Peak:** | 12.8777 | 10.977 | 10.6578 | 10.977 |
| **PeakTime (sec):** | 850 | 803.8980 | 880 | 803.8980 |

## 6.4 Decoupled MRAC results analysis and discussion

The dynamic behaviour of the controlled system can be seen in Figure 6.5. By observation, it can be assumed that the MRAC design objective has been achieved to a certain degree. The simulation results show clear evidence of reference model tracking. However, the MRAC characteristics do not exactly match that of the reference model. It does show improvement as opposed to the decoupled PI design where $H_f$ is considered. The decoupled MRAC controller design demonstrates a degree of stability and resilience to disturbances occurring at the flotation process flowrates Qw and Qg. Table 6.13 shows a comparison of the characteristics of both the decoupled PI controller and decoupled MRAC design per test case.

**Table 6.13:** **Decoupled PI controller and Decoupled MRAC characteristics per Test Case**

| Case: | Control loop | RiseTime (s): | SettlingTime (s): | Overshoot (%): | Peak: | PeakTime (s): | Ess: |
|---|---|---|---|---|---|---|---|
| 1 | Hf PI | 50.6268 | 850.3920 | 55.9666 | 1.5597 | 131.8340 | -0.004 |
| | Hf MRAC | 244.6465 | 523.6977 | 29.1733 | 1.292 | 328.3780 | -0.002 |
| | Eg PI | 58.6045 | 474.8497 | 5.2085 | 1.0521 | 122.4387 | 0.0102 |
| | Eg MRAC | 284.9500 | 500.0000 | 6.7557 | 1.0674 | 361.1478 | 0.0001 |
| 2 | Hf PI | 50.6268 | 850.3920 | 55.9666 | 1.5597 | 131.8340 | -0.004 |
| | Hf MRAC | 244.6465 | 523.6977 | 29.1733 | 1.292 | 328.3780 | -0.002 |
| | Eg PI | 58.6045 | 474.8497 | 5.2085 | 1.0521 | 122.4387 | 0.0102 |
| | Eg MRAC | 284.9500 | 500.0000 | 6.7557 | 1.0674 | 361.1478 | 0.0001 |
| 3 | Hf PI | 74 | 1200 | 99.69 | 1.9969 | 1200 | 0.0031 |
| | Hf MRAC | 260 | 750 | 28.7764 | 1.2878 | 350 | 0.0021 |
| | Eg PI | 91 | 1200 | 99.41 | 1.9941 | 1200 | 0.0102 |
| | Eg MRAC | 310 | 1200 | 8.45 | 1.0850 | 310 | -0.01 |
| 4 | Hf PI | 74 | 1200 | 99.69 | 1.9969 | 1200 | 0.0031 |
| | Hf MRAC | 260 | 850 | 28.7764 | 1.2878 | 350 | 0.0014 |
| | Eg PI | 91 | 1296 | 0.1302 | 1.1302 | 1202 | 0.0209 |
| | Eg MRAC | 310 | 1330 | 8.0547 | 1.0805 | 380 | -0.01 |

The MRAC implementation brings about its merits, for example, the plant parameters can be unknown. Whereas the decoupled PI design increases the order of the system, the decoupled MRAC design ensures that the flotation process system order remains the same.

The MIT rule is highly sensitive to large amplitude setpoint variation, causing instability as seen in the figures above. By observing Figure 6.6 and Figure 6.7, the froth height shows improved stability over the gas holdup response. This is mainly due to the magnitude of the set point variation induced into the system. To improve the sensitivity the gamma value is reduced significantly. The effects of this cause the controller to respond much slower giving the illusion that the system does not respond to setpoint variations with a lower amplitude. This now makes the system overdamped, but the inclusion of MRAC has improved the system's performance significantly.

## 6.5 Challenges and limitations

The initial challenge of the adaptive controller is determining a suitable reference model. The MRAC controller is most used in a coupled system using state space modelling. The reference model theoretically should consist of the same order as that of the plant to be controlled. In this design, it is assumed that the plant parameters are unknown. Therefore, a second-order system is used to achieve the desired characteristics.

In addition, the froth height decoupled control loop possessed a negative gain. The assumption generally made when designing an MRAC controller is that the process gain is always positive. Thus, the adaptive gain (gamma) for the MRAC controller is always negative. However, with the decoupled froth height control loop the adaptive gain is made positive.

The MRAC controller does, however, demonstrate its limitations when applying the MIT rule. One of those limitations is the controller's adaptive gain. As mentioned in the analysis, the controller exhibits sensitivity and instability to larger setpoint adjustments. This can be resolved by having the adaptive gain automatically adjust itself.

## 6.6 Conclusion

In this chapter, a brief description of MRAC was given. A reference model was developed for the design of the MRAC controller using the MIT rule. With the use of MATLAB and SIMULINK the adoption gain was achieved through trial and error. The MRAC controller performance was measured against the reference model to monitor its tracking capabilities. It provided a reasonable degree of control that can be improved by means of applying other MRAC strategies or by improving the designed reference model. However, that is beyond the scope of this research. The decoupled MRAC design displayed several merits compared to the decoupled PI controller. The work in this chapter shows that a controller can be developed with the process parameters being unknown. The reference model was developed using a second-order characteristic equation. Irrespective of the order of the plant or process the controller can be tuned by simply tuning the reference model. The setbacks for the decoupled MRAC design are common as per the MIT rule, that is the sensitivity to large setpoint variations. This work demonstrates an adequate method of advance control for a column flotation process. The following chapter will focus on implementing the work from the current chapter onto a controller for real-time evaluation.

# CHAPTER 7: IMPLEMENTATION OF ADVANCE DECOUPLED CLOSED-LOOP FLOTATION SYSTEM USING A PLC AND TWINCAT3

## 7.1 Introduction

The closed-loop flotation system controllers are developed and analysed in the previous chapters 5 and 6 using the MATLAB/Simulink environment. The advanced decoupled controlled flotation system developed in Chapter 6 is practically implemented and presented in this chapter using the TwinCAT 3.1 software environment. The TwinCAT 3.1 automation software allows for real-time simulation with the use of a C60xx Beckhoff PLC utilizing model transformation. This strategy is based on the conversion of continuous-time controllers developed in MATLAB/Simulink to the Beckhoff PC-based PLC automation software through the TwinCAT 3.1 simulation environment for real-time control.

In this chapter, the multivariable column flotation process is implemented within a real-time environment using real-time control strategies. This is done to monitor the practical effectiveness of the controller developed in chapter 6. The real-time control strategies are centred on the generation of software algorithms for implementing closed-loop control systems to capture and analyse data over a predetermined period. The MATLAB/Simulink environment is used to generate the code for the TwinCat 3.1 environment for real-time implementation. The generated code gets downloaded onto the Beckhoff C60xx PLC for Hardware-In-Loop (HIL) implementation. The ethernet communication protocol EtherCAT designed by Beckhoff Automation, is used to communicate between the Beckhoff C60xx PLC and the embedded PC.

Chapter 7 consists of the following subsections. An overview of Beckhoff Automation and TwinCAT 3.1 in section 7.2. Section 7.3 covers the information necessary to migrate from MATLAB/Simulink to the Beckhoff environment. The Hardware implementation and runtime are described in section 7.4. The real-time implementation is given in section 7.5. The results of section 7.5 are discussed in section 7.6. The limitations and challenges of implementation are listed and discussed in section 7.7 before the chapter is concluded in section 7.8.

### 7.2 Overview of Beckhoff Automation and TwinCAT3

Beckhoff Automation focuses on the implementation of an automation system using PC-based control technology. The Automation technology targets markets within the control industry such as industrial PCs, I/O, fieldbus technology, and automation software. Beckhoff is renowned for its innovative PC-based control technology and TwinCAT automation software. For the implementation of the closed-loop flotation control, a C6015 series embedded PC or PLC will be utilized. Beckhoff refers to the C60xx series as embedded PCs due to its ability to combine the processing power of an industrial PC and the I/O modules. The C6015 can be seen in Figure 7.1.

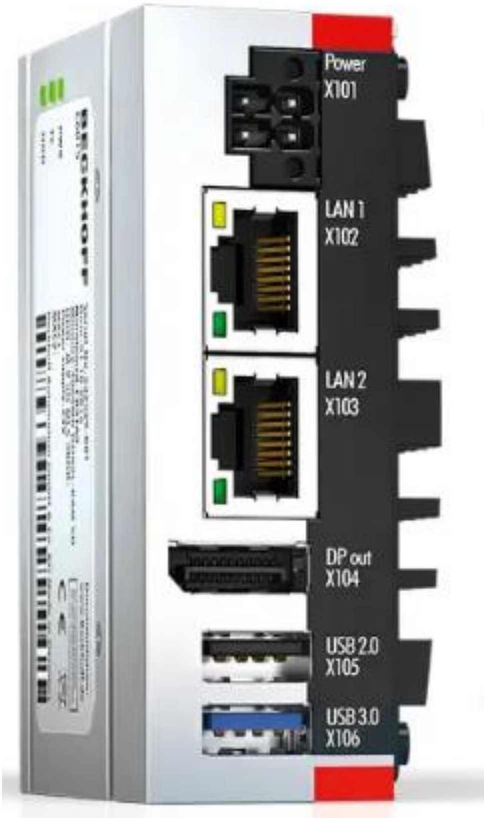


**Figure 7.1:** **Beckhoff C6015 PLC, (https://www.beckhoff.com/en-gb/products/ipc/pcs/c60xx-ultra-compact-industrial-pcs/c6015.html)**

The C6015 PLCs are from Beckhoff Automation, C60xx series is based on the Intel Atom processor. The device has a 1.7 GHz Intel Atom processor. Beckhoff Automation does allow the user sub-variants of the C6015 PLC. The sub-variants are defined by the number of cores the processor holds. The dual virtual cores are essential for effectively executing more complexed software. Based on the installed TwinCAT runtime environment, any C6015 variant that has at least 2 cores could be used for implementing PLC or motion control projects with or without visualization, (Beckhoff, 2023). Some of the features of the C60xx series include two RJ-45 ethernet connectors (labelled “*X102 and X103*” in Figure 7.1), one DisplayPort connector (labelled “*X104*” in Figure 7.1), one USB 2.0 and USB 3.0 connector (labelled “*X105 and X106*” in Figure 7.1). Additional technical details on the Beckhoff C6015 can be found in Appendix A.

### 7.3 Migration of MATLAB/SIMULINK to TwinCAT3

This section describes the migration process from the MATLAB/SIMULINK environment to the TwinCAT3.1 environment. The migration process between the two mentioned environments plays a critical role in the implementation of the advanced control method of a column flotation system. In this study, MATLAB/SIMULINK environment is used to design and analyse the advanced control theory applied to the column flotation process. The analysis entails several scenarios and test conditions to monitor the real-time performance of the controller designed in Chapter 6. The MATLAB/SIMULINK environment possesses the ability to generate code of a SIMULINK model with the use of an Embedded Simulink Coder. The Embedded Simulink Coder and Beckhoff Automation’s TwinCAT 3.1 software package “*Target for MATLAB/SIMULINK (TC1400)*” are used together to generate the C++ programming code. The generated C++ code is compiled into a TwinCAT 3.1 modular arrangement. The generated C++ code is then loaded into the TwinCAT 3.1 development environment.

The TE1400 software is developed by Beckhoff Automation to allow the user the ability to interface with the development of real-time modules using the TwinCAT 3.1 runtime environment. These real-time modules possess the ability to be instantiated several times for debugging and analysis. The Interface for MATLAB/SIMULINK TE1410 is a Beckhoff Automation software package that serves as an interface between the MATLAB/SIMULINK and the TwinCAT 3.1 environment to allow for data exchange. A real-time model containing the SIMULINK inputs and outputs may be imported into the TwinCAT environment. The real-time capable model is referred to as the TwinCAT Component Object Module or TcCOM, refer to Figure 7.2 below.

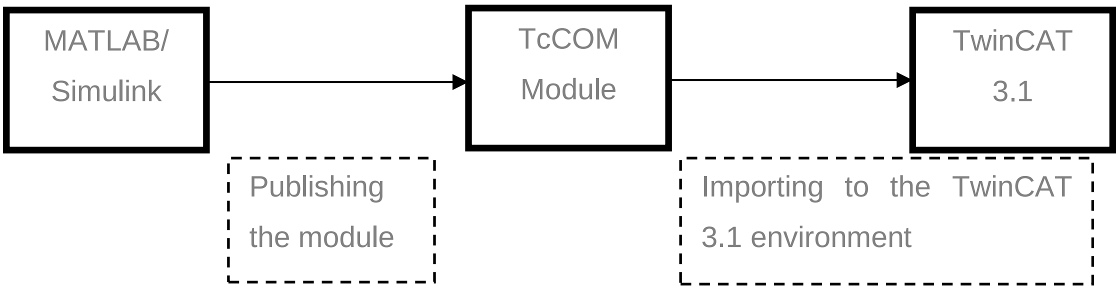


**Figure 7.2:** **Simulink to TwinCAT 3.1 migration block diagram**

TcCOM enables modules written in various languages to interact with the real-time environment.

### Process of migration from SIMULINK to TwinCAT 3.1

The steps below are the necessary procedures taken when migrating from SIMULINK to the TwinCAT 3.1 development environment.

### Step 1: Simulink Configuration

In the SIMULINK software, open the SIMULINK model and navigate to the Parameter Configuration. Under the solver tab set the solver selection type to “Fixed-step” and the Fixed-step size to 0.01 as seen in Figure 7.3.

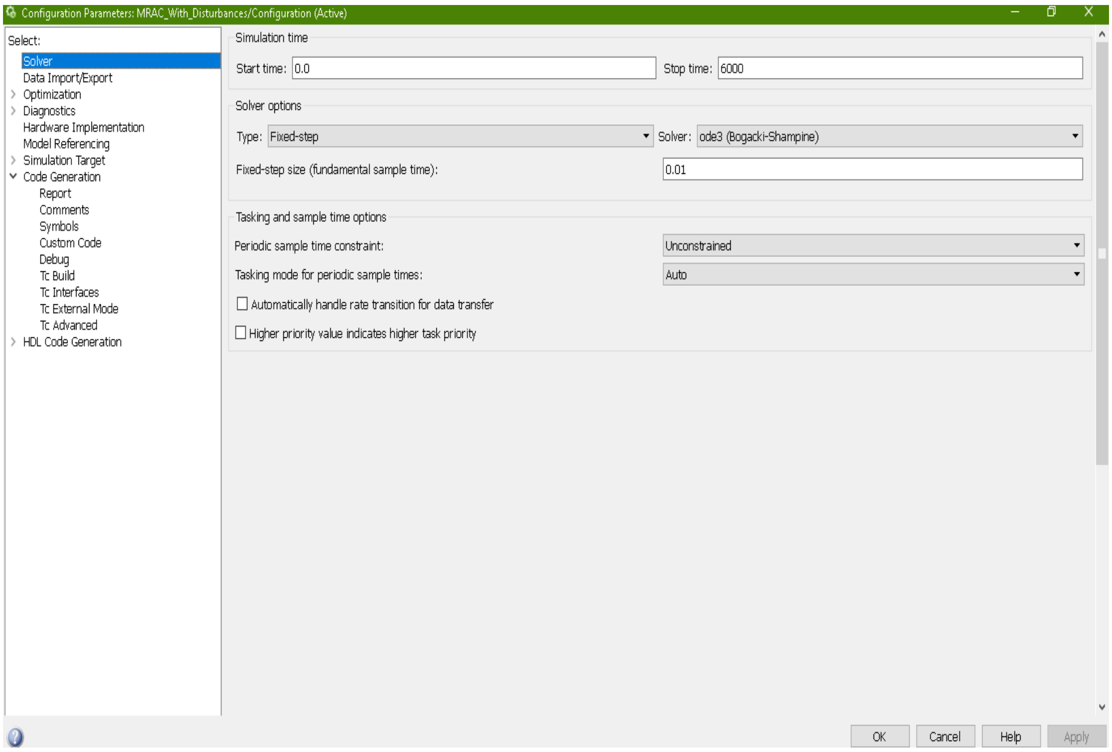


**Figure 7.3:** **Simulink Configuration**

Under the code generation tab, set the system target file to “TwinCAT.tlc” for the TwinCAT target to be selected. If “TwinCAT.tlc” is not already selected, click the Browse button and a drop-down menu should appear with the option to select “TwinCAT.tlc”. The code generation tab can be seen in Figure 7.4.

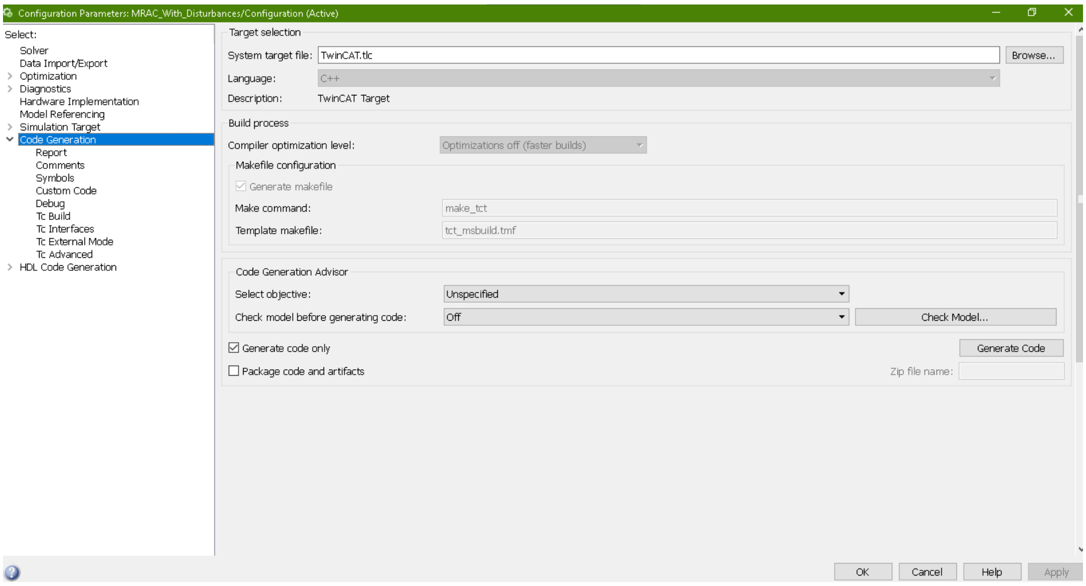


**Figure 7.4:** **Simulink System target file**

### Step 2: Simulink Code Generation

The code generation procedure is then initiated by selecting the Generate Code block under the Code Generation tab. The build process then begins and can be monitored on the MATLAB workspace as shown in Figure 7.5. Once the build process is completed, all the necessary model files for migration will be ready for use in the TwinCAT environment. If the Visual Studio C++ compiler isn’t recognised by MATLAB, the C++ code can be published in the Visual Studio platform under the TwinCAT environment.

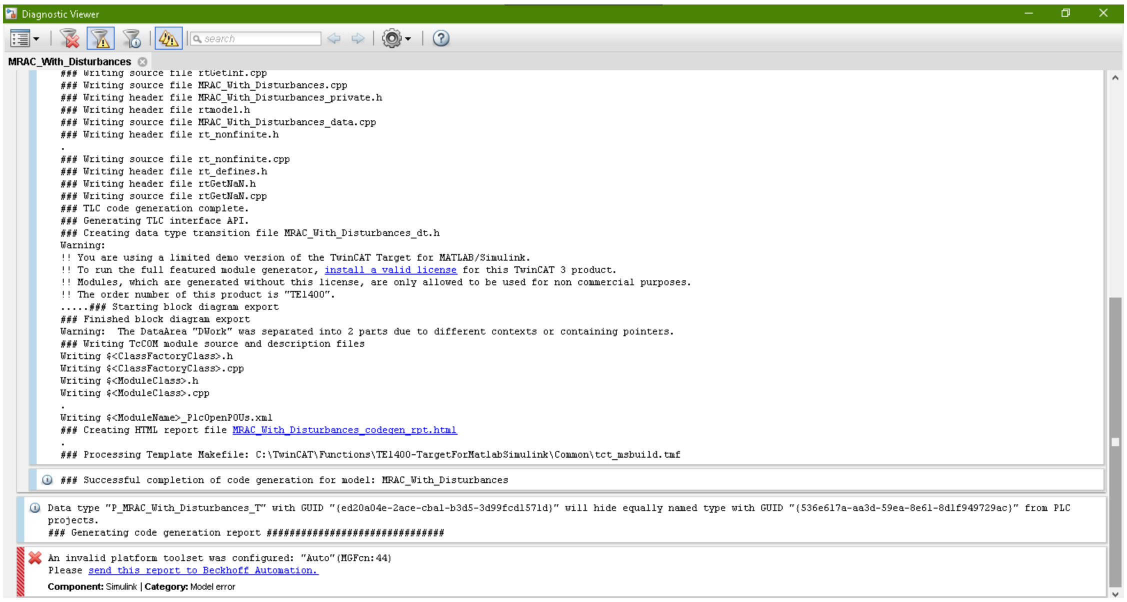


**Figure 7.5:** Simulink model build process

### Step 3: Visual Studio interface for TwinCAT 3

Open the TwinCAT engineering platform (XAE) using the Visual Studio 2019 interface and create a new TwinCAT project. Navigate to the C++ tab and add an existing item. The C++ project should be in the MATLAB path directory. Import the desired VC++ project file, refer to Figure 7.6 and Figure 7.7.

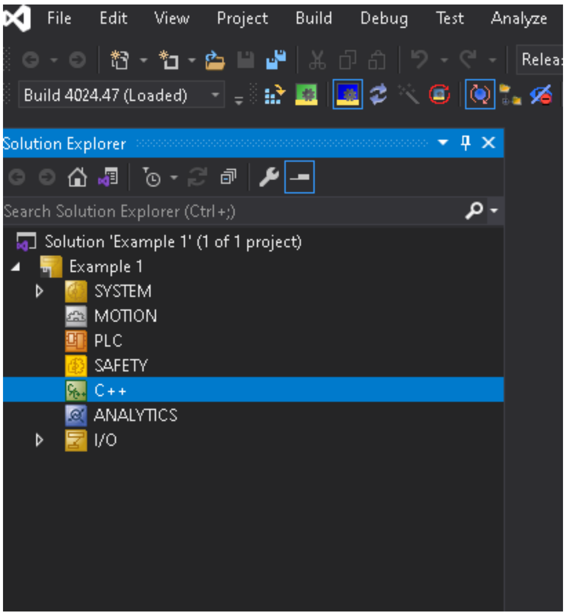


**Figure 7.6:** TwinCAT 3 C++ project

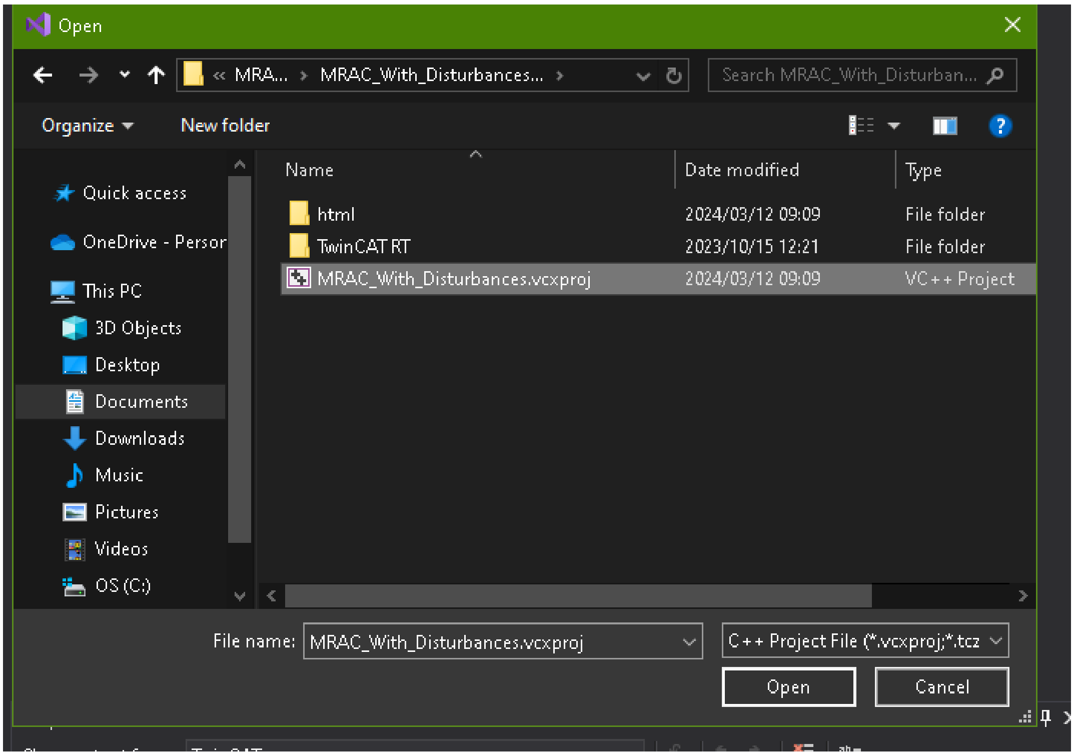


**Figure 7.7:** Simulink C++ project selection

Once the VC++ file is loaded, right-click on the C++ project file, and navigate to properties. From properties select the Tc Sign and configure its Certificate Name to the appropriate assigned certificate and select apply, as seen in Figure 7.8. The C++ project can now be built and published.

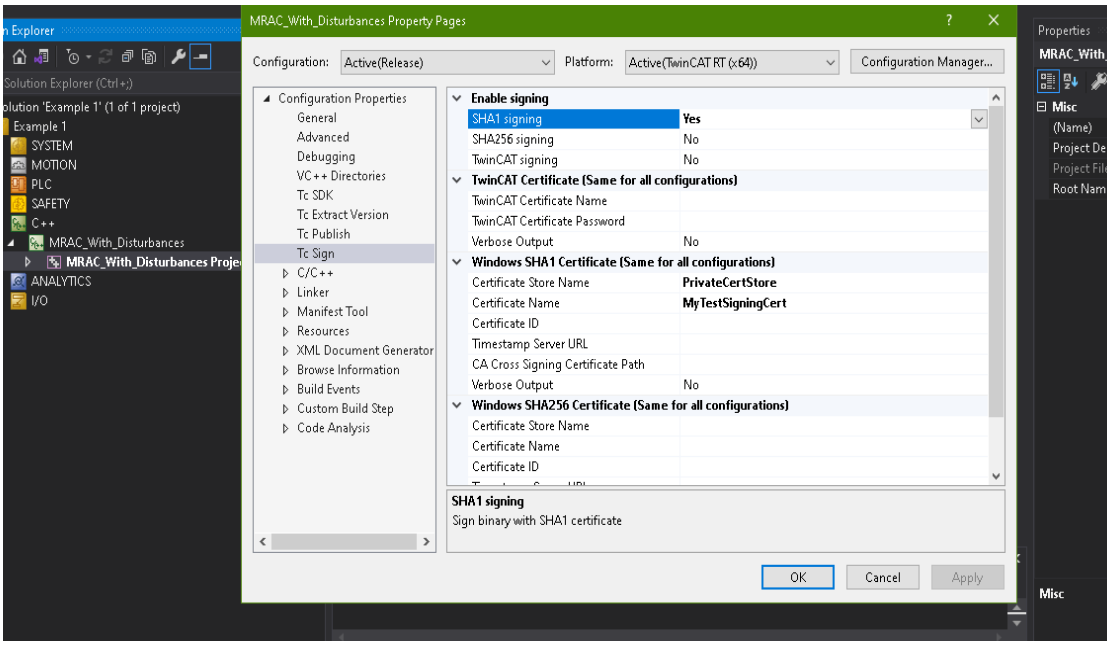


**Figure 7.8:** Visual Studio Tc Sign settings

With the C++ project successfully built, the TcCOM objects can now be loaded onto the projects, as seen in Figure 7.9. This is done by navigating to the Systems tab, right-clicking on the TcCOM Objects, and selecting “Add New Item”. Create a Task with the same “Cycle ticks” as your Simulink Fixed Step size. In this case, the Cycle ticks would be 10 milliseconds. From the object node, select configure the TcCOM “Context” and select the recently configured Task. The model is now configured and ready to be loaded onto the target system.

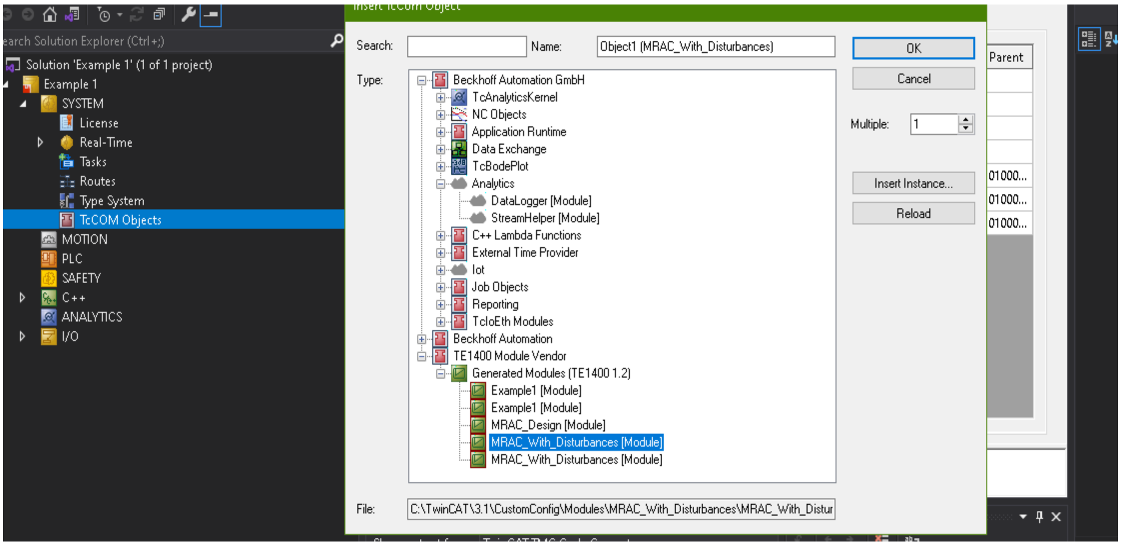


**Figure 7.9:** **Object file selection**

### Step 4: Selecting the Target System

The user is given the option of running the Model on either the local machine (Engineering PC) or on an Industrial Beckhoff PC. For this study, the Module is loaded onto the Industrial Beckhoff PC. The configuration is therefore activated for the execution of the Simulink model onto the Beckhoff PLC.

### Step 5: Real-time running

Once the activated system is configured onto the target system, the target status icon will alter from blue to green indicating that the system is now running in real-time. The block diagram’s status can be monitored online by selecting the block diagram tab.

### Step 6: TwinCAT Measurements

A TwinCAT Measurements project can be created in addition to the TcCOMs project. The TwinCAT Measurements wizard is used to easily configure the scopes needed for analysis. The TcScopes server is configured locally with the inputs and outputs of the TcCOMs module inputs and outputs are displayed on each scope.

### 7.4 TwinCAT 3 Runtime and hardware implementation

This section describes some of the TwinCAT 3 components used in this study to successfully implement the Adaptive Controller. The aspects of the TwinCAT environment and runtime are explained, along with the Automation Device Specification (ADS) communications protocol. The TwinCAT measurements are also mentioned as the software provides a critical analysis tool for the implemented Adaptive Controller.

#### 7.4.1 TwinCat Integrated environment

The focus of TwinCAT 3 is to make software engineering a much simpler undertaking. TwinCAT 3 is integrated with Visual Studio 2010 or higher as an extension for the development environment. This environment along with the TwinCAT System Manager is all the developer requires to train, program, configure, and fault-find the Beckhoff Automation devices. The environment utilizes the PLC programming languages of the IEC 61131-3 standard, C, C++ or MATLAB/Simulink as presented in Figure 7.10.

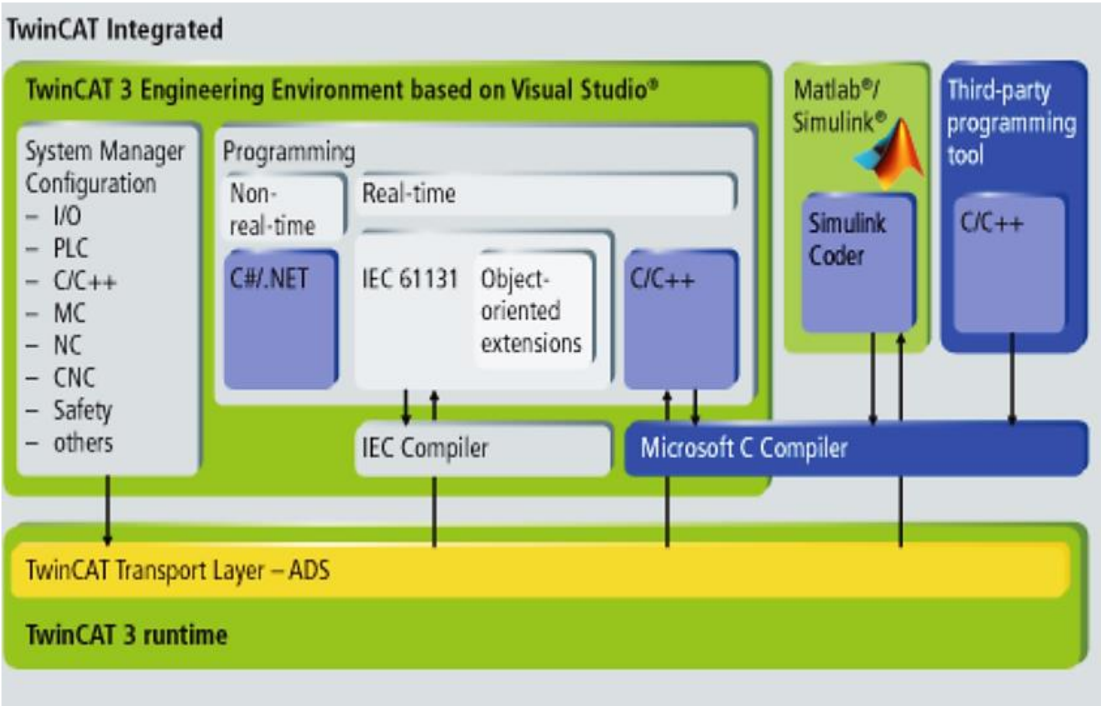


**Figure 7.10:** **TwinCAT 3 Environment layout, *(*https://www.beckhoff.com)**

#### 7.4.2 TwinCAT 3 Runtime

TwinCAT 3 Runtime is a real-time environment for TwinCAT modules to be loaded, implemented, or managed. The TwinCAT modules are to be created with a different compiler for independent programming by the developer. The created modules are called cyclically from the Task. Due to the nature of different modules (C, C++ or

MATLAB compiled), they possess the ability to call themselves in the TwinCAT 3 Runtime. Therefore, rendering the possibility to complete an automated application. These automated applications are generally defined as a combination of several modules each possessing their functionality. There is no limit to the number of modules to which a task can call, however, it is dependent on the system properties of the runtime device. The runtime layout can be seen in Figure 7.11.

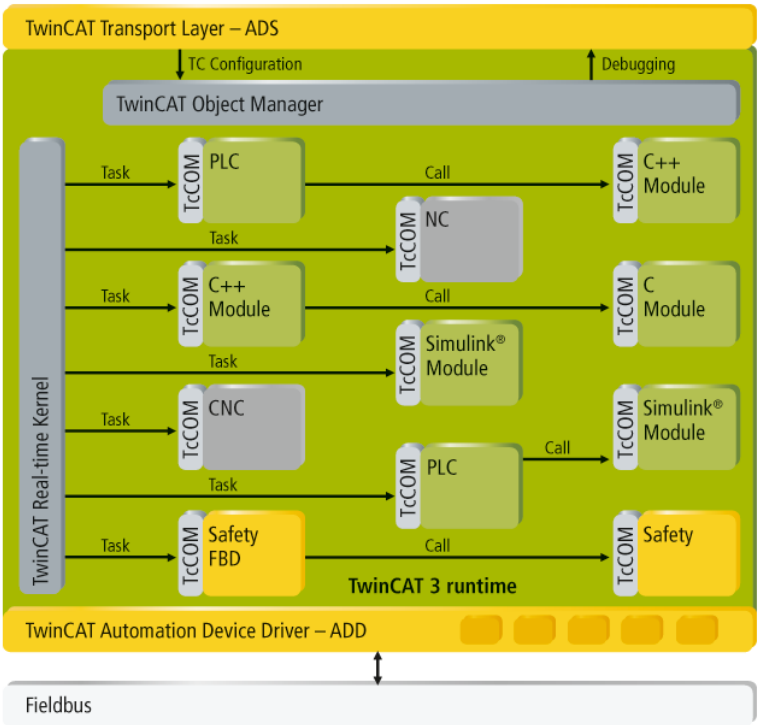


**Figure 7.11:** **TwinCAT 3 Runtime Layout, (Beckhoff Automation, 18 August 2023)**

### 7.4.3 Interface application based on automation device specification

The TwinCAT system arrangement offers individual modules to be treated as autonomous devices, each task having its software module (either a server or client). The server executes these devices in the form of software, allowing for virtual device implementation within the software. The clients are programs that request the services of servers. These client programs could be shaped as visualisations or programming devices. Automation Device Specification (ADS) is an interface used by the TwinCAT system to transfer messages between modules using a message router. All messages in the system are managed and distributed via TCP/IP communications. The message router exists on all TwinCAT devices, allowing the exchange of commands and data between client and server devices. Figure 7.12 displays the concept of ADS.

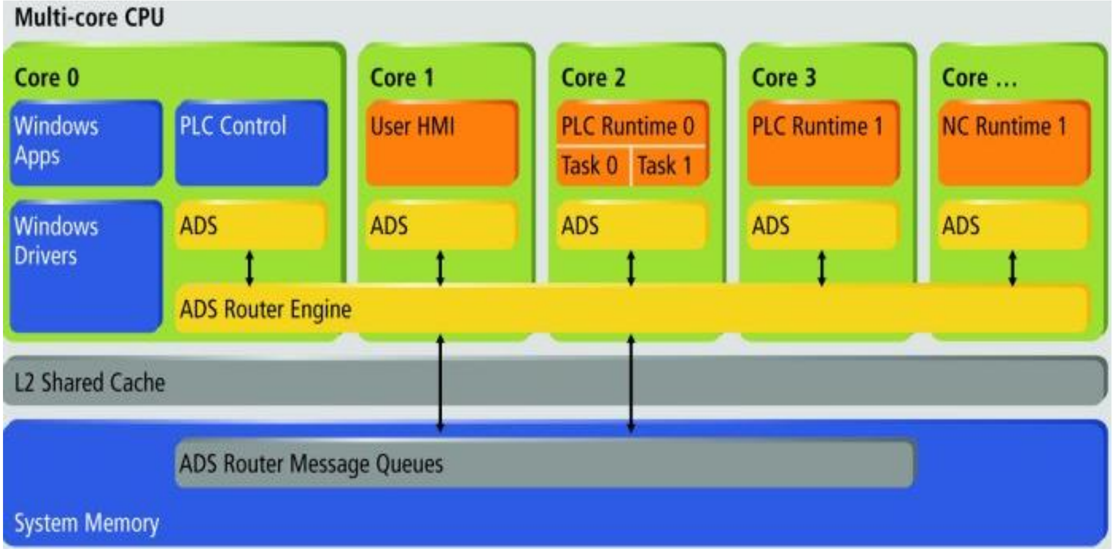


**Figure 7.12:** **TwinCAT ADS concept, (Beckhoff Automation, 18 August 2023)**

### 7.4.4 Project measurements

TwinCAT provides developers with a tool for analysis and charting called TwinCAT 3 Scope. This allows variables in TwinCAT to be recorded and displayed graphically. The tool is integrated with Microsoft Visual Studio, making it possible for a TwinCAT 3 project and Scope project to share a single solution. TwinCAT 3 project variables can easily be shifted and configured into the Scope Project. A Scope Server software package is often installed on distributed devices or local target devices to record and log data. TwinCAT 3 Scope is often used for machine commissioning and process monitoring. For this research, the project measurements will be used to monitor the status of the controlled variables (Froth height and Gas Holdup).

## 7.5 Real-time implementation of the advanced decoupled control for flotation process

This section is based on the implementation of the advanced decoupled control strategy for the flotation process. The objective of this section is to demonstrate real-time results of the closed-loop flotation column being controlled by the advanced decoupled controller. The flotation column under study is a 2x2 model presented in Chapter 4 for open-loop analysis. The implemented advanced decoupled controller for the flotation column is presented in Chapter 6. This section presents a modified SIMULINK model with the ability to accommodate the migration from SIMULINK to TwinCAT 3, as presented in Figure 7.13. Using the TwinCAT 3 environment the model is deployed onto a Beckhoff Programmable Logic Controller (PLC).

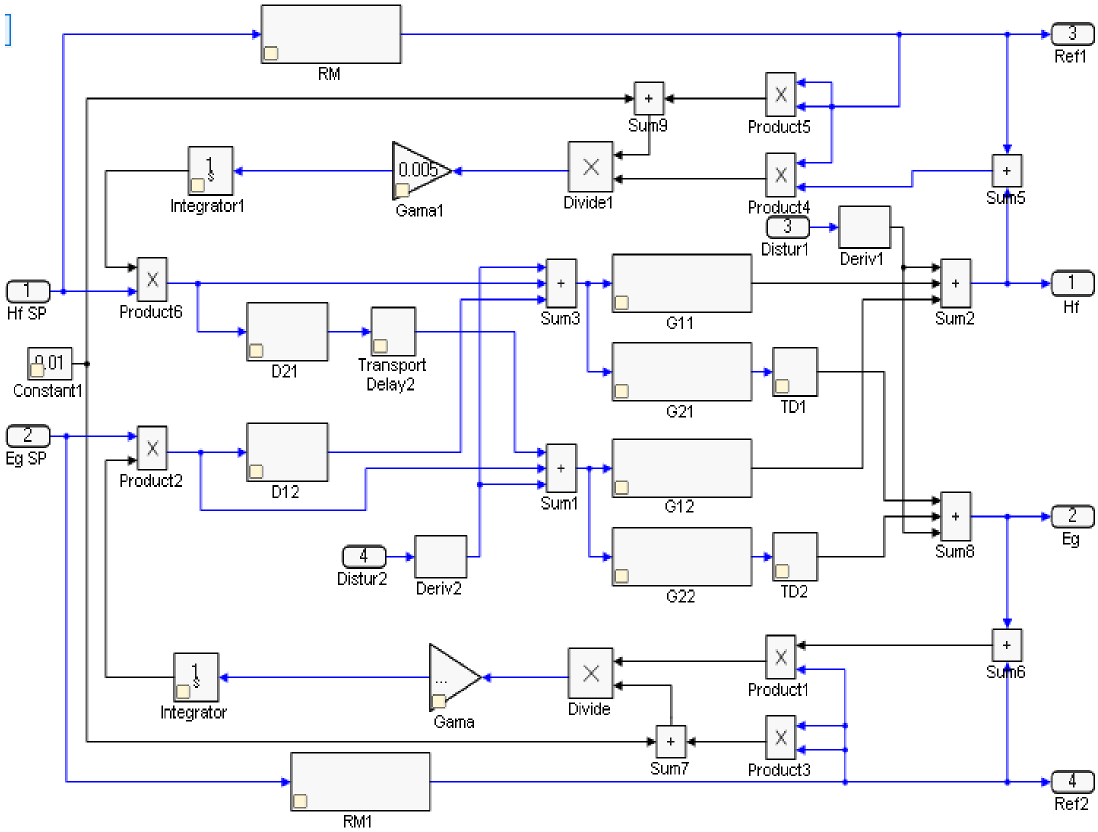


**Figure 7.13:** Advanced Decoupled TwinCAT real-time model

Table 7.1 shows a list of test equipment used for the duration of the experiments. An image of the test setup can be seen in Appendix B.

**Table 7.1:** Equipment used for the experiments.

| List of Test Equipment used | | | |
|---|---|---|---|
| | **Equipment** | **Part Number** | **Serial Number** |
| 1 | Programmable Logic Controller (PLC) | C6015 | 182138 |
| 2 | DC Power Supply | | 90626 |
| 3 | **Windows OS Computer with the following software:** | N/A | N/A |
| | MATLAB/SIMULINK | 2015a | |
| | TwinCAT3 | 4024 | N/A |
| | Visual Studio | 2019 | N/A |

To accomplish real-time implementation of the Beckhoff PLC the results are imported via the TwinCAT Measurements Tool described in section 7.4. The TwinCAT simulation environment also allows for real-time monitoring, system blocks, and variables to be updated and loaded onto the PLC. This method is used to update the control loop setpoint values HfSP and EgSP respectively. The implementation is evaluated using two test case conditions described in Table 7.2. The results of these test conditions are displayed in the subsections of this chapter, partitioned as per case number in the table below.

**Table 7.2:** **TwinCAT model test case conditions**

| Cases | Hf | | Eg | | Description |
|---|---|---|---|---|---|
| | **Setpoints (cm)** | **Time (min)** | **Setpoint (%)** | **Time (min)** | |
| **1** | 1-5-3-4 | 0-15-30-45 | 1-8-5-5 | 0-15-30-45 | This case simulates four changes made to the setpoint pulse signal. As indicated in the height loop, the changes are made from 1,5,3, and 4 at different intervals of 15min alongside the air-loop changes. The Time columns now represent when the setpoint change occurs within the 60-minute test interval. The aim is to observe the hardware implementation of MRAC controller performance under numerous setpoint changes. |
| **2** | 0-1 | 0 | 0-1 | 0 | An impulse response is modelled into the system as a disturbance for both the froth height and gas holdup control loops. This case aims to observe the controller's ability to stabilize the system as the disturbances are applied under different conditions. |

The changes mentioned above were all completed in the real-time TwinCAT simulation environment and the results are presented case by case in the following subsections.

### 7.5.1 Case 1: Real-time setpoint tracking of model reference adaptive controlled flotation column

#### Test description

The MRAC TwinCAT model of a flotation process in Figure 7.13 is subject to several setpoint variations best described in Table 6.3. This is to monitor the MRAC controller performance under different adaptation gains or gamma $\gamma$ settings. The real-time simulation only allows the variables to be recorded for a duration of 60 min. Thus, the setpoint change will occur every 15 min to allow for all 4 setpoint changes to be recorded. The gamma setting will have a series of four test runs for each setpoint change. The time in Table 6.3 represents the time at which the setpoint occurs in each test run.

**Table 7.3:** **Set point variations for MRAC simulation.**

| Hf | | Eg | |
|---|---|---|---|
| **Setpoint** | **Time (min)** | **Setpoint** | **Time (min)** |
| 1 | 0 | 1 | 0 |
| 5 | 15 | 8 | 15 |
| 3 | 30 | 5 | 30 |

| | | | |
|---|---|---|---|
| 4 | 45 | 5 | 45 |

**Test results when gamma = 0.005**

Figure 7.14 presents the real-time implementation results of the closed-loop flotation system under the Model Reference Adaptive Controller (MRAC). It can be seen that the MRAC responds positively to minor setpoint variations when implemented onto the Beckhoff PLC.

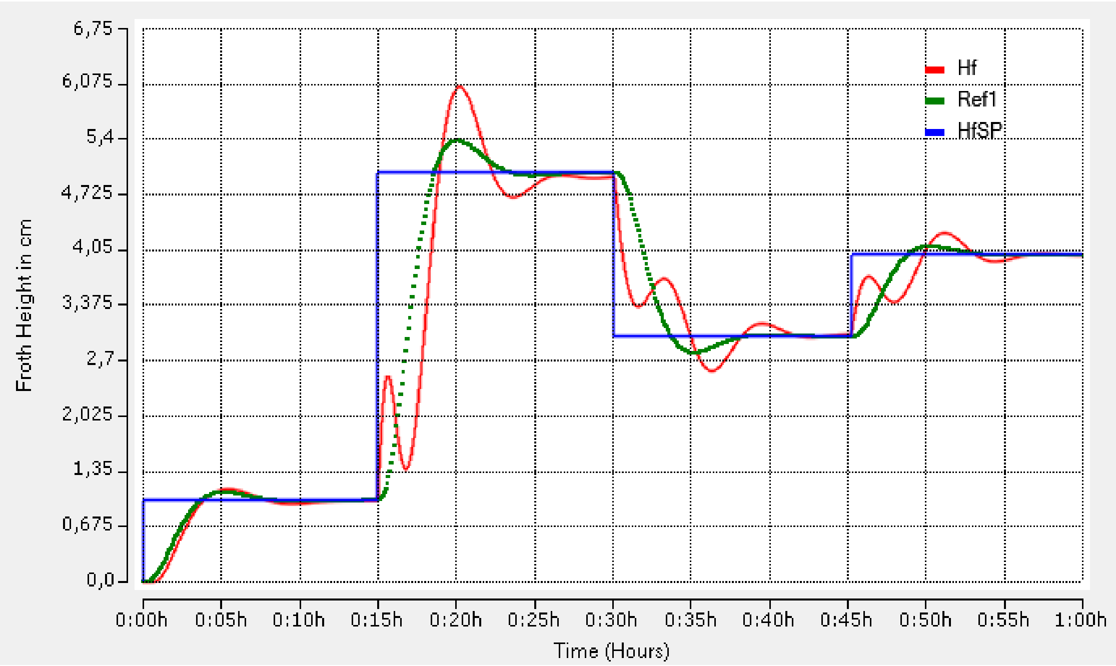


**Figure 7.14:** **Real-time simulation results of Froth Height and Reference Module 1 with respect to time (hours), gamma = 0.005**

It is also noted that there is a delay from when the step input occurs and to when the system begins to respond. The overshoot and time delay of the froth height seen in Figure 7.14 do match with the simulated responses of the Simulink model presented in Chapter 6. However, the Froth height exhibits some oscillations as the response transitions between setpoints occur, as seen at t = 0:15hr; t =0:30hr, and t = 0:45hr. This could be caused by the calibration of the rise time of the reference model being too slow and the controller attempting to adjust the response to duplicate the reference model.

The next step is to look at the second loop and see the effect of the Model Reference Adaptive controller implementation. The result shows that the Beckhoff PLC implementation system has a positive response when minor setpoint variations are made, however, as a step input variation range gets bigger as presented in Figure 7.15, with a magnitude of 1% to 8%, the gas holdup experiences instability at t = 0:15hr, before it followed the command.

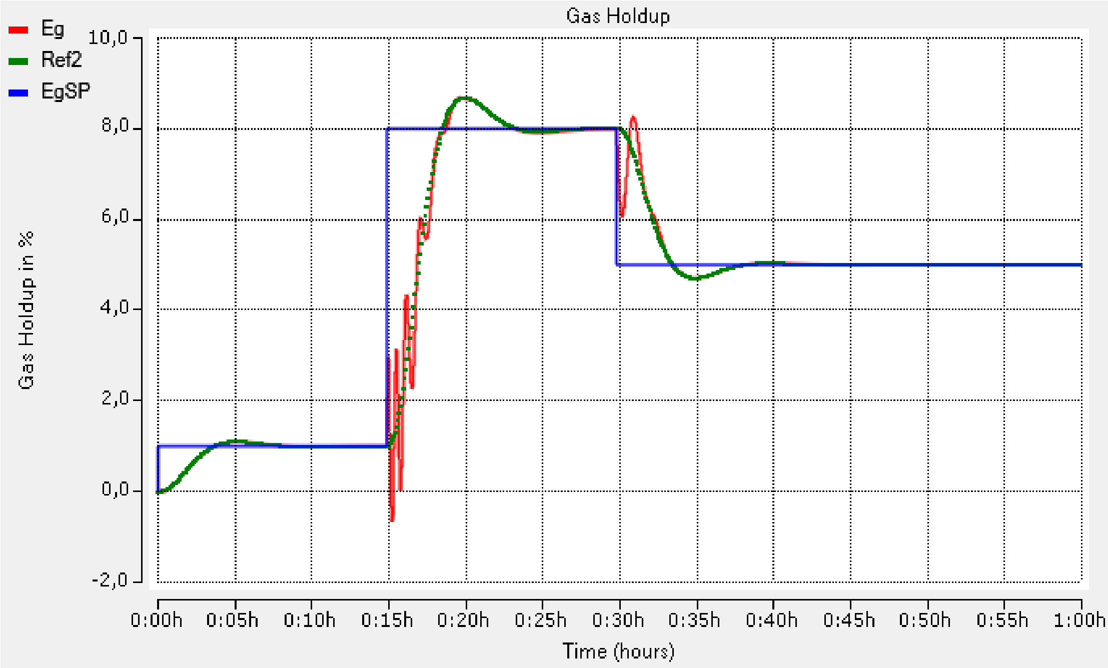


**Figure 7.15:** **Real-time simulation results of Gas Holdup and Reference Module 2 with gamma = 0.005**

Figure 7.15 above indicates a delay from when the step input occurs and to when the system begins to respond. A slight oscillation occurs just after the setpoint is changed. However, the response does stabilize and reach a steady state before the next setpoint change. The overshoot and time delay of the gas holdup seen in Figure 7.15 does match the simulated responses of the Simulink model presented in Chapter 6. However, oscillations in the gas holdup do occur as the response transitions between setpoints., see Table 7.4 for the system's characteristics under this test condition. This could be caused by the calibration of the rise time of the reference model being too slow and the controller attempting to adjust the response to duplicate the reference model. A possible solution would be to further develop and tune the reference model.

**Table 7.4:** **Step response characteristics of the flotation system with Gamma = 0.005**

| Characteristics | Hf (cm) | RM1 | Eg (%) | RM2 |
|---|---|---|---|---|
| **RiseTime (min):** | 3:10 | 2:52.7 | 4:18 | 2:52.7 |
| **SettlingTime (min):** | 11:29 | 9:55 | 16:37 | 9:55 |
| **SettlingMin:** | 0.98 | 0.9025 | 0.98 | 0.9025 |
| **SettlingMax:** | 0.99 | 1.1000 | 0.99 | 1.1000 |
| **Overshoot (%):** | 13 | 9.75 | 4.5 | 9.75 |
| **Peak:** | 1.13 | 1.097 | 1.04 | 1.097 |

| | | | | |
|---|---|---|---|---|
| **PeakTime (min):** | 5:07 | 4:57.4 | 6.23 | 4:57.4 |
| **ess** | 0.001 | 0 | 0.001 | 0 |

The next step is to reduce gamma and examine the performance of the advance controller under the same setpoint variations. In theory, this should increase stability for larger setpoint variations. See the reference model response in Figure 7.16.

**Test results when gamma = 0.00005**

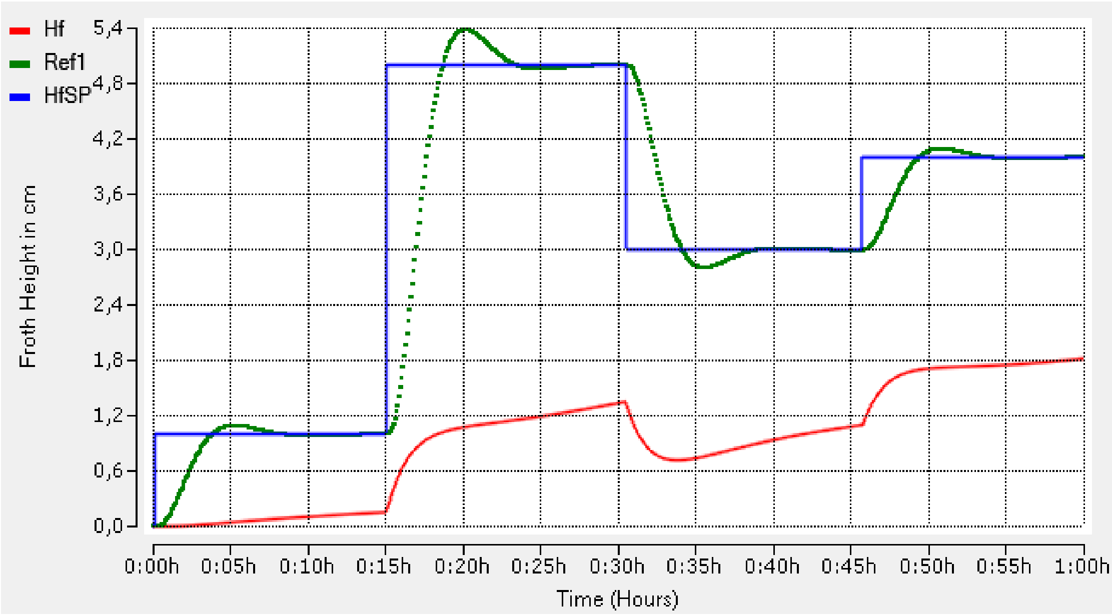


**Figure 7.16:** **Real-time simulation results of Froth Height and Reference Model 1 with gamma = 0.00005**

The implementation of the Model Reference Adaptive controller onto the Beckhoff PLC is displayed in Figure 7.16, the response is poor to both minor and major setpoint variations as the gamma is reduced to 0.00005 from 0.005. The response of froth height appears to be overdamped, not reaching the desired setpoint within the 15-minutes interval before the next setpoint changes occur.

In Figure 7.17 the PLC responds poorly to both minor and major setpoint variations as the gamma is reduced to 0.00005 from 0.005. The response of Gas holdup appears to be overdamped, not reaching the desired setpoint within the 15 min interval before the next setpoint change occurs.

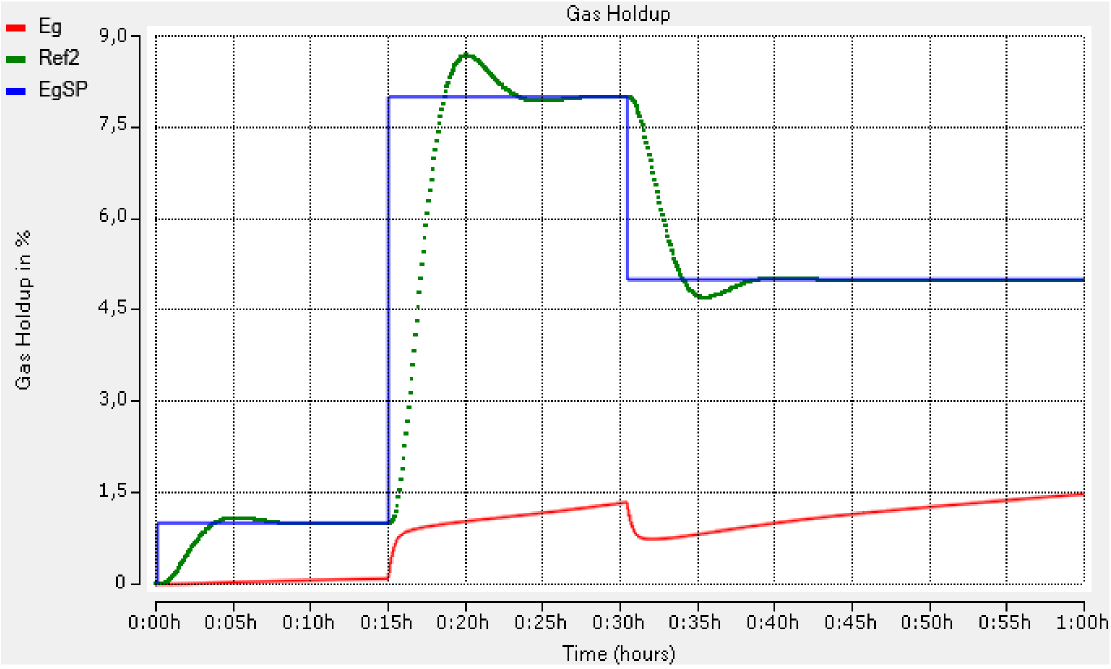


**Figure 7.17**: Real-time simulation results of Gas Holdup and Reference Model 2 with respect to time (hours), gamma = 0.00005

The response seen in Figure 7.17 does not seem to represent any similarity to the SIMULINK model simulation in Chapter 6, as setpoint changes do not achieve a steady state. The response characteristics for both froth height and gas holdup can be seen in Table 7.5. Based off Table 7.5, the control loops of both froth height and gas holdup underperform when the gamma value is reduced.

**Table 7.5:** Characteristics of the flotation system with Gamma = 0.00005

| Characteristics | Hf (cm) | RM1 | Eg (%) | RM2 |
|---|---|---|---|---|
| **RiseTime (min):** | inf | 2:52.7 | Inf | 2:52.7 |
| **SettlingTime (min):** | inf | 9:55 | Inf | 9:55 |
| **SettlingMin:** | inf | 0.9025 | Inf | 0.9025 |
| **SettlingMax:** | inf | 1.1000 | Inf | 1.1000 |
| **Overshoot (%):** | inf | 9.75 | Inf | 9.75 |
| **Peak:** | inf | 1.097 | Inf | 1.097 |
| **PeakTime (min):** | inf | 4:57.4 | Inf | 4:57.4 |
| **ess** | inf | 0 | Inf | 0 |

Due to the responses presented in Figures 7.16 and 7.17, it is noted that reducing gamma has a negative effect on the system. Hence, the next implementation step is to increase the gamma value to identify the controller limitations while implementing the design.

**Test results when gamma = 0.05**

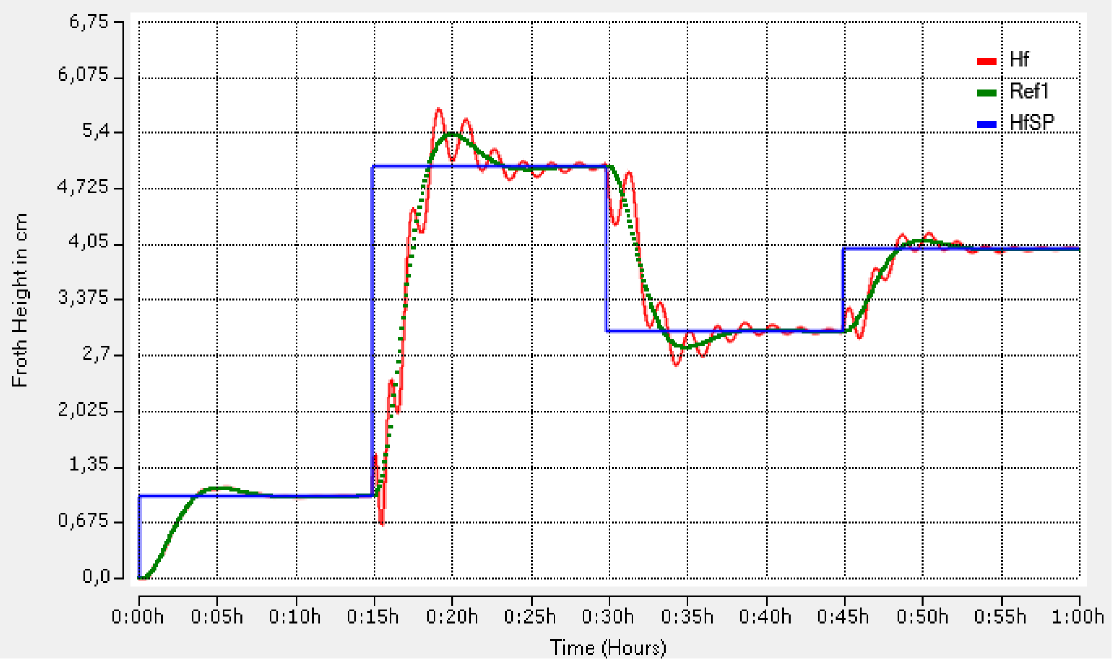


**Figure 7.18:** **Real-time simulation results of Froth Height and Reference Model 1 with respect to time (min), gamma = 0.05**

In Figure 7.18 the Model Reference Adaptive controller when implemented onto the Beckhoff PLC responds poorly to major setpoint variations as the gamma is increased to 0.05. The controller does respond well with the initial step response when t = 0h. The Froth Height response in Figure 7.18 does however resemble that of the froth height response when gamma was set to 0.05 with respect to Figure 7.14. Oscillations in the Froth height does seem to occur as the response transitions between setpoints. (t = 0:15hr; t =0:30hr, and t = 0:45hr). This phenomenon is seen in both responses when gamma is set to 0.005 and 0.05. The SIMULINK simulations in Chapter 6 did not contain any measurements with gamma set to 0.05 as it would display minor oscillations around the steady state.

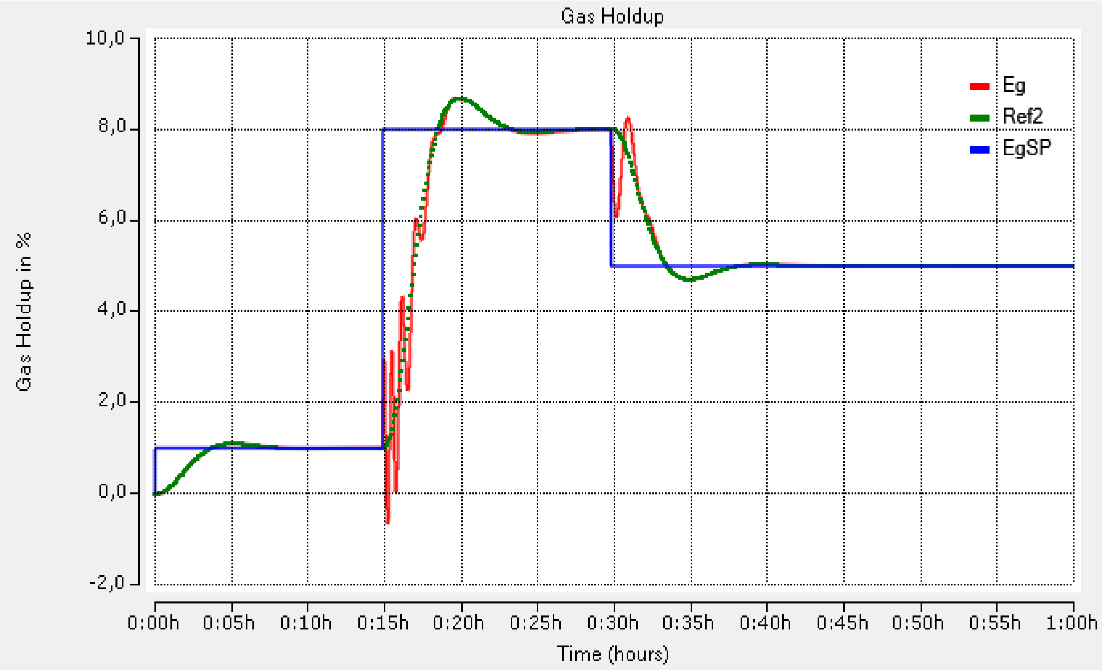


**Figure 7.19:** **Real-time simulation results of Gas Holdup and Reference Model 2 with gamma = 0.05**

The Model Reference Adaptive controller implemented onto the Beckhoff PLC demonstrates a reasonable response to major setpoint variations as the gamma is increased to 0.05 as presented in Figure 7.19. The controller does respond well with the initial step response when t = 0h. The gas holdup response in Figure 7.19 seem to display some resemblance to that of the froth height response when gamma was set to 0.05 in Figure 7.15. The Gas holdup response seen in Figure 7.19 does begin to oscillate once a major setpoint occurs, as seen when t = 0:15h. However, this can only be seen as the controlled variable transitions to the new setpoint (from 1% to 8%). hen gamma is set to 0.005 and 0.05. The characteristics with the gamma set to 0.05 can be seen in Table 7.6, with the steady-state error completely eliminated.

**Table 7.6:** **Step response characteristics of the flotation system with Gamma = 0.05**

| Characteristics | Hf (cm) | RM1 | Eg (%) | RM2 |
|---|---|---|---|---|
| RiseTime (min): | 3:01 | 2:52.7 | 4:18 | 2:52.7 |
| SettlingTime (min): | 11:29 | 9:55 | 16:37 | 9:55 |
| SettlingMin: | 0.98 | 0.9025 | 0.98 | 0.9025 |
| SettlingMax: | 0.99 | 1.1000 | 0.99 | 1.1000 |
| Overshoot (%): | 13 | 9.75 | 4.5 | 9.75 |
| Peak: | 1.13 | 1.097 | 1.04 | 1.097 |
| PeakTime (min): | 5:03 | 4:57.4 | 6.15 | 4:57.4 |
| ess | 0.0002 | 0 | 0.001 | 0 |

The system demonstrates a degree of stability after large setpoint changes occur at t =0:15h for both the froth height and gas holdup. This means that the maximum gamma value that causes instability has not been achieved yet. Therefore, the gamma is then set to 0.5 before undergoing the setpoint tracking test case.

**Test results when gamma = 0.5**

Figure 7.20 displays the real-time implementation of the Model Reference Adaptive controller onto the Beckhoff PLC when gamma is increased to 0.5.

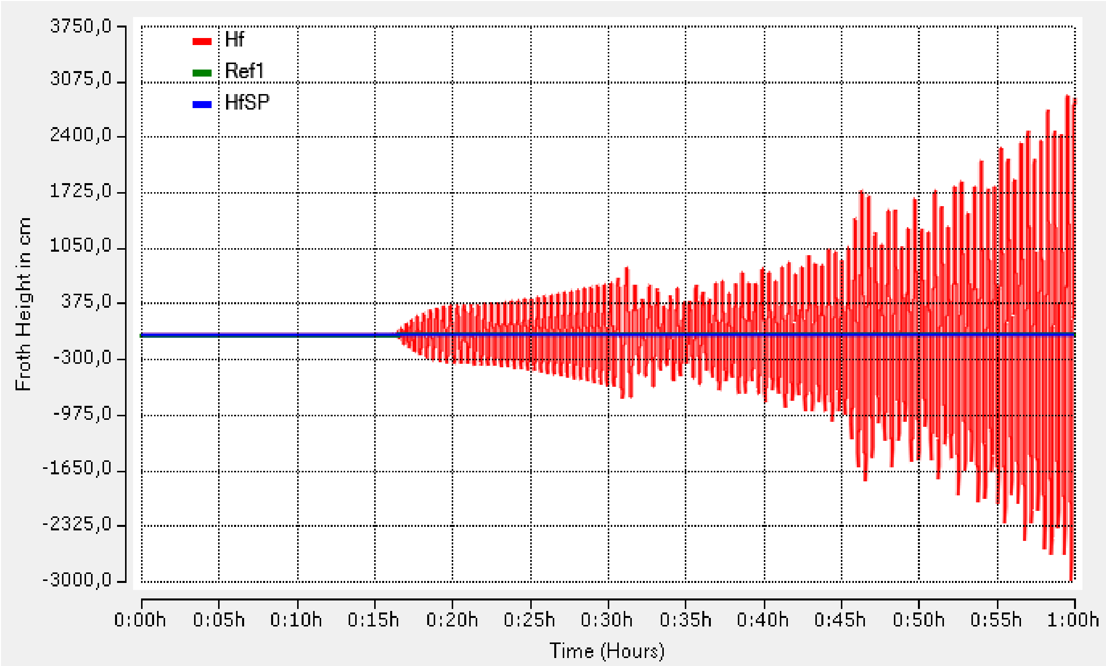


**Figure 7.20: Real-time simulation results of Froth Height and Reference Model1 for gamma = 0.5**

It can be seen that the controller responds poorly to major setpoint variations as the gamma is increased to 0.5. The results show that the controller does respond well with the initial step response when t = 0h. However, the Froth Height response with the gamma set to 0.5 is seen to become unstable when the setpoint change of 1cm-5cm occurs at t = 0:15h. The upper gamma limits for the froth height control loop that causes instability in the system is now chosen as 0.5. The SIMULINK simulations in Chapter 6 did not contain any measurements with gamma set to 0.5 as it would display oscillations around the steady state. This was mainly due to the Simulink results demonstrating sufficient performance with gamma set to 0.005.

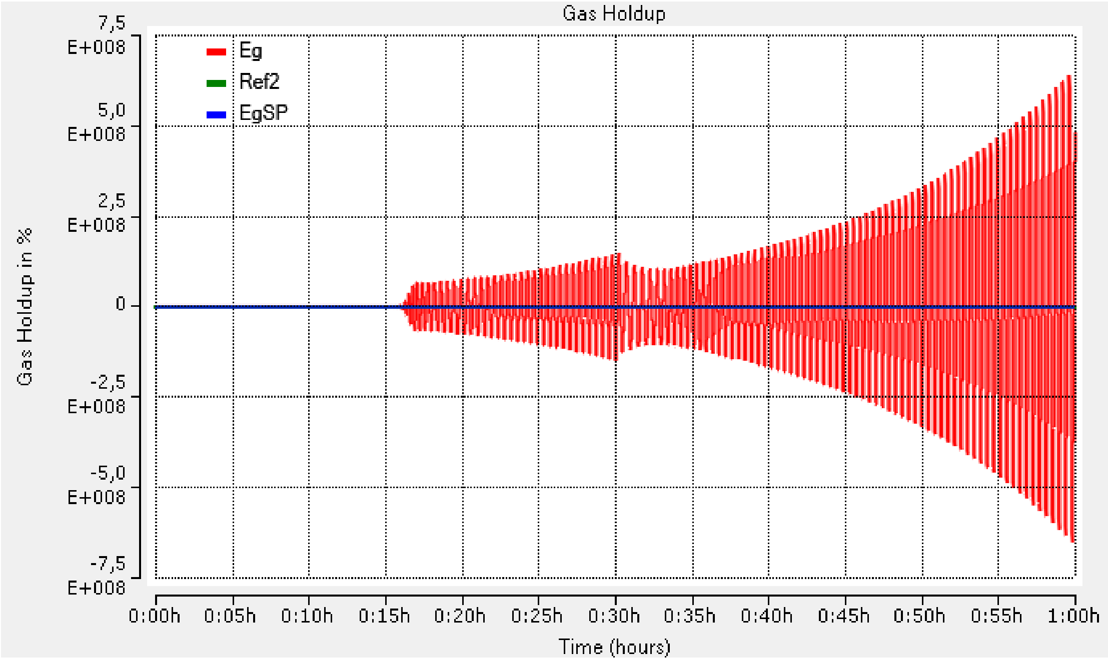


**Figure 7.21:** **Real-time simulation results of Gas Holdup and Reference Model 2 with gamma = 0.5**

Figure 7.21 demonstrates the gas holdup response of the Model Reference Adaptive controller when implemented onto the Beckhoff PLC. The gas holdup is seen to respond poorly to major setpoint variations as the gamma is increased to 0.5. The conclusion drawn here is that the controller does respond well with the initial step response when t = 0h. However, the response becomes unstable when the setpoint change of 1cm-5cm occurs at t = 0:15h. The instability to the gas holdup response now means that the upper limit for gamma is now achieved. The characteristics of the flotation system with Gamma set to 0.5 can be seen in Table 7.7.

**Table 7.7:** **Step response characteristics of the flotation system with Gamma = 0.5**

| Characteristics | Hf (cm) | RM1 | Eg (%) | RM2 |
|---|---|---|---|---|
| **RiseTime (min):** | inf | 2:52.7 | inf | 135.5231 |
| **SettlingTime (min):** | inf | 9:55 | inf | 437.8855 |
| **SettlingMin:** | inf | 0.9025 | inf | 0.9025 |
| **SettlingMax:** | inf | 1.1000 | inf | 1.1000 |
| **Overshoot (%):** | inf | 9.75 | inf | 9.75 |
| **Peak:** | inf | 1.097 | inf | 1.1000 |
| **PeakTime (min):** | inf | 4:57.4 | inf | 6:53 |
| **ess** | inf | 0 | inf | 0 |

As seen in Table 7.7, the characteristics of both Hf and Eg are “inf” due to the uncontrollable oscillations. The next step is to perform the hardware implementation of the process under study with Case 2 conditions, which is the evaluation of the advanced controller against disturbances.

### 7.5.2 Case 2: Real-time Evaluation of Model Reference Adaptive Controlled Flotation Column Against Disturbances

In this subsection, the designed Decoupled MRAC is measured against disturbances induced before and after the plant. The procedure is separated into two scenarios based on where the disturbances occur. The first scenario introduces the disturbance at the output of each loop, whereas the second scenario introduces the disturbance to the flotation plant flow rates. The Model generated for the disturbance scenarios can be seen in Figure 7.22. Input ports 3 and 4 are added to the system to generate the disturbances.

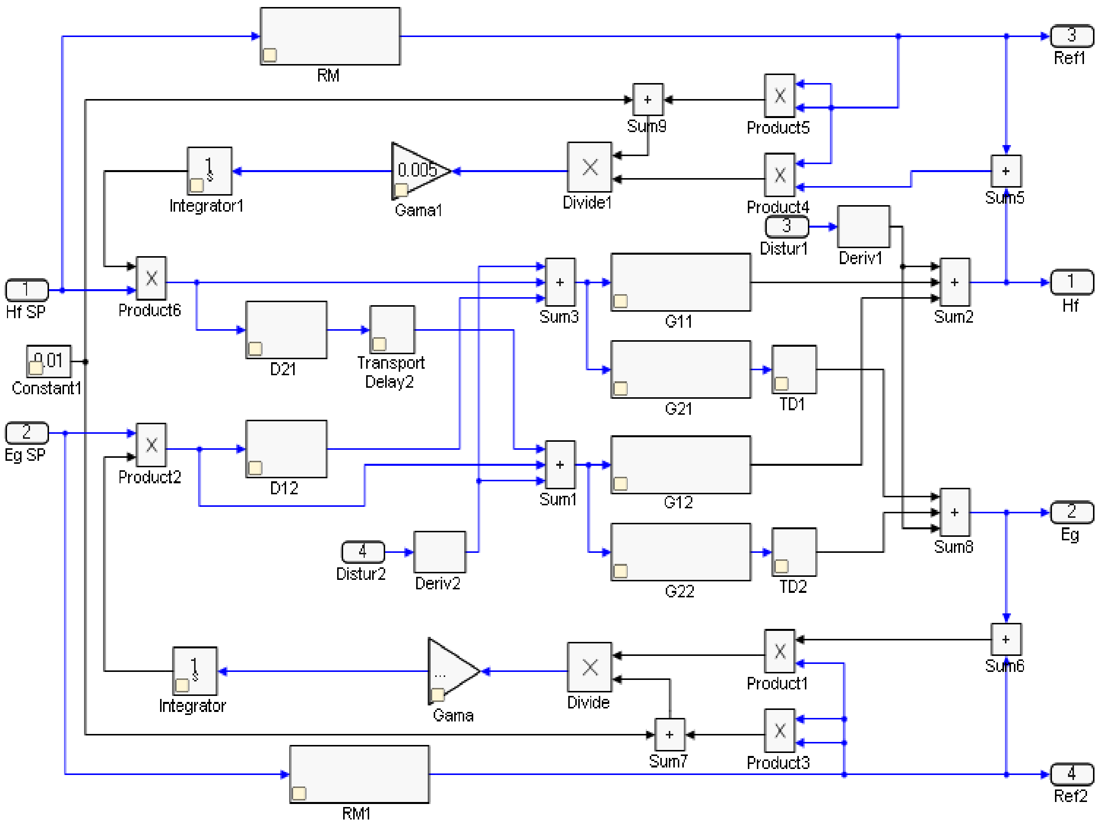


**Figure 7.22:** **MRAC TwinCat Model of a Flotation Process with Disturbance**

#### 7.5.2.1 Scenario 1

The purpose of this scenario is to monitor the effects of the system and controller under the disturbance of the plant outputs (froth height and gas holdup in the collection zone). The test conditions are defined in Table 7.8 below, indicating the setpoint changes in froth height and gas holdup. As well as the disturbances induced at the given time in columns 4 and 5 of Table 7.8. The disturbances and step inputs are applied to Figure 7.22. For scenario 1 Distur2 is left at 0 and Distur1 is applied.

**Table 7.8:** **Disturbance Test Cases for the flotation process**

| Gamma = 0.005 | | | | |
|---|---|---|---|---|
| **TC** | **Setpoint of Hf & Eg** | **Setpoint Time (min)** | **Distur1 & Distur2** | **Disturbance Time (min)** |
| **A** | 1 | 2.5 (2min30sec) | 0.01 | 15 |
| **B** | 1 | 2.5 (2min30sec) | 0.1 | 5 |

**Test condition A:**

The real-time implementation based on Test condition A's values described in Table 7.8 were used in the TwinCat Model displayed in Figure 7.22. The setpoints of the froth height (Hf) and gas hold up (Eg) were changed to 1 at a time of t = 2.5 min. The step response settles well until the disturbance is implemented at a time of t = 15 min. The controller response is plotted against its respective reference models in Figure 7.23 and Figure 7.24. The aim of this test condition is to monitor the controlled system stability when a disturbance occurs after a minor change in setpoint.

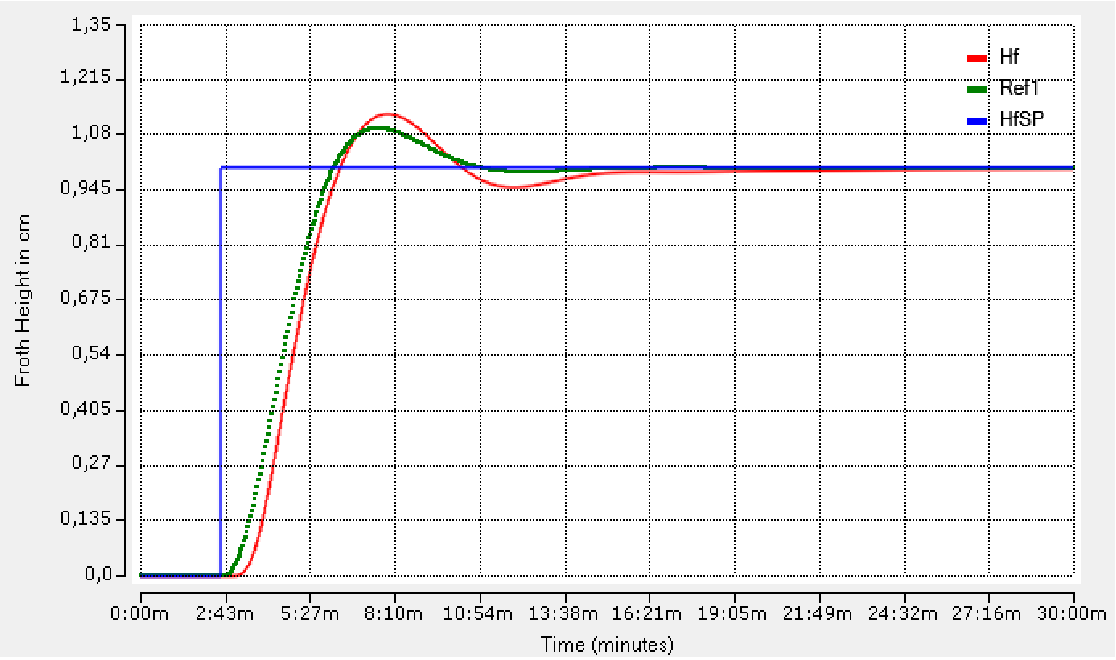


**Figure 7.23:** **Real-time implementation results for Scenario 1 Test Case A of Froth Height and Reference Model 1 for gamma = 0.005**

In Figure 7.23 the reaction of the Froth Height and the reference model 1 response, it can be noted that the response with reference model rejected well and effectively managed the disturbance. Even with the disturbance applied the system remained stable. However, the simulation in chapter 6 clearly displays when the disturbance occurred whereas the implementation response seen in Figure 7.23 does not any evidence of disturbance.

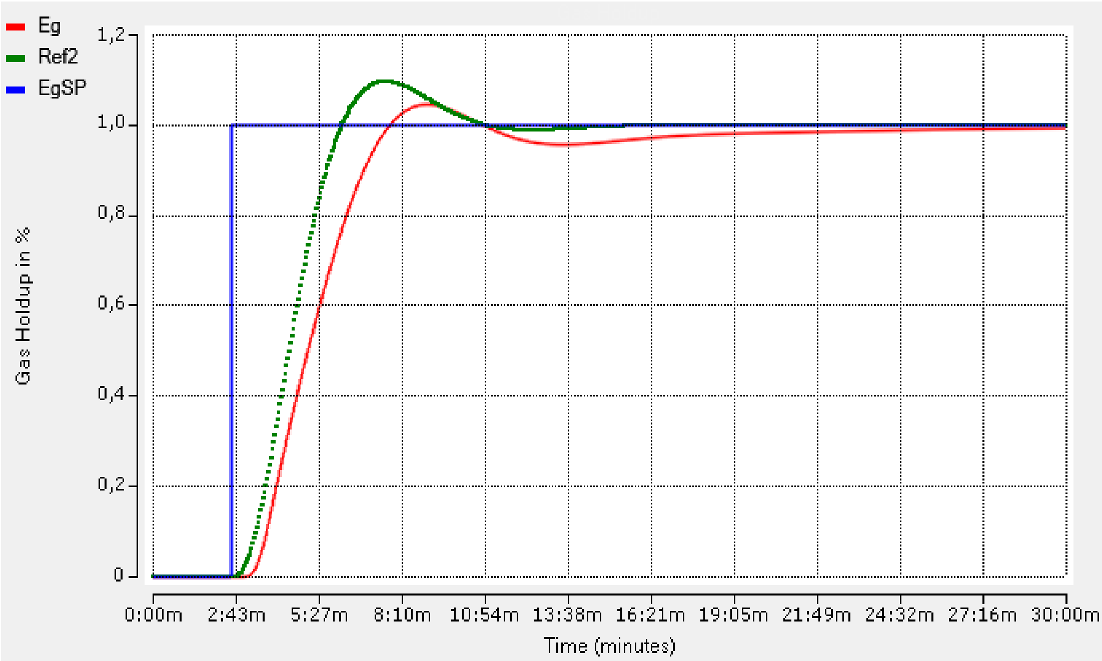


**Figure 7.24:** **Real-time simulation results for Scenario 1 Test Case A of Gas Holdup and Reference Model 2 with respect to time (min), gamma = 0.005**

The reaction of the Gas Holdup and the reference model 2 response is compared against each other in Figure 7.24. It can be noted that the response with the reference model was able to reject and effectively manage the disturbance well. Even with the disturbance applied the system remained stable.

**Test condition B:**

Test condition B test values described in Table 7.8 are used in the Twincat3 model displayed in Figure 7.22. The setpoints of the froth height (Hf) and gas hold up (Eg) are set to stay at zero until a step change of 1 is applied at a time of t = 10 min. The disturbance impulse occurred at a time of t = 2.5 min before the occurrence of a step input into their respective setpoints. The controller response is plotted against its respective reference models in Figure 7.25 and Figure 7.26. This test condition aims to monitor the controlled system stability when a disturbance occurs before a minor change in setpoint.

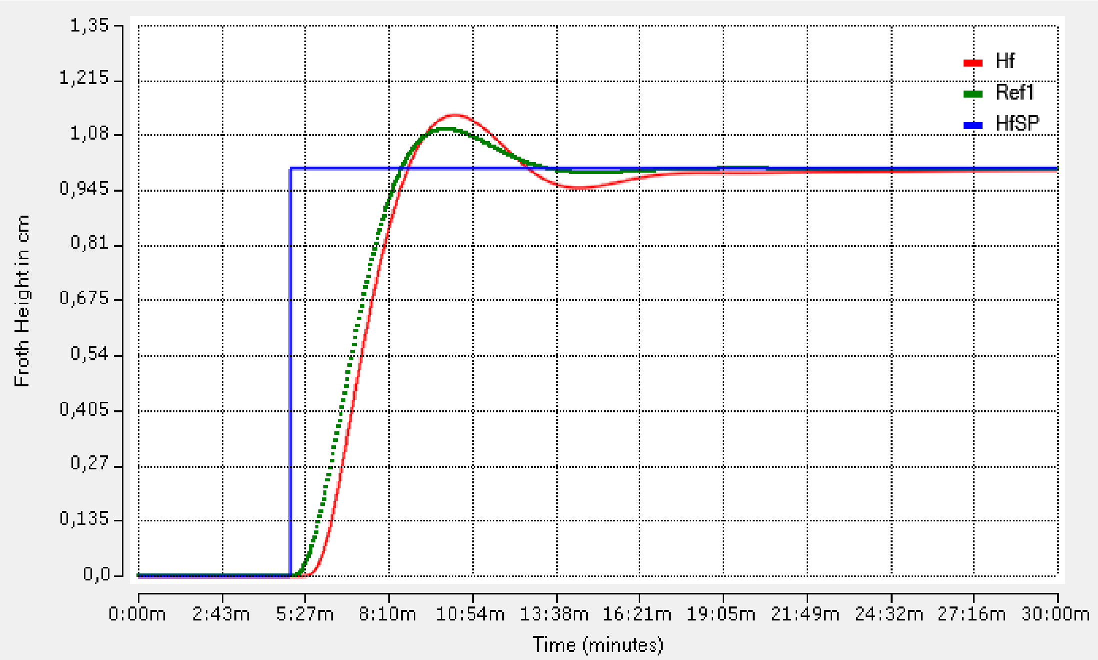


**Figure 7.25:** **Real-time simulation results for Scenario 1 Test Case B of Froth Height and Reference Model 1 with respect to time (min), gamma = 0.005**

In Figure 7.25 the reaction of the Froth Height and the reference model 1 response, it can be noted that the response with the reference model rejected well and effectively managed the disturbance. Even with the disturbance applied the system remained stable. However, the simulation in Chapter 6 displays when the disturbance occurred whereas the implementation response seen in Figure 7.25 does not show any evidence of disturbance.

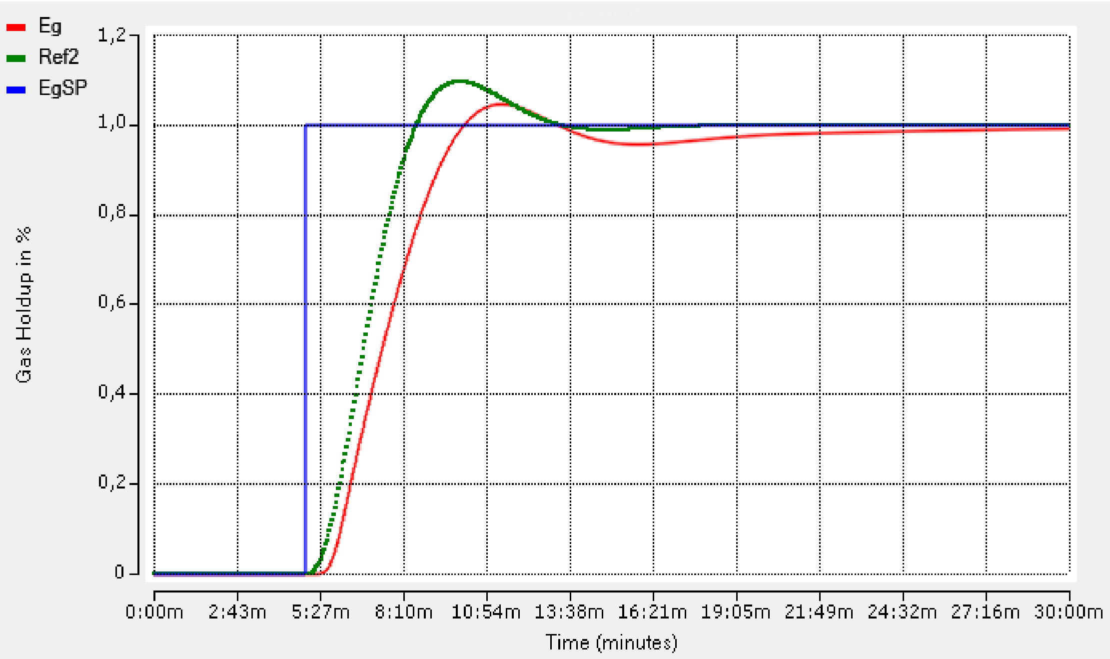


**Figure 7.26:** **Real-time simulation results for Scenario 1 Test Case B of Gas Holdup and Reference Model 2 with respect to time (min), gamma = 0.005**

The reaction of the Gas Holdup and the reference model 2 response is compared against each other in Figure 7.26. It can be noted that the response with the reference model rejected well and effectively managed the disturbance. Even with the disturbance applied the system remained stable.

#### 7.5.2.2 Scenario 2

Impulse responses (Distur2) are added to the input of the plant and the decoupler of each loop to check the effectiveness of disturbance rejection imposed onto the froth height (y1) or the gas holdup (y2). The purpose of this scenario is to monitor the effects of the system and controller under the disturbance of the plant inputs (wash water flowrate and gas flowrate).

The test conditions are the same as scenario 1 which is described in Table 7.8 indicating the setpoint changes in froth height and gas holdup. Only one gamma value will be used in this experiment. The disturbances are induced at the given time in columns 4 and 5. For this scenario, the flow rates $Q_w$ and $Q_g$ experience disturbances labelled as distur2 in Figure 7.22 to simulate irregularities that may occur with the flow rates of the flotation plant.

**Test condition A:**

The simulation based on the Test condition A values described in Table 7.8 were used in the SIMULINK diagram displayed in Figure 7.22. The setpoints of the froth height (Hf) and gas hold up (Eg) were changed to 1 at a time of t = 2.5 min. The step response settles well until the disturbance is implemented at a time of t = 15 min. The controller response is plotted against its respective reference models in Figure 7.27 and Figure 7.28. This test condition aims to monitor the controlled system stability when a disturbance in the flowrates occurs after a minor change in setpoint.

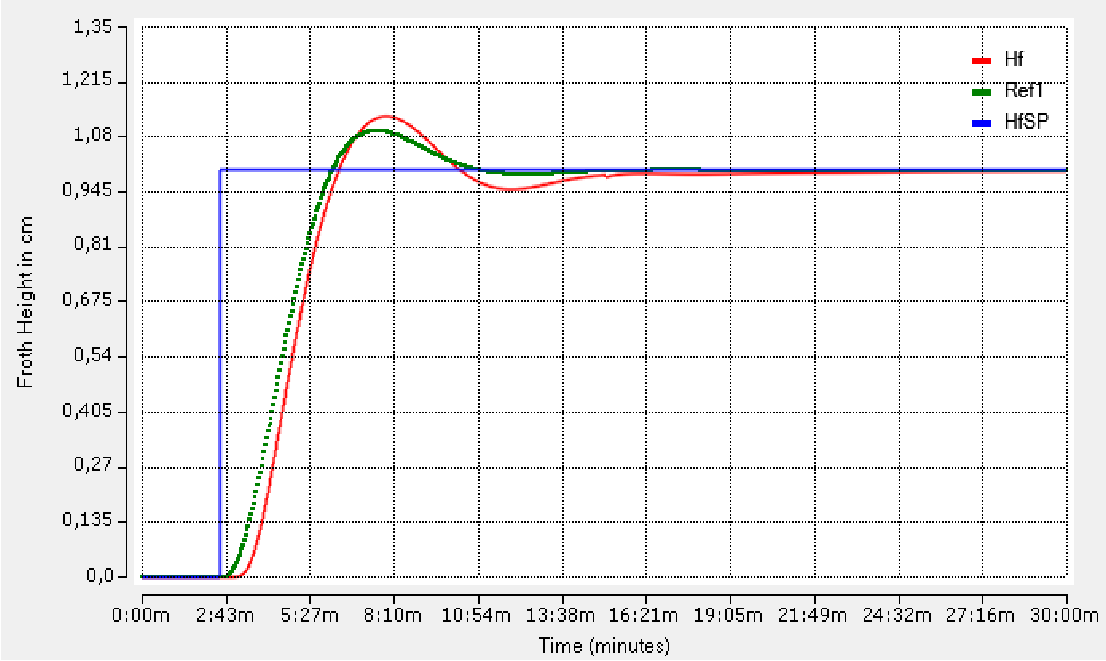


**Figure 7.27**: **Real-time simulation results for Scenario 2 Test Case A of Froth Height and Reference Model 1 with respect to time (min), gamma = 0.005**

By observing the froth height in Figure 7.27, the froth height experiences a slight delay but then follows the Reference Model 1 response labelled Ref1. A step input is introduced at the setpoint of t = 2.5min. Once both the reference model and the froth height start to settle an impulse response is introduced to the flowrates $Q_w$ and $Q_g$ of 0.01 at t = 15min. A minor disruption can be seen between 13:38min and 16:21min, however it is hardly noticed. The froth height remains stable, both before and after the disturbance is introduced.

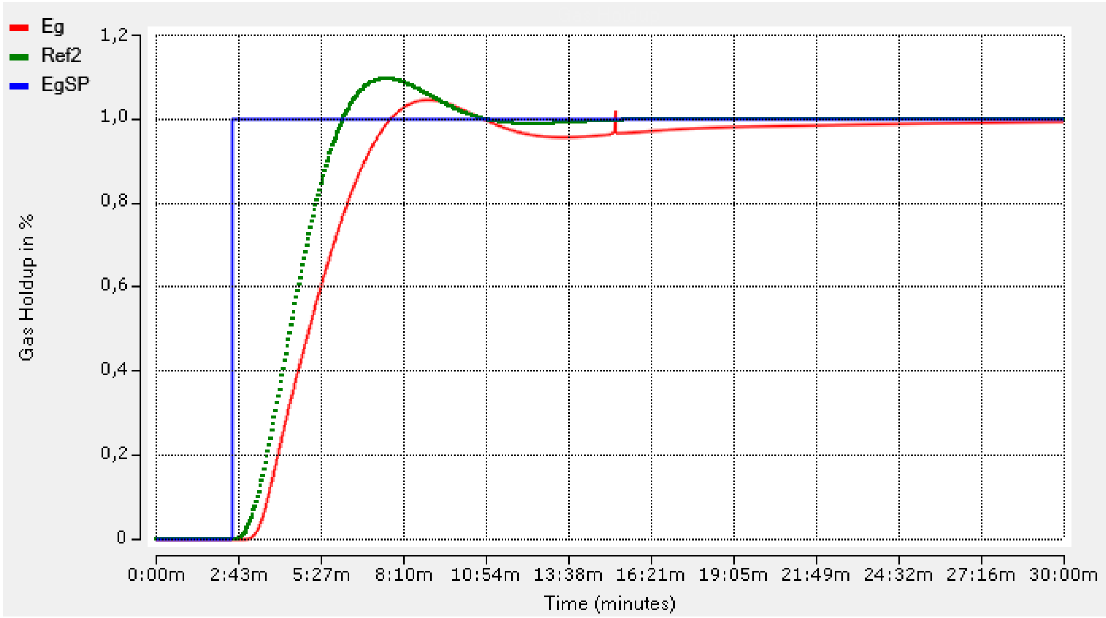


**Figure 7.28: Real-time simulation results for Scenario 2 Test Case A of Gas Holdup and Reference Model 2 with respect to time (min), gamma = 0.005**

By observing the gas holdup in Figure 7.28, the gas holdup experiences a slight delay but then follows the Reference Model 2 response labelled as Ref2. A step input is introduced at the setpoint at t = 2.5min. Once both the reference model and the gas holdup begin to settle an impulse response is introduced to the flowrates $Q_w$ and $Q_g$ of 0.01 at t = 15min. A minor disruption can be seen between 13:38min and 16:21min. Unlike the froth height, the disturbance is more noticeable in the gas holdup. This is due to the flow rates being more effective in the gas holdup control loop. Aside from the visibility of the disturbance, the gas holdup remains stable both before and after the disturbance is introduced.

**Test condition B:**

The real-time simulation based on the Test Condition B values described in Table 7.8 was used in the TwinCAT model diagram displayed in Figure 7.22. A disturbance is implemented at a time of t = 2.5 min before the setpoint change occurs. The setpoints of the froth height (Hf) and gas hold up (Eg) were changed to 1 at a time of t = 10 min. The controller response is plotted against its respective reference models in Figure 7.29 and Figure 7.30. The aim of this test condition is to monitor the controlled system stability when a disturbance in the flowrates occurs before a minor change in setpoint.

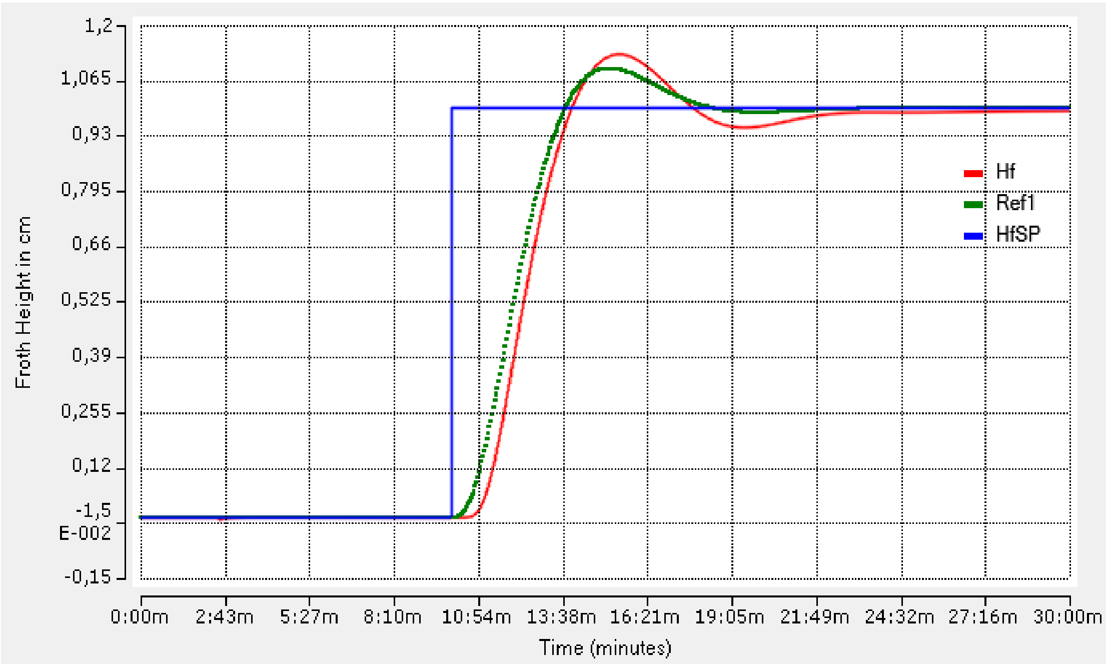


**Figure 7.29:** **Real-time simulation results for Scenario 2 Test Case B of Froth Height and Reference Model 1 with respect to time (min), gamma = 0.005**

By observing the froth height in Figure 7.29, the froth height experiences a slight delay but then follows the Reference Model 1 response labelled Ref1. An impulse response is introduced to the flowrates $Q_w$ and $Q_g$ of 0.01 at t = 2.5min. A minor disruption can be seen between 2.5min and 5min, but it is hardly noticed. A step input is introduced at the setpoint at t = 10min. Once both the reference model and the froth height start to settle. The froth height remains stable both before and after the disturbance and setpoint change is introduced.

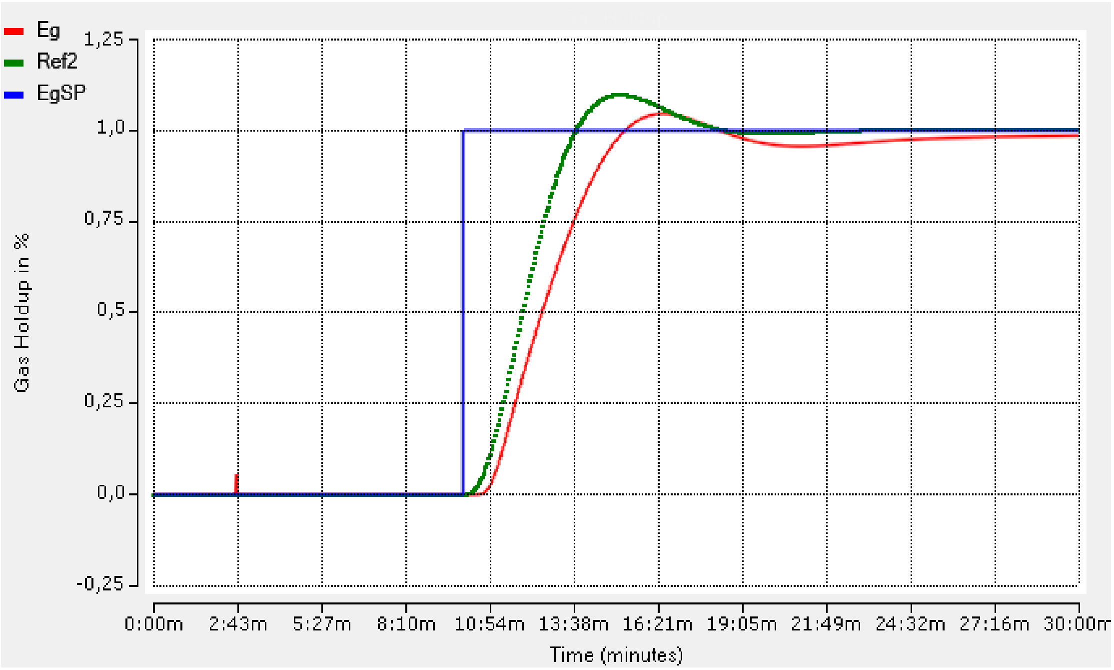


**Figure 7.30**: **Real-time simulation results for Scenario 2 Test Case B of Gas Holdup and Reference Model 2 with respect to time (min), gamma = 0.005**

By observing the gas holdup in Figure 7.30, the gas holdup experiences a slight delay but then follows the Reference Model 2 response labelled as Ref2. An impulse response is introduced to the flow rates $Q_w$ and $Q_g$ of 0.01 at t = 2.5 min. A minor disruption can be seen between 2min and 5min and is noticed. A step input is introduced at the setpoint at t = 10min. Unlike the froth height, the disturbance is more noticeable in the gas holdup. This is due to the flowrates being more effective in the gas holdup control loop. Aside from the visibility of the disturbance, the gas holdup remains stable both before and after the disturbance is introduced.

The next section will focus on examining the real-time simulation results presented in both case 1 and case 2 of this section.

## 7.6 Real-time simulation results analysis of model reference adaptive controlled flotation column

The behaviour of the implemented MRAC design displays an improved performance as opposed to the design simulation results seen in the previous chapter. Figure 7.14 and Figure 7.15 represents the implemented MRAC designs Froth Height and Gas Holdup respectively. In each of the mentioned figures the Froth Height and Gas Holdup both display good setpoint tracking capabilities by following their respective reference models. For larger setpoint changes the implemented MRAC controller displays moderate aggression with regards to tracking the reference models when the gamma is set to 0.005.

Decreasing the Gamma to 0.00005 should have stabilized the large variation in setpoint change. This however caused the implemented system to become overdamped as seen in Figure 7.16 and Figure 7.17. Increasing gamma displays a more aggressive reference model tracking approach as seen in Figure 7.18 and Figure 7.19, where the gamma of both the Froth Height and Gas Holdup has increased to 0.05. With the gamma set to 0.05, the system displayed optimal setpoint tracking for minor setpoint variations. However, based on Figure 7.18 and Figure 7.19 the response displays minor steady-state oscillations for major setpoint variations (e.g. t = 0:15h) for both Froth Height and Gas Holdup. Figure 7.20 and Figure 7.21 confirm that the MIT rule is sensitive to large amplitude setpoint variations by demonstrating uncontrollable oscillations after a large setpoint change.

The results of the second case demonstrate the implemented MRAC controller’s resilience to interference imposed on both the before and after the controller. Scenario 1 demonstrates stability when an impulse response is imposed on the Froth Layer Height and Gas Holdup. Scenario 2 demonstrates evidence of a disturbance within the response but still maintains stability in Figure 7.27, Figure 7.28, Figure 7.29, and Figure 7.30. It may appear in both Scenarios 1 and 2 that the responses of both systems are dependent on their respective reference models.

## 7.7 Challenges and limitations

The biggest challenge of implementing the adaptive controller design is the migration of the Simulink model to the TwinCAT 3 environment. Although Beckhoff provides sufficient documentation on how to go about the migration. If the MATLAB version does not correspond with the Visual Studio version (e.g. MATLAB 2015 and Visual Studio 2019). The C++ compilers installed by the Visual Studio now become incompatible with the installed MATLAB version. As a result, the C++ project must be built via Simulink, and then imported into the TwinCAT environment for the project to be successfully published and digitally signed.

In addition, having the incorrect Windows drivers installed can lead to ADS errors. This often prevents the user from connecting to the Programmable Logic Controller. Beckhoff Automation also provides a step-by-step guide on how to correctly install and assign Windows drivers.

## 7.8 Conclusion

This chapter concludes with a successful method of implementing an adaptive controller that uses the MIT rule for a column flotation process. This is done by migrating the Simulink model to the TwinCAT 3.1 environment for controller implementation. The implemented adaptive controller is subjected to setpoint variations to monitor the setpoint tracking capabilities as well as controller resilience to disturbance. The implemented controller demonstrated exceptional performance as expected from an adaptive controller, however, the results show some room for improvement. The Model Reference Adaptive Controller displays dependency on both the gamma and reference models. Highlighting these two factors and emphasizing their design could further improve the controller's performance. The following chapter concludes and discusses the results and findings of this study.

# CHAPTER 8: RESEARCH CONCLUSION

## 8.1 Introduction

This chapter offers a summary of the thesis deliverables, approaches and methods used in the thesis as well as future research that could be conducted to improve the work presented in this thesis. The chapter also contains the number of publications or future publications based on the studies conducted in this thesis. The focus of this study is on the control design methodology implemented in the flotation process.

The chapter can be broken down into four sections. The first section, section 8.2 outlines the output product of the thesis. The probable research and industrial applications of the thesis output are discussed in section 8.3. A recommendation or consideration for future work is mentioned in section 8.4. The number of published articles and future considerations thereof can be seen in section 8.5.

## 8.2 Thesis deliverables

The objective of the thesis was to establish a method of designing an advanced control system for a flotation column. In addition, the advanced control system was then implemented within a real-time environment. The findings in the thesis are as follows: The Literature Review of Flotation, Column Flotation Control Methodology, and System Modelling, Decentralized decoupled PI and Advanced Controller Design and Real-time Implementation.

### 8.2.1 Literature Review

The second chapter of the thesis consists of the literature review. In the second chapter, the concepts of flotation are thoroughly explained with a brief history of the practice. In the same chapter, numerous advanced control methodologies and applications are mentioned and discussed. Advance control methods such as Adaptive control, Multivariable Control, and Model Predictive Control are frequently used in industrial applications. The literature review also mentions and summarizes decentralized control theory applications in flotation. Similarities within the study of decentralized control theory for flotation are discussed based on recently published articles. Despite flotation being an important process for mineral refinery, research on decentralized control theory for the process is still a scares resource. Based on the Literature review of flotation for the past 5 years, researchers and scholars have trended away from the decentralized control theory. Recent trends in publications have seen research and development into the modelling and evaluation of bubble size distribution (BSD) and the utilization of frother dosage as a controlled variable. Despite advanced control theory in the flotation process being widely available within the industry, processing plants often opt for the manual operation of lower-level systems.

### 8.2.2 Column Flotation Methodology and System Modelling

In Chapter three, the concept of column flotation control is introduced. The relevance of the third chapter is to grasp the understanding of regulatory control of a flotation column. The manipulated and controlled variables of the flotation column are defined at this point of the thesis. The manipulated variables in question would be the wash water flow rate and gas flow rate. Whereas the controlled variables would be the froth layer height and gas holdup within the collection zone. Some concerns about the system modelling of a flotation column are highlighted, with the main factor being the interacting variables. Thus, the introduction of a decentralized decoupled controller for the flotation process.

In Chapter four, A flotation column presented by Nasseri et al, (2020) was modelled and simulated within the MATLAB/Simulink environment. The simulation results of the 2x2 modelled system confirmed variable interaction between the two control loops. Therefore, assuring the requirement of a decoupled system to nullify the variable interaction. The design process can be seen in the fourth chapter, along with the simulation results demonstrating the effectiveness of the decoupled design. However, the chapter concludes with a need for some control action for the decentralized decoupled flotation system.

### 8.2.3 Decentralized decoupled PI and Advanced Control of a flotation process

A decentralized decoupled PI controller design is presented in Chapter five. The controller was evaluated against the decoupled flotation process. The evaluation is partitioned into four different test cases. The first test case was a typical step response. The decoupled PI controlled process performed better by demonstrating stability for the froth height step response. The second test case was the system's response to a set number of setpoint variations. The third and fourth test cases were based on the reaction of the system to disturbances. In the remaining three test cases the decentralized decoupled PI controlled system demonstrated moderate performance when compared to the decentralized and decoupled flotation system without any control action applied.

The decentralized decoupled Model Reference Adaptive Controller is introduced in Chapter Six as the Advanced Control method of a flotation system. The Chapter also displays the detailed design process of the Model Reference Adaptive Controller. The Advanced controller was evaluated against the desired reference response utilizing the same test cases as seen in Chapter five. The controller displayed instability at higher setpoint changes for both control loops. To combat this, the adaptation gain (gamma) is reduced significantly, this does however cause the system to become overdamped. Aside from this drawback, the advanced controller simulations show improvements against the PI controller. The Froth Height response displays some characteristic improvement with a reduction in overshoot as opposed to the PI controlled system. The findings and contribution of the evaluations conducted in Chapter Six demonstrated the controllability of a column flotation process using only a second-order reference model per control loop.

### 8.2.4 Real-time Implementation

The objective of this thesis is to develop and implement a decentralized control method for a flotation process. The seventh Chapter of this thesis is dedicated to implementing the advance controller for the flotation process that is mentioned in Chapter six. Chapter seven demonstrates the transformation from the MATLAB/Simulink environment to Beckhoff Automation's TwinCAT3 runtime platform. The discoveries of such a transformation display the accessibility and availability of utilizing a Beckhoff PLC to interface with MATLAB/Simulink generated models via the TwinCAT3 environment. Despite the Adaptive controller being more complex than the conventional PI controller, the TwinCAT3 platform demonstrates its convenience by conducting the transformation effortlessly. The biggest challenge with the implementation was the licensing, despite being limited to the number of Simulink blocks that can be transformed, it was still possible to implement the controller.

As for the performance of the Implemented Advanced controller, it was tested under the same test conditions as the Simulink simulations. However, the implemented controller response demonstrates fewer oscillations for larger setpoint changes when compared to the simulated results. This is mainly due to the Real-time operating mode of the Beckhoff PLC. Real-time operations, according to Beckhoff Automation, are computing operations that enable continuous data processing so that the processing outcomes are available in a specific amount of time. This indicates that an application's output values are made available within a specified, guaranteed amount of time, whereas the simulated results are almost instantaneous.

The implemented advance controller also demonstrated adequate disturbance rejection for both the disturbance scenario test cases. As a result of the evaluation, it is safe to conclude that the implemented advanced control design displays its effectiveness. The adaption gain is then increased to establish the upper limitations of the controller at which the system can remain stable. The range of the adaptation gain is found to be more than 0.00005 but less than 0.5, at 0.5 both the froth height and gas holdup demonstrate uncontrollable oscillations at larger set point variations. This is common to the adaptive control method utilizing the MIT rule.

## 8.3 Research and industrial applications

The methodology and algorithms pertaining to the thesis may be used for the following:

- The Real-Time engineering industrial implementation, and additional investigation
- An adequate outline of translating MATLAB/Simulink generated projects to the TwinCAT3 environment.
- Industrial application and implementation of adaptive and advanced control theory.
- For Academic research and training in the arena of engineering and automation.

A large portion of the contribution would tend towards the column flotation and the flotation process in general. The research can contribute to the improvement of the performance and efficiency of the flotation process.

## 8.4 Future work and recommendations

Further research on advance control theory of a column flotation system should be focused on the following:

- Improving the stability of the system for larger setpoint variations.
- Improvements on the design of the Reference model for the advanced controller.
- The addition of a National Instruments compact RIO to emulate a flotation plant.
- The addition of plausible disturbance scenarios to the flotation process simulation.

Based on the findings of the thesis, it would be advisable to concentrate on the development of the reference model when working with the Model Reference Adaptive Controller using the MIT rule. The controller's performance can be drastically improved by simply adding emphases to the reference model's step response. A simple unity feedback system could resolve offset and time-delay of the controller.

## 8.5 Publication

Samodien M.T., Tshemese N., Mnguni M. E. S. 2024. The Implementation of a Decoupled MRAC design for a column flotation process. The article has been submitted to the International Journal of Electrical Engineering and Applied Sciences (IJEEAS).

Samodien M.T., Tshemese N., Mnguni M. E. S. 2024. A inclusive study on the robustness of A decoupled PI control and a Decoupled MRAC design of a column flotation process. This article is sent to the International Journal of Electrical Engineering and Applied Sciences (IJEEAS).

## 8.6 Conclusion

This chapter describes the aim and objectives of the thesis and gives the direction for the thesis deliverables. for the. This includes the strategies, algorithms and software developed in this research. The application of the thesis outcomes and future research trends are mentioned.

## REFERENCES


Beckhoff Automation, 18 August 2023. *Beckhoff Information System.* [Online] Available at: https://www.beckhoff.com/en-gb/
[Accessed 15 January 2024].

le Roux, J. D. & Craig, I. K., 2019. *State controllability of froth flotation cell,* Pretoria: International Federation of Automatic Control.

Maurice, F., Jamson, G. j. & Yoon, R. H., 2007. *Froth Flotation.* s.l.:Littleton, Colo. : Society for Mining, Metallurgy, and Exploration.

Quintanilla, P., Neethling, S. J. & Brito-Parada, P. R., 2021. Modelling for froth flotation control: A review. *Minerals Engineering,* 162(0892-6875), pp. 1-19.

Saifadin, G., 2020. *statista.* [Online] Available at: https://www.statista.com/statistics/1121214/mining-sectors-value-added-to-gdp-in-south-africa/#statisticContainer
[Accessed 20 June 2021].

Afolabi, A.S., Muzenda, E. & Abdulkareem, S.A. 2011. Effect of pH on the floatability of base metal sulphides PGMs. In *Proceedings of the World Congress on Engineering and Computer Science*. San Francisco: 239–248.

Ahmed, Y., Oumar, A. & Cherkaoui, M. 2024. Nonlinear robust control applied to the six-phase induction machine. *International Journal of Power Electronics and Drive Systems*, 15(4): 2089–2096.

Airikka, P. 2004. Advanced control methods for industrial process control. *IEE Computing and Control Engineering*, 15(3): 18–23.

Alsafasfeh, A., Alagha, L. & Al-Hanaktah, A. 2024. The Effect of Methyl Isobutyl Carbinol “MIBC” on the Froth Stability and Flotation Performance of Low-Grade Phosphate Ore. *Mining, Metallurgy & Exploration*, 41(1): 353–361.

Alsamia, S. & Koch, E. 2024. Applying clustered artificial neural networks to enhance contaminant diffusion prediction in geotechnical engineering. *Scientific Reports*, 14(1).

Besta, C.S. & Chidambaram, M. 2016. Tuning of multivariable PI controllers by BLT method for TITO systems. *Chemical Engineering Communications*, 203(4): 527–538.

BİLİR, K. 2022. INVESTIGATION OF THE ENTRAINMENT OF FINE SIZED CALCITE AND CHROMITE PARTICLES BY A FLOTATION COLUMN WITH NEGATIVE BIAS REGIME. *Eskişehir Osmangazi Üniversitesi Mühendislik ve Mimarlık Fakültesi Dergisi*, 30(1): 123–129.

Bu, X., Zhou, S., Sun, M., Alheshibri, M., Khan, Md.S., Xie, G. & Chelgani, S.C. 2021. Exploring the Relationships between Gas Dispersion Parameters and Differential Pressure Fluctuations in a Column Flotation. *ACS Omega*, 6(34): 21900–21908.

Calisaya, D., Poulin, É., Desbiens, A., del Villar, R. & Riquelme, A. 2012. Multivariable Predictive Control of a Pilot Flotation Column. In *American Control Conference*. Montréal, Canada: Department of Mining, Materials and Metallurgical Engineerin: 4022–4027.

Candy, J. 2021. Model Reference Adaptive Control (MRAC) for Additive Manufacturing (AM). *Lawrence Livermore National Laboratory*.

CEYLAN, A. 2021. Investigation of the Frother Effect in Two and Three Phases Systems on Bubble Size, Surface tension, Recovery and Grade in Chalcopyrite Flotation. *Physicochemical Problems of Mineral Processing*.

Ceylan, A., Aydın, Ş.B., Göktepe, F. & Bulut, G. 2024. Relation of bubble size, grade and recovery in the copper flotation systems. *Colloids and Surfaces A: Physicochemical and Engineering Aspects*, 692: 133929.

Choi, J.Y., Lee, J. & Edgar, T.F. 2000. Use of the sequential loop closing method for iterative identification of ill-conditioned processes. *Industrial and Engineering Chemistry Research*, 39(7): 2404–2409.

Choi, J.Y., Lee, J., Jung, J.H., Lee, M. & Han, C. 2000. Sequential loop closing identification of multivariable process models. *Computers and Chemical Engineering*, 24(2–7): 809–814.

Doubra, P., Carelse, C., Chetty, D. & Manuel, M. 2023. Experimental and Modelling Study of Pt, Pd, and 2E+Au Flotation Kinetics for Platreef Ore by Exploring the Influence of Reagent Dosage Variations. *Minerals*, 13(10): 1350.

Emmanuella Onyinye Nwulu, Tari Yvonne Elete, Adeoye Taofik Aderamo, Andrew Emuobosa Esiri & Ovie Vincent Erhueh. 2023. Promoting plant reliability and safety through effective process automation and control engineering practices. *World Journal of Advanced Science and Technology*, 4(1): 010–024. https://zealjournals.com/wjast/node/203.

Euzebio, T.A.M., Silva, M.T.D. & Yamashita, A.S. 2021. Decentralized PID Controller Tuning Based on Nonlinear Optimization to Minimize the Disturbance Effects in Coupled Loops. *IEEE Access*, 9: 156857–156867.

Ferreira, F. de S., Silva, J.F., José Netto, A. & Pessoa, E.G. 2024. ADVANCES IN SMART HOME AUTOMATION THROUGH FUZZY LOGIC SYSTEMS. *Revista Sistemática*, 14(5). https://sevenpublicacoes.com.br/RCS/article/view/5644.

Fuerstenau, M.C. & Somasundaran, P. 2003. Flotation. In *Principles of Mineral Processing*. Littleton: Society for Mining, Metallurgy & Exploration, Incorporated: 245–306.

Garrido, J., Vázquez, F. & Morilla, F. 2012. Centralized multivariable control by simplified decoupling. *Journal of Process Control*, 22(6): 1044–1062.

Halters, F., Zondervan, E. & de Haan, A. 2010. Integrated optimization of a waste water treatment plant using statistical analysis. *Journal of hazardous materials*, 179(1): 480–487.

Huang, H., Yang, X., Wu, Z., Qiao, B., Ma, G., Shao, H. & Tao, D. 2023. An investigation of nanobubble enhanced flotation for fly ash decarbonization. *Colloids and Surfaces A: Physicochemical and Engineering Aspects*, 679: 132563.

I, C.A., Chennakesavulu, K., Reddy, G.R., Vasumathi, N., Kumari, A., Gharai, M., Kumar, T.A. & Kumar, T.V.V. 2024. Utilizing a sustainable surfactant from Cucurbita pepo seeds for eco-friendly flotation of non-coking coal in sustainable energy applications. *Biomass Conversion and Biorefinery*.

Imhof, R. 1988. Pneumatic flotation - a modern alternative. *Aufbereitungs-Technik*, 29(8): 451–458.

Jain, P. & M.J, N. 2013. Design of a Model Reference Adaptive Controller Using Modified MIT Rule for a Second Order System. *Advance in Electronic and Electric Engineering*, 3(4): 477–484.

Jiang, S., Du, L., Li, Y., Yang, L. & Luo, B. 2024. LCL APF control strategy based on model predictive control. *Frontiers in Energy Research*, 12.

Kämpjärvi, P. & Jämsä-Jounela, S.L. 2003. Level control strategies for flotation cells. *Minerals Engineering*, 16(11): 1061–1068.

Kukita, S., Kiya, H. & Kondo, Y. 2024. Optimal quantum controls robust against detuning error. *Physica Scripta*, 99(11): 115124. https://iopscience.iop.org/article/10.1088/1402-4896/ad8281.

Kyriazos, T. & Poga, M. 2024. Exploring Fuzzy Logic as an Alternative Approach in Psychological Scoring. *The Open Psychology Journal*, 17(1). https://openpsychologyjournal.com/VOLUME/17/ELOCATOR/e18743501337527/.

Leiva, C., Acuña, C., Luukkanen, S. & Cruz, C. 2024. Enhancing bubble bize prediction in flotation processes: a drift flux model accounting for frother type. *Physicochemical Problems of Mineral Processing*.

Li, Y., He, Q., Liu, X., Zhang, W. & Jing, X. 2024. Robust flight control based on a nonlinear-L1 adaptive control with modified piecewise-constant and HIL experiments. *Nonlinear Dynamics*. https://link.springer.com/10.1007/s11071-024-10600-3.

Liang, J., Tang, S. & Jia, B. 2024. Control of Parallel Quadruped Robots Based on Adaptive Dynamic Programming Control. *Machines*, 12(12): 875. https://www.mdpi.com/2075-1702/12/12/875.

Liao, Q. & Sun, D. 2021. Sparse and Decoupling Control Strategies Based on Takagi-Sugeno Fuzzy Models. *IEEE transactions on cybernetics*, 51(2): 947–960.

Liu, L., Tian, S., Xue, D., Zhang, T., Chen, Y. & Zhang, S. 2019. A Review of Industrial MIMO Decoupling Control. , 17(X): 1–9.

Liu, T., Cui, Q. & Xu, D. 2024. Optimal trajectory control for the yaw system vibration and crawling jitter of a wind turbine. *Journal of Vibroengineering*. https://www.extrica.com/article/24220.

Liu, Y., Si, W., Xvshang, H., Li, L., Qin, Y. & Lin, Y. 2024. *Biomedical Engineering Research: Computer Translating and Teaching System and Neural Network*.

Maldonado, M., Desbiens, A. & del Villar, R. 2009. Potential use of model predictive control for optimizing the column flotation process. *International Journal of Mineral Processing*, 93(1): 26–33.

Martín-sánchez, J.M. 2014. *Advances in Industrial Control ADEX Optimized Adaptive Controllers and Systems*. illustrate. M. J. Grimble & M. A. Johnson, eds. Springer.

Nabiel Algshat. 2024. Evaluating Students' Academic Progress in the Role of Fuzzy Logic. *AlQalam Journal of Medical and Applied Sciences*: 984–989. https://journal.utripoli.edu.ly/index.php/Alqalam/article/view/326.

Nasseri, S., Khalesi, M.R., Ramezani, A., Abdollahi, M. & Mohseni, M. 2020. An Adaptive Decoupling Control Design for Flotation Column: A Comparative Study Against Model Predictive Control. *IETE Journal of Research*, 0(0): 1–14.

Oliveira, A., Junior, J., Pinto, T. & Filho, L. 2023. The Influence of Static Pressure on Bubble Size and Contact Angle of Quartz: Mimicking What May Happen Inside a Hypothetical Flotation Column. *Minerals*, 13(3): 417.

Panjipour, R., Karamoozian, M. & Albijanic, B. 2021. Bubble size distributions in gas–liquid–solid systems and their influence on flotation separation in a bubble column. *Chemical Engineering Research and Design*, 167: 96–106.

Persechini, M.A.M., Peres, A.E.C. & Jota, F.G. 2004. Control strategy for a column flotation process. *Control Engineering Practice*, 12(8): 963–976.

Quintanilla, P., Neethling, S.J. & Brito-Parada, P.R. 2021. Modelling for froth flotation control: A review. *Minerals Engineering*, 162(November 2020): 106718.

Ramadan, M. & Anitescu, M. 2024. Dampening parameter distributional shifts under robust control and gain scheduling. http://arxiv.org/abs/2411.16566.

Le Roux, J.D. & Craig, I.K. 2019. State controllability of a froth flotation cell. In *IFAC-PapersOnLine*. Elsevier B.V.: 54–59.

Rudakov, R. V., Serzhantova, M. V., Boikov, V.I., Bushuev, A.B., Nuyya, O.S., Litvinov, Y. V. & Bystrov, S. V. 2024. Adaptive control of robots for high-temperature operations. *Informatsionno-Upravliaiushchie Sistemy*, (4): 12–23.

Salgado, M.E. & Conley, A. 2004. MIMO interaction measure and controller structure selection. *International Journal of Control*, 77(4): 367–383.

Sasi, M., Marimi, R.M. & Masoud, A. 2024. Design Fuzzy Logic Controller of MPPT for Photovoltaic System. *International Science and Technology Journal*, 35(1): 1–18. https://www.stcrs.com.ly/istj/article-details.php?id=954.

Schmidt, H. 2002. *Model Based Design of Decentralized Control Configurations*. Royal Institute of Technology.

Shean, B.J. & Cilliers, J.J. 2011. A review of froth flotation control. *International Journal of Mineral Processing*, 100(3–4): 57–71.

Shen, Y., Cai, W.J. & Li, S. 2010. Multivariable process control: Decentralized, decoupling, or sparse? *Industrial and Engineering Chemistry Research*, 49(2): 761–771.

da Silva Lima, G., Amorim Savi, M. & Moreira Bessa, W. 2024. Adaptive control of cardiac rhythms. *Scientific reports*, 14(1): 23284.

Srikanth, M., Venkata Pavan Kumar, Y., Pradeep Reddy, C. & Mallipeddi, R. 2024. Multivariable Control-Based dq Decoupling in Voltage and Current Control Loops for Enhanced Transient Response and Power Delivery in Microgrids. *Energies*, 17(15).

Syrmakezis, K.C., Tsakalakis, K.G. & Sammas, I.P. 2023. Valorisation of base metals contained in fine particles of End-of-Life Printed Circuit Boards with the use of column flotation process. *Sustainable Chemistry and Pharmacy*, 33: 101062.

Szrama, S. 2024. Turbofan engine health status prediction with neural network pattern recognition and automated feature engineering. *Aircraft Engineering and Aerospace Technology*, 96(11): 19–26.

Taghavi Zinjenab, Z., Azimi, E., Shadman, M. & Hosseini, M.R. 2024. Maximization of ultrafine poly-mineral ore sequential flotation recovery through synergistic effect of conventional and nano-size bubble combination. *Journal of Molecular Liquids*, 401: 124698.

Tang, M.A., Wang, X.M., Jie, C. & Li, C. 2017. On lyapunov stability theory for model reference adaptive control. *Proceedings - 2017 4th International*

*Conference on Information Science and Control Engineering, ICISCE 2017*: 1055–1060.

Tsave, P.K., Kostoglou, M., Karapantsios, T.D. & Lazaridis, N.K. 2023. Enhancing Fines Recovery by Hybrid Flotation Column and Mixed Collectors. *Minerals*, 13(7): 849.

Tsave, P.K., Kostoglou, M., Lazaridis, N.K. & Karapantsios, T.D. 2024. Hydrodynamic Study of a Hybrid Electro-Flotation Column. *Minerals*, 14(4): 344.

Tshemese-Mvandaba, N., Tzoneva, R. & Mnguni, M.E.S. 2021. Decentralised PI controller design based on dynamic interaction decoupling in the closed-loop behaviour of a flotation process. *International Journal of Electrical and Computer Engineering*, 11(6): 4865–4880.

Verma, B. & Padhy, P.K. 2020. Robust Fine Tuning of Optimal PID Controller with Guaranteed Robustness. *IEEE Transactions on Industrial Electronics*, 67(6): 4911–4920.

Viteckova, M. & Vitecek, A. 2021. Robust Tuning of PI and PID Controllers for Integrating Plants with Time Delay. *2021 22nd International Carpathian Control Conference, ICCC 2021*: 2–7.

Vu, T.N.L. & Lee, M. 2010. Independent design of multi-loop PI/PID controllers for interacting multivariable processes. *Journal of Process Control*, 20(8): 922–933.

Wang, Y. & Hsiao, T. 2024. Multivariable Iterative Learning Control Design for Precision Control of Flexible Feed Drives. *Sensors*, 24(11).

Wills, B.A. & Finch, J.A. 2016. Froth Flotation. In *Wills' Mineral Processing Technology*. Elsevier: 265–380.

Wu, T., Qi, Y., Liao, L., Ji, F. & Chen, H. 2021. Research on equalization strategy of lithium-ion batteries based on fuzzy logic control. *Journal of Energy Storage*, 40(May): 102722.

Xiong, Q., Cai, W.J., He, M.J. & He, M. 2006. Decentralized control system design for multivariable processes - A novel method based on effective relative gain array. *Industrial and Engineering Chemistry Research*, 45(8): 2769–2776.

Yin, M., Han, N., Yang, T. & Li, Y. 2024. Study of a Novel Fluidized Bed Flotation Column with Enhanced Bubble Dispersion. *Minerals*, 14(1): 84.

Yu, Y., Yang, H., Wan, S., Liu, Q. & Yan, J. 2024. A cooperative control method and application for series multivariable coupled system. *Scientific Reports*, 14(1).

Zhang, J., Wang, Z., Li, L., Yang, K. & Lu, Y. 2024. Trajectory tracking control of autonomous vehicles based on event-triggered model predictive control. *IET Intelligent Transport Systems*. https://ietresearch.onlinelibrary.wiley.com/doi/10.1049/itr2.12589.

Zhang, S., Bai, H. & Zhang, W. 2024. Optimization control of the D-shaped cylinder flow with genetic algorithm and Coanda pulsation jets. *Physics of Fluids*, 36(12). https://pubs.aip.org/pof/article/36/12/125138/3324007/Optimization-control-of-the-D-shaped-cylinder-flow.

Zhang, Y., Li, C., Wang, L. & Wang, H. 2020. Application of froth flotation in the separation of polyvinyl chloride and polycarbonate for recycling of waste plastic based on a novel surface modification. *Waste Management*, 110: 43–52.

Zhang, Z., Miao, Z., Chen, Y. & Deng, X.-H. 2024. Smolyak algorithm assisted robust control for quantum systems with uncertainties. https://www.researchsquare.com/article/rs-5313186/v1.

Zhao, D., Li, B., Lu, F., She, J. & Yan, S. 2024. Deep Bilinear Koopman Model Predictive Control for Nonlinear Dynamical Systems. *IEEE Transactions on Industrial Electronics*.

Zhou, G., Swaminathan, S., Raju, R.V., Guntupalli, J.S., Lehrach, W., Ortiz, J., Dedieu, A., Lázaro-Gredilla, M. & Murphy, K. 2024. Diffusion Model Predictive Control. http://arxiv.org/abs/2410.05364.

Zhou, H., He, W., Ji, C., Yang, X., Li, H., Dong, W., Jia, L. & Liu, B. 2024. Mathematical modeling of the effect of SEN outport shape on the bubble size distribution in a wide slab caster mold. *Metallurgical Research & Technology*, 121(3): 301.

## APPENDIX A

The product specifications for the Beckhoff Automation Industrial PC C6015-002 are given in Table A.1 below.

**Table A.1:** **C6015 Product specification, (https://www.beckhoff.com/en-gb/products/ipc/pcs/c60xx-ultra-compact-industrial-pcs/c6015.html)**

| **Beckhoff Industrial PC: C6015** | |
|---|---|
| **Criteria** | **Product Specification** |
| Dimensions ( Width X Height X Diameter) | 82 x 82 x 40 mm, excluding mounting plate |
| Weight | 400g without mounting plate |
| | 450g with mounting plate |
| Power Consumption | 17 Watt |
| Power Supply | 24 V DC |
| Processor | Intel Atom® x5-E3930, 1.3 GHz, 2 cores (TC3: 40) |
| Memory | 4 GB DDR4 RAM |
| Protection rating | IP20 |
| Vibration Resistance (Sinusoidal) | EN 60068-2-6: 10 to 58 Hz: 0.035 mm |
| | 58 to 500 Hz: 0.5 G (approx. 5 m/ s2) |
| Shock resistance (shock) | EN 60068-2-27: 5 G (approx. 50 m/s2), duration: 30 ms |
| EMC interference immunity | conforms to EN 61000-6-2 |
| EMC interference emission | conforms to EN 61000-6-4 |
| Permissible operating temperature | 0 °C to +50 °C (operation) |
| | -25 °C...+65 °C (transport / storage) |
| Permissible air humidity | Maximum 95 %, no condensation |

## APPENDIX B

The test setup used to implement the adaptive control for the flotation process can be seen in Figure B.1. The I/O card displayed in this image was not powered and thus not used for the purpose of demonstration. The 24 V DC is supplied to the Industrial PC with the Ethernet1 adapter connected to the engineering PC for ADS implementation and TwinCAT Scope View.

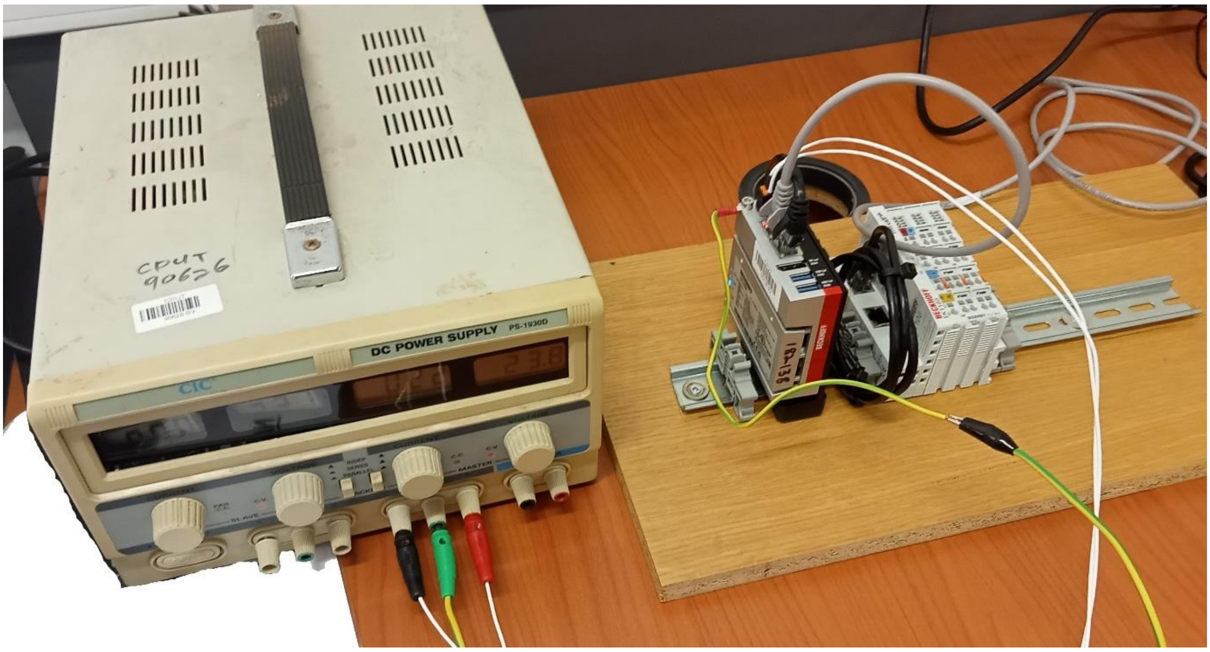


**Figure B.1: Implementation test setup**